Functional Connectivity of Auditory Statistical Learning

Erica R. Peterson

A dissertation

submitted in partial fulfillment of the

requirements for the degree of

Doctor of Philosophy

University of Washington

2026

Reading Committee:

Patricia K. Kuhl, Chair

Adrian K.C. Lee

Andrew Brown

Program Authorized to Offer Degree:

Speech and Hearing Sciences

University of Washington

Abstract

Functional Connectivity of Auditory Statistical Learning

Erica R. Peterson

Chair of the Supervisory Committee:

Patricia K. Kuhl

Department of Speech and Hearing Sciences

Statistical learning is a key mechanism underpinning language acquisition in infancy. Using electrophysiological functional imaging, researchers have demonstrated neural adaptation to statistical probabilities in a speech stream using event-related paradigms, but the role of functional connectivity is unknown. The current study investigates the functional connectivity of statistical learning using magnetoencephalography (MEG) recordings of adults and adolescents listening to a speech stream composed of tri-syllabic pseudowords. Data were source localized using the eLORETA inverse method and band-pass filtered into canonical bands, theta (4-7 Hz), alpha (8-12 Hz), low beta (13-18 Hz), high beta (19-30 Hz), and low gamma (31-55 Hz). Two methods of connectivity estimation are compared, amplitude envelope correlations, which are sensitive to slow modulations in cortical activity, and the instantaneous amplitude correlation, which has a higher temporal resolution. Functional networks are derived and characterized using both methods. Support vector regression is used to assess whether network features predict statistical learning. Results of the investigation show that high temporal

resolution metrics predict auditory statistical learning above chance, independently of event-related measures of neural adaptation.

Table of Contents

List of Figures

List of Tables

Chapter 1: Motivation, Background, Goals, and Approach

Humans display a remarkable ability to acquire languages over the course of their lifetimes. Infants typically start to learn their own names by six months and say their first words by the end of the first year of life, despite apparently having no direct instruction. This astonishing cognitive feat has been under investigation for many decades as educators, psychologists, linguists, and neuroscientists have examined various facets of the language acquisition process.

A key cognitive ability underlying language acquisition is human statistical learning. Statistical learning is the ability to pick up on regularities in the environment. Sensitive statistical learners are highly attuned to the probabilistic landscape of their surroundings; likely events are expected and unlikely events are detected by successful statistical learners. In the context of language learning, statistical properties of speech emerge from the fact that language is structured in hierarchical groupings from the phonemic to the discourse level, structure that makes human utterances highly patterned and predictable. Detecting the patterns embedded in utterances in their environment allows infants to segment individual words from speech streams, enabling semantic encoding. Auditory statistical learning is therefore an essential ability for developmental scientists and language researchers to understand.

Over the past two decades, researchers have made significant progress illuminating neural changes resulting from auditory statistical learning (ASL) using neuroimaging, but mysteries about statistical learning remain. Electrophysiological measures of cortical function, magneto- and electroencephalography (M/EEG), show that the transitional probability of a syllable in a SL speech stream modifies the transient event-related response to the stimulus in two time windows of interest, 100 milliseconds following stimulus onset, known as the N100,

and in a late processing window approximately 400 ms after stimulus onset, known as the N400 (Cunillera et al., 2009; Daikoku, 2018; Sanders et al., 2002; Teinonen & Huotilainen, 2012). Prior work has shown that the syllables with low transitional probability, syllables that are not predictable, evoke a larger amplitude response in the N400 late processing window than syllables with a high transitional probability that are expected by the participant (Abla et al., 2008; Bosseler et al., 2016; Teinonen & Huotilainen, 2012). These effects involve not only the primary auditory cortex, but also higher-level cortical regions involved in speech processing like the superior temporal gyrus and inferior frontal gyrus (Karuza et al., 2013; Orpella et al., 2022; Teinonen & Huotilainen, 2012).

The multiplicity of cortical regions supporting auditory language processing poses a mystery for researchers seeking to understand statistical learning from speech. Prior neuroimaging studies of ASL using event-related paradigms have examined the roles of specific auditory regions in isolation. How does the cortex integrate different functional regions like the primary auditory cortex, the superior temporal gyrus, and the inferior frontal gyrus during learning?

Unearthing evidence of functional integration of the cortex during auditory statistical learning is the goal of this investigation.

In this introduction to my study, I begin by highlighting the significance of ASL research and the significance of a functional connectivity approach to the ASL task. Next, I review relevant prior literature providing evidence about oscillatory activity related to the auditory statistical learning task and to functional integration of the cortex. I explain the key considerations for selecting functional connectivity (FC) metrics appropriate for assessing

cortical connectivity during an auditory statistical learning task. Finally, I delineate the core aims, research questions, hypotheses, and approach of my study.

The Significance of Understanding Auditory Statistical Learning from Speech

Auditory statistical learning is important topic for research because the ability is broadly relevant, not just to infants, but to people of all ages, and furthermore, understanding mechanisms supporting ASL may shed light on many other types of learning.

Auditory statistical learning is not only essential for early development (Kuhl, 2004), but important throughout the lifespan (Erickson & Thiessen, 2015; Sherman et al., 2020). Successful acquisition of language in the first year of life has long-term impacts on learning outcomes for children (Kuhl et al., 2005; Singh et al., 2012; Zhao et al., 2021); as a key cognitive ability allowing language acquisition, auditory statistical learning is important to non-invasively measure, evaluate, and facilitate – goals that require profound understanding at the neural level. ASL correlates with multiple language learning skills such as vocabulary development and second language acquisition (Frost et al., 2013; Singh et al., 2012) and deficits in SL have been associated with language impairments such as dyslexia (Gabay et al., 2015; Pavlidou et al., 2010).

ASL has both modality-specific and domain-general features, which means that understanding adaptation related to ASL opens a window to cortical plasticity broadly (L. J. Batterink et al., 2019; Fan et al., 2024). For example, a participant's ability to track transitional probabilities in an SL task depend upon the sensory processing required to encode and recognize the stimulus (Frost et al., 2019); inevitably, explorations of statistical learning prompt refinements to our knowledge of intersecting sensory, executive, and memory abilities. Moreover, statistical learning abilities in specific modalities relate to abilities in other modalities

and therefore have surprisingly broad implications; for example, visual statistical learning and language learning are correlated (Daltrozzo et al., 2017).

Neuroimaging indicators of statistical learning are especially desirable. Reliable online measures of statistical learning, e.g. measures derived from MEG signal, do not suffer from response confounds that impact offline measures (Siegelman et al., 2017) and are applicable to pre-verbal subjects like infants and adults recovering from stroke. Currently word segmentation measures do not offer high sensitivity and specificity for tracking ASL, and therefore more work is needed.

The Significance of Functional Connectivity Investigation of Statistical Learning

One area of word segmentation research that remains almost entirely unexplored is the role of functional connectivity during language learning. Auditory statistical learning from speech necessitates significant cortical functional integration for two reasons: first, like most language tasks, it requires sensory integration across auditory, visual, and motor modalities, and second, it requires expectation-related integration between sensory, memory, and executive regions.

Language is multimodal. For speech processing in particular, auditory, motor, and frontal areas all contribute, and these contributions must be integrated into a coherent whole (Ahveninen et al., 2006; Lau et al., 2008; Price, 2000). Functional connectivity analyses offer a way to explore the integration of auditory, visual, motor, and social regions of the brain during language processing, and multiple studies examining functional connectivity during various language tasks such as sentence processing, musical tone sequence learning, and verb generation have generated novel insights (Doesburg et al., 2016; Gaudet et al., 2020; Paraskevopoulos et al., 2017; Schoffelen et al., 2017).

Beyond multi-sensory integration, expectation-related functional connections ought to be prevalent during auditory statistical learning, as has been shown in visual statistical learning studies (Betti et al., 2021; Molinaro et al., 2016; Spaak & Lange, 2020). This process in known as predictive coding, and it necessitates inter-regional communication (Friston et al., 2015; Lewis et al., 2016).

While the motivation for expecting significant functional integration to occur during ASL is powerful, no investigations of electrophysiological functional connections during ASL currently exist. Does functional connectivity relate to event-related measures? When, where, and how do connections form? The mystery surrounding language learning integration begs for attention.

Oscillations in Auditory Statistical Learning

For language researchers seeking to understand how humans acquire language, the role of neural oscillations in supporting statistical learning in the auditory domain is important to understand, yet largely undetermined at present. Why study oscillations? The discovery of the alpha rhythm reported by Hans Berger in his seminal 1929 paper “The Electroencephalogram of Man” launched the discipline of electromagnetic functional imaging of the brain (La Vaque, 1999). Today, ongoing research continues to explore and explain oscillatory neural behavior and its significance for cognition for multiple reasons.

First, oscillations emerge from fundamental neural mechanics and therefore are an important indicator of neural function. While spike timing of individual neurons may seem largely stochastic, electromagnetic activity observed at the population level demonstrates the ubiquitous presence of neural oscillations (X.-J. Wang, 2010). Oscillations emerge from the interplay between excitatory and inhibitory neural connections (Buzsáki & Wang, 2012) as

populations of neurons get rhythmically inhibited and fire synchronously as inhibition decays (Siegel et al., 2012). Excitation, neural drive to fire, balanced by inhibition, preventing neural firing, regulate the timing of neural firing over ensembles of neurons, producing oscillations (Atallah & Scanziani, 2009; Siegel et al., 2000; X.-J. Wang, 2010). Neural timing matters because of time-related mechanisms that alter how neurons connect, interact, and sever their connections. Spike-timing dependent plasticity is an example of the importance of the timing of neural activations. As neurons fire over time, neural synaptic connections either strengthen via potentiation or decay through depression and the factor deciding whether a synaptic connection will strengthen or decay is the timing of when the pre- and postsynaptic neurons fire with respect to each other. If a presynaptic neuron fires slightly before the postsynaptic neuron (less than 20 ms), and the postsynaptic neuron fires after that, the strength of the synaptic connection is increased (i.e. the presynaptic neuron becomes more influential on the firing patterns of the postsynaptic neuron). On the other hand, if the postsynaptic neuron fires before the presynaptic neuron, the influence of the presynaptic neuron decreases. This is called spike-timing-dependent plasticity, and in this way, neurons strengthen or ignore their connections to each other by coordinating the timing of their firing. Inhibitory interneurons contribute significantly to the generation of neural rhythms by tapping the brakes to prevent pyramidal cells from firing for a brief period of time, allowing rhythmic firing patterns to emerge (Andrade-Talavera et al., 2023). Synchronous firing from many neurons generates large fluctuations in potential at the scalp and magnetic flux near the head.

These large fluctuations at the population level are readily observable with M/EEG (Hari & Puce, 2023). Modeling work at the microcircuit level gives insight into mechanisms for the generation of neural oscillations and the significance of neural oscillations for circuit function,

but how do these basic mechanisms relate to the cognitive tasks underlying language in the human brain? M/EEG detects summative activity across the whole brain, and this means that the signal is dominated by large neural ensembles in the preferred spatial orientation and location given the imaging modality. Therefore, M/EEG imaging provides an excellent platform for examining oscillatory cortical dynamics — in other words, how oscillations in large neural assemblies roughly localized to coarse-grained regions of the cortex relate to each other, to stimulus properties, and to subject behavior over time. Discriminable differences in the power or phase of neural oscillations are known to relate to cognitive and behavioral outcomes (Engel et al., 2001; Fries, 2015; Klimesch, 1999).

Because oscillations are an important avenue for insights about how the brain does what it does, oscillations offer a promising topic of investigation for auditory statistical learning. Statistical learning in the auditory domain, particularly from speech, is a core ability enabling language acquisition (Kabdebon et al., 2015; Kuhl, 2010; Saffran et al., 1996; Sanders et al., 2002). Historically, neuroimaging studies of statistical learning from speech have used tri-syllabic pseudowords in a continuous stream, eliminating prosodic and timing cues that separate words in order to test neural adaptation to statistical regularities alone (Frost et al., 2019). The key variable used by Saffran and subsequent language researchers was transitional probability between stimuli, the likelihood of one stimulus being succeeded by another. Over time, if statistical regularities are learned through exposure, participant response to low probability transitions should differ from participant response to high probability transitions. Event-related studies using M/EEG have demonstrated that neural responses to speech syllables differ as a function of transitional probability, and moreover that these differences emerge over the course of learning (Abla et al., 2008; Sanders et al., 2002; Teinonen & Huotilainen, 2012).

What role do oscillations play in supporting statistical learning in the auditory domain? So far, very little direct experimental evidence is available to answer this question, since most auditory statistical learning studies have been event-related (i.e. they examine transient responses time-locked to the onset of a stimulus averaged over multiple trials). However, hypotheses may be formed by drawing insights from related experiments. Several related lines of research contribute useful knowledge. First, domain-general cognitive abilities, such as attention, recruited during a statistical learning task will likely elicit modulations of oscillatory activity known to be related to the ability. Second, oscillatory modulations related to auditory processing will be present during an auditory statistical learning task. Third, predictive coding research in the auditory domain lends useful insight about modulations of oscillatory activity in response to expectations and probability. Oscillatory modulations during statistical learning in the visual domain may translate into the auditory domain or at least suggest directions for investigation. And finally, known relationships between oscillations and event-related transient waves may suggest trade-offs that may be present in SL paradigms.

Domain-General Oscillatory Roles

The fact that oscillations in the M/EEG signal arise from such basic neural mechanisms results in widespread detection of oscillatory activity and modulation across tasks in all sensory modalities and cognitive domains. Known oscillatory modulations associated with domain-general cognitive abilities, like attention, contribute to the electromagnetic signal evoked during language tasks. Therefore, an account of oscillatory dynamics during a specific task like auditory statistical learning starts with an acknowledgement of contributing domain-general influences. For auditory statistical learning research, as in studies of other cognitive abilities, the putative functional role of oscillatory activity depends on the frequency of the oscillation.

Sensory Processing

High frequency oscillations in the gamma band are considered to reflect the synchronization of neuronal assemblies during sensory processing in general. Fries proposed that presynaptic neurons entrain postsynaptic neurons with gamma-band oscillations and that this entrainment causes phase-based enhancement and inhibition of incoming signals. Specifically, he posited that postsynaptic neurons have enhanced responsivity to presynaptic neurons with which they synchronize (Fries, 2015). However, the degree of recruitment for processing of language inputs is dependent on several factors. For example, the predictability of the language input modulates the oscillatory response (in predictive contexts, expected language inputs result in reduced gamma power compared to incongruent inputs) (L. Wang et al., 2018).

Concept and Task Maintenance

Engel and Fries suggest that oscillations in the beta band, which are temporally appropriate for long-distance coordination between cortical regions, allow the brain to sustain ideas and tasks (Engel & Fries, 2010). Beta band oscillations are mostly well-known for involvement in motor processing; however, they are also thought to play a role in the maintenance of neurocognitive networks representing stimuli in general and have been shown to respond to language tasks in multiple contexts (Weiss & Mueller, 2012). This is a phenomenon found across multiple modalities; for example, Betti et al. found that beta band networks support the activation of stable priors that inform expectations during naturalistic scene viewing (Betti et al., 2021). Finally, beta has been shown to be related to memory (Hanslmayr et al., 2012). Together, these studies underline the importance of beta any task in which representations must be sustained over time.

Attentional Control

In the alpha band, oscillations inhibit unattended stimuli and help with selective attention. The classical view holds that alpha power increases result from the activation of inhibitory neurons during a task, which is supported by evidence indicating that alpha increases selectively in regions that are not activated in direct stimulus processing (for example, in ipsilateral visual regions compared to contralateral visual regions during hemifield tasks) (Klimesch, 2012). Alpha activity is associated with rhythmic GABA-ergic activity and inhibitory interneurons that help block unattended signal (Lozano-Soldevilla et al., 2014). Alpha power drops prior to an anticipated stimulus, and this drop is thought to reflect the onset of information retrieval (Foxe & Snyder, 2011). The classical view is complicated by evidence that alpha inhibition is related to task difficulty. For example, Wang et al. found that the attenuation of alpha power during stimulus processing in temporal and parietal cortical regions was associated with comprehension of sentences (P. Wang et al., 2022). Degree of alpha drop-out correlated with complexity of the sentences, which the authors attributed to increased excitability in functionally relevant regions due to task demands. Therefore, alpha modulations can be a key indicator of the engagement of attentional processes as well as cortical excitability due to effort.

Learning and Memory

Oscillations are known to change over time in response to learning and the consolidation of novel sequences or stimuli to memory. For example, theta power was shown to be lower following the introduction of novel words when compared to known words, and theta power was shown to increase to a level comparable to known words after novel words were committed to memory (Bakker-Marshall et al., 2018).

Auditory statistical learning paradigms involve all of the cognitive abilities listed above in some form, and therefore neural activity supporting the exercise of these cognitive abilities will contribute to the signal during a statistical learning task. However, these contributions may or may not be modulated by the primary experimental condition, the probability contrasts created by the paradigm. This must be determined experimentally.

Auditory Processing of Speech

During listening to language, oscillatory activity in the brain can be more precisely related to aspects of auditory processing. Importantly, oscillations are related to speech features such as the speech envelope, formant transitions, voicing, vocal pitch and intonation, in addition to higher order language processing tasks like semantic retrieval. Investigations into the relationship between oscillatory activity and speech processing are somewhat unique in that many speech processing studies focus on entrainment, or phase relationships between the stimulus signal and the neural signal, rather than simply power modulations in the neural signal. Oscillatory responses to speech processing will necessarily contribute during speech-based statistical paradigms and are therefore a potential target for modulation by the probability contrasts.

An important issue underlying auditory processing of language is that signal characteristics of heard speech align occur at rates that overlap with oscillatory brain signal, and brain signal has been found to be entrained to features of speech signals. Slow features of language such as the intonation contour of words and phrases occurs at 1-2 Hz, in the delta band range (Giraud & Poeppel, 2012). The acoustic envelope of speech modulates at the rate of the theta band, approximately 4-7 Hz. In higher frequency range, phonemic attributes such as formant transitions and voicing coding happen at rates between 30 - 50 Hz, corresponding to low

gamma frequencies. Giraud and Poeppel propose that endogenous delta, theta, and gamma oscillations in the primary auditory cortex work cooperatively to encode incoming auditory signal by discretization and grouping of spike trains. Specifically, they suggest that theta oscillations in superficial layers of the cortical column, together with gamma oscillators, sample spike trains in layer 4 of the cortex, generating discontinuous spike packages that are entrained to features of speech, tying them together across multiple time scales – for example, integrating phoneme features with intonation to represent the full information of the utterance.

Gross et al. generated experimental evidence supporting the role of oscillations in the delta, theta, and gamma bands in processing speech (Gross et al., 2013). In MEG recordings of participants listening to stories with a control condition of backwards-presented speech, the authors used mutual information to measure phase-locking in low frequencies to the speech envelope as well as cross-frequency coupling in the auditory cortex (theta phase modulating gamma amplitude). Both types of coupling were stronger for the story condition than the backward speech condition, showing that stimuli must be meaningful speech, not merely speech-like in terms of acoustic characteristics, to propagate oscillatory entrainment and nesting.

Phase-amplitude coupling in the auditory cortex is an essential process underlying language learning in infancy and in adults. Studies of infants have shown the importance of low-frequency tracking of the speech envelope. Infants have higher modulation energy in the delta band compared to adults as well as enhanced phase synchronization of delta and theta oscillations, corresponding to greater modulation energy found in infant directed speech (IDS) compared to adult-directed speech; in other words, speech directed to infants has exaggerated pitch contours to which cortical oscillations entrain, assisting with language acquisition. Attaheri et al. found that infants at 4 months of age already showed delta-band tracking of infant-directed

sung speech, and that theta entrainment emerged over the first year of development, statistically significant at the age of 11 months. Furthermore, significant coupling was observed between gamma and delta as well as gamma and theta bands (Attaheri et al., 2022). In adults, phase-amplitude coupling was shown to be critical for second-language learning. Lizarazu et al. found that phase-amplitude coupling in adult native Spanish speakers learning Basque was modulated by language proficiency and by speech intelligibility, while overall power in the gamma band did not differ by proficiency (Lizarazu et al., 2021). In other words, the cooperation between theta and gamma bands is essential for speech processing beyond the participation of the gamma band alone.

Low frequency oscillations, even without correlation to gamma amplitude, have been found to be predictive of word learning. Using a speech stream of 11 tri-syllabic pseudowords and EEG recordings, Batterink tracked phase-locking in the theta band using intertrial phase coherence over the course of learning (L. Batterink, 2020). She found that phase-locking to individual pseudo-words predicted behavioral indices of word learning, and she also found that phase locking increased over time at the rate of word presentations. Similarly, the theta band was also implicated in a study of word learning from a speech stream of nonsense words comparing musicians and non-musicians (Elmer et al., 2018). In this study, a connectivity metric called the Asymmetry Index, measured as the difference between left hemisphere and right hemisphere lagged coherence, in the dorsal auditory stream was shown to be significantly higher in more successful word learners (participants with high d prime values, indicating that they learned nonsense words from speech stream exposure). A review of functional connectivity studies in pediatric populations found that theta band coherence in the left hemisphere was widely associated with a range of measures of expressive and receptive language proficiency (Gaudet et

al., 2020). The authors noted increasing left lateralization of functional connectivity with age was associated with higher language ability, not only in theta but in higher frequency bands as well.

These studies show that language learning is associated with oscillatory phase modulation and coupling; however, the dependence of these responses on the semantic content of the material is unclear. Participants learning from an auditory statistical learning paradigm learn sets of associated syllables without semantic meaning, whereas infants and second language learners are exposed to semantic indicators as well as probabilistic segmentation information during learning. Experimentation is needed to determine which responses arise from perceived syllable groupings alone and which are associated with semantic operations.

Other oscillatory modulations associated with speech processing represent potential experimental confounds. Basic acoustical differences in speech elicit oscillations in the canonical oscillatory bands; for example, auditory processing of pitch information elicits cortical gamma oscillations. Ross et al found that cortical gamma oscillations modulate to follow the pitch contours of speech during listening to spoken syllables (Ross et al., 2020). Poor controls in the construction of the speech stream could potentially result in confounds that obscure the true nature of the oscillatory response to statistics in the speech stream. For example, systematic differences in the pitch of onset and medial syllables in tri-syllabic pseudowords could result in oscillatory differences due to pitch characteristics rather than to transitional probability characteristics. Checking acoustical features of the speech stream to ensure equality between probability conditions is an essential step to ensure that modulations of the oscillatory response in an auditory statistical learning experiment are truly due to neural adaptation to probability.

Oscillations and Probability, Expectation, and Prediction

Literature on oscillatory responses to probability contrasts in the context of auditory statistical learning from speech streams is extremely limited. However, indirect evidence from other branches of research offer insight into oscillations and statistical learning.

Auditory Paradigms that Manipulate Probability or Expectation

First, significant research has demonstrated oscillatory responses to auditory paradigms that manipulate probability. Multiple studies have reported that power in alpha and beta bands drops following a stimulus that violates expectations. Lam et al. investigated band-limited response to sentence processing in Dutch-speaking young adults, comparing word processing between sentences and words lists in addition to comparing words in early parts of the sentence to words in later parts of the sentence to examine the contribution of additive predictability afforded by sentence context. They compared oscillatory power following words in a word list to words in a sentence and found significantly different results in theta, alpha, beta, low gamma and high gamma bands. Theta, alpha and beta bands had reduced power for sentences than for word lists, whereas in the low gamma band, higher power for sentences was shown in left temporal and frontal regions. Furthermore, early and late sentence contexts showed significant effects in theta, alpha, and beta bands that varied in direction by region of interest. The authors interpreted lower power, particularly in anterior temporal regions, during sentences and particularly the late parts of sentences, as indicating less effortful lexical retrieval due to the facilitatory effect of sentence context (Lam et al., 2016). Wang et al. found that beta power dropped lower following incongruent sentence endings compared to congruent sentence endings (L. Wang et al., 2012). Armeni et al. found that beta power dropped lower following high perplexity words during auditory story listening compared to low perplexity words (Armeni et al., 2019). High entropy

words in the same paradigm were followed by lower beta power and increased theta power. Beta power modulates during violations of syntax (Bastiaansen et al., 2010; Davidson & Indefrey, 2007). Beta power modulates to semantic incongruities (Kielar et al., 2014; Luo et al., 2010; L. Wang et al., 2012), and theta power has also been shown to respond to semantic violations at the end of sentences (Pu et al., 2020). Syntactically intact sentences result in an increase in beta power compared both to sentences with syntactic violations and to word lists (Bastiaansen & Hagoort, 2015). The bulk of these studies of probability use syntactic structure and semantic content of sentences to create the probability contexts in which participants' expectations are either fulfilled or violated. It is unclear whether participant expectations based on syllable order are enough to elicit similar responses in the absence of semantic information.

Research on the neural basis of predictive coding offers multiple insights relevant to statistical learning. Predictive coding is a theoretical mechanism of cognition centered on the ability of the brain to generate predictions about the environment based on incoming sensory input and then compare input to predictions (Bastos et al., 2012). Predictive coding in the context of auditory language processing is reflected in multiple aspects of the neural response. Lewis et al examined the effect of expectation on beta oscillations during sentence comprehension. Lewis hypothesized that beta oscillations within a neurocognitive network associated with the maintenance of a concept should increase from higher to lower levels of the processing network during processing of a highly predictable stimulus and decrease during network changes. In this sense, beta oscillations are a signature of top-down predictions at a neural level. Lewis et al constructed sentences in which an auxiliary verb could refer to one of two referents, a standard reference (subject-relative condition) and one unexpected or uncommon (object-relative condition). Auxiliary verbs could be singular or plural, which differentiates the two grammatical

conditions such that Dutch readers expect the common referent, but are sometimes cued to the unexpected referent following the presentation of the auxiliary verb. Lewis et al found that beta power decreased following auxiliary verbs in the unexpected object-relative condition, which the authors interpreted as evidence that the neurocognitive network supporting the processing of the sentence underwent change following the introduction of an unexpected linguistic cue (Lewis et al., 2016). In support of this view, multiple studies have found that increased syntactic complexity results in greater beta power (Bastiaansen & Hagoort, 2006; Muller & Meyer, 2014). Beta oscillations may similarly offer a mechanism for predictive coding based on probability information in a speech stream made of pseudowords. If so, it should emerge over the course of learning.

While most of the studies above examined oscillatory responses after the introduction of the stimulus, there has also been evidence for anticipatory modulations of oscillatory power prior to stimulus onset using auditory stimuli. For example, Gastaldon et al. found that beta power was lower prior to predictable end words in sentences compared to unpredictable end words in sentences (Gastaldon et al., 2020). Therefore, it is necessary to examine both pre- and post-stimulus windows for potential effects. Since post-stimulus band-limited power is usually calculated with a baseline period, traditionally in a window from 200 to 50 ms before the onset of the stimulus to stimulus onset, anticipatory effects represent an important potential confound to the calculation of power modulations (Pfurtscheller & Lopes da Silva, 1999). Short interstimulus intervals between syllables in a speech stream may conflate processing and anticipatory effects, which may limit the interpretation of study results.

Visual Statistical Learning

Aside from auditory paradigms that manipulate expectation or probability, statistical learning paradigms in the visual modality offer insight into the potential role of oscillations to auditory statistical learning. In the visual domain, more work has focused on anticipatory activity in windows preceding the onset of a stimulus. For example, using a visual statistical paradigm with triplet sequences of stimuli, Bogaerts et al. found that beta power in the significant beta-range cluster revealed significantly higher power for the interval preceding a triplet transition compared to intervals within triplets (Bogaerts et al., 2020). Altamura et al found that oscillatory activity in the alpha and beta bands modulated in a 500 ms window prior to stimulus onset under a visual-motor paradigm manipulating the probability of trial types (Altamura et al., 2014). In this study, poor statistical learners with small reaction time differences demonstrated greater alpha power, while strong statistical learners had anticipatory dampening of the alpha and beta rhythms prior to probable events in the contralateral motor cortex, anterior cingulate, inferior frontal gyrus and the caudate.

Studies examining oscillatory responses after stimulus onset also found modulations of band-limited power when using visual stimuli. Meindertsma et al used a visual statistical learning paradigm to manipulate stimulus surprise and found that more surprising events were associated with reduced power in the beta band in parietal and prefrontal cortices (Meindertsma et al., 2018). Roehe et al found that gamma power increased following the presentation of random images compared to expected images, whereas alpha and beta power increased following the onset of a predictive stimulus but prior to the stimulus that it predicted (Roehe et al., 2021). Since power for expected images was increased relative to random images, an alternate interpretation of the findings would be that random stimuli were followed by greater drop-out for

alpha and beta. However, not all visual SL paradigms associated mid-frequency drop-out with the violation of expectations. Zhou et al found that alpha power increased following presentation of unexpected images in the occipito-temporal cortex (Zhou et al., 2020). In that paradigm, high probability pairs and low probability pairs were trained, then on the subsequent day, expected pairs were presented along with violation trials where the trailing images were unexpected given the training from the day before. Images that violated expectation resulted in significantly increased alpha power from the onset of the violation image for about 400 milliseconds.

Results have also been found in the theta band for visual SL paradigms. Spaak et al found that theta power is responsive to statistical probability using a visual statistical learning paradigm (Spaak & Lange, 2020). In this experiment, participants searched for a target letter T, which was probabilistically likely to occur in characteristic locations, but occasionally appeared in unexpected locations (violation trials). Theta power following the onset of images in expected locations was greater than following the onset of violation locations in superior frontal regions. Tóth et al examined functional connectivity in connection with a visual statistical learning task with a button press response (Tóth et al., 2017). Reaction times for the button press reflect statistical learning, as high probability events should result in reduced reaction times for strong statistical learners. Phase lag index as the metric of connectivity in sensor space using groups of channels clustered into 13 regions of interest showed that reduced frontal functional connectivity in theta and beta bands correlated with better statistical learning.

Auditory Statistical Learning: ERPs and Oscillations

Evidence of oscillatory contributions to auditory statistical learning is scarce since most M/EEG studies of auditory statistical learning have used event-related paradigms. However, there are known associations between ERP properties and oscillatory activity; therefore, ERP

studies themselves offer some indirect suggestions. For example, Davidson and Indefrey showed that expectation violations during language processing resulted in higher amplitude event-related potentials and lower-amplitude oscillations, particularly in the alpha and beta bands. They found an inverse relationship between oscillatory and ERP amplitude in late time windows following stimulus presentation (Davidson & Indefrey, 2007). Similarly, Wang et al. found that late waves in event related fields increased in amplitude in response to semantic incongruities while oscillations in the beta band showed suppressed power (L. Wang et al., 2012). The authors localized the drop in beta power to the left inferior frontal gyrus, and they interpreted the trade-off between transient and oscillatory amplitudes to reflect more effortful processing of incongruencies.

Daikoku et al found that early waves, termed P1m and N1m, are modulated in amplitude and latency by the transitional probability of the auditory stimulus. High probability transitions are followed by attenuated P1m and N1m waves with low latency, whereas low probability transitions are followed by slightly slower, higher amplitude P1m and N1m waves. The authors interpreted the attenuated response to predictable stimuli as a reduction in neural recruitment to predictable stimuli (Daikoku et al., 2017). Similarly, Teinonen et al found that the amplitude of the 100 ms response was lowest for high transitional probability medial syllables in tri-syllabic pseudowords. Teinonen et al also found that responses from 380-420 ms had enhanced amplitude when syllables were unexpected (Teinonen & Huotilainen, 2012). Pairing these findings with other findings showing that mid-frequency oscillations in the alpha and beta bands drop-out during high level recruitment resulting in high-amplitude event-related waves, the natural suggestion is that mid-frequency oscillations and event-related waves should maintain an inverse relationship in amplitude during an auditory statistical learning paradigm.

Implications for the Current Study: Oscillatory Dynamics to Expect

Based on findings reviewed above, several points about oscillatory activity likely to occur during an ASL paradigm are worth noting. First, unpredictable moments in a speech stream ought to elicit increased recruitment or activation, as this is a common response to language paradigms that create high entropy trials. In contrast, moments of heightened predictability ought to cause response suppression. This general pattern of response comes with a caveat, however: variations in subject attention may alter typical response patterns expected during implicit learning (Kok et al., 2012), representing a potential confound to detection of implicit learning. Fortunately, confounds from oscillatory dynamics responding solely to the acoustic features of speech syllables ought to be washed out in trial averages of onset and medial syllables. A known oscillatory phenomenon induced by pseudo-word learning is that phase-locking across multiple oscillatory frequencies occurs at word onsets (L. Batterink, 2020; Gross et al., 2013). Because phase-resets at onsets can impact band-limited oscillatory power, measures based on band-limited power envelopes must be viewed as incorporating phasal influences. Finally, it is important to remember that prior studies of oscillatory power indicating timing of power modulations are a valuable source of insight, but peak power within a single cortical region may not temporally align with periods of maximal coupling between distant regions. Therefore, the timing of oscillatory information transfer may vary significantly from the timing of power modulations; the relationship between the two must be tested experimentally.

Functional Connectivity for Auditory Statistical Learning

When testing for oscillatory functional coupling during a cognitive task, appropriate methods for FC estimation may vary depending on the research question and the degree of prior knowledge about the paradigm. From initial exploratory efforts to targeted tests of directed

influence, methodological choices must navigate known confounds that impact FC estimation from electrophysiological recordings.

Descriptive Functional Connectivity: Associations Between Signals

The goal of exploratory research – to uncover previously unknown patterns, relationships, and associations between phenomena of interest – is perhaps the most common motivation for connectivity studies over the past two decades, as connectomics as a discipline has been in its infancy (Rossini et al., 2019). Exploratory connectivity studies aim to demonstrate associations between signals and to show behavioral or cognitive relevance of those associations. Successful exploratory connectivity studies should produce connectivity estimates with high descriptive validity. In other words, the estimate should faithfully reflect properties of the neural activity being studied, not artifacts of the environment or imaging device. There are multiple aspects of estimation to consider when evaluating the descriptive validity of a study. Is the connectivity metric appropriate in the type of signal relationship assessed, its temporal or frequency domain, its dimensionality, and temporal scale? Is it likely to reflect neural activity rather than volume conduction or field spread? If connectivity estimation is performed in source space, are the inversion and source space properties appropriate to the type of signal relationships tracked? Methodological choices by the researcher must take all of these factors into account.

Types of Functional Relationships

The simplest scenario for connectivity estimation uses bi-variate measures of statistical dependency between two or more signals. Statistical dependencies may be measured via phase, amplitude, or phase-amplitude relationships between signals (van Diessen et al., 2015; Wei et al., 2021). Theoretically, the goal of measuring phase relationships between regions is to assess

synchronization between cell assemblies, since regional communication is hypothesized to be dependent on synchronization between neural groups (Marzetti et al., 2019). Effects of an incoming signal are thought to be enhanced if the receiving population is in a favorable phase of the oscillation, and therefore oscillatory synchronization and maintenance of the enhancing or attenuating phase relationship must be maintained across an ensemble to a measurable degree. However, measurement of oscillatory phase relationships using non-invasive devices like M/EEG is difficult for multiple reasons, the foremost reasons being field spread and volume conduction effects on the signal (Schoffelen & Gross, 2009). Alternatives to phase-based connectivity include amplitude-based measures and phase-amplitude based measures. Amplitude-based measures, such as amplitude envelope correlations, measure correlations in modulations of the amplitude of the oscillatory signal, working under the assumption that transient increases and decreases in the amplitude of an oscillation across regions may be indicative of functional integration (Tewarie, Hunt, et al., 2019). In contrast, phase-amplitude measures examine connections between low and high frequency oscillations, under the premise that the phase of low frequency oscillators, for instance, in the theta band, modulate the amplitude of high frequency oscillations, for instance in the gamma band (Gross et al., 2013). Each of these measures targets a different mechanism or set of mechanisms by which functional integration of brain regions might occur, and each measure comes with a set of unique challenges for measurement from a whole-head device like M/EEG. Some measures do not entirely separate phase and amplitude influences on the estimation of connectivity; coherence and weighted Phase Lag Index are examples of connectivity metrics that include amplitude information in the connectivity estimation (Bastos & Schoffelen, 2016; Vinck et al., 2011). Therefore, the

researcher must carefully consider what mechanism or set of mechanisms should be captured by the connectivity metric when choosing methods for connectivity estimation.

Frequency or time domain

Even within a given category of connectivity measures, such phase-based measures, specific measures may differ in whether they operate in the frequency or time domain. Some metrics are based on the time series of the signal; in contrast, frequency-based metrics such as phase-locking value, transform the signal into the frequency domain and then probe relationships between two regions (Bastos & Schoffelen, 2016). Furthermore, metrics may be sensitive to either linear or non-linear relationships between signals (Schoffelen & Gross, 2009). For example, coherence, a popular phase-based measure unfortunately subject to strong effects from volume conduction, is a linear measure whereas phase-locking value is not. Since nonlinear phenomena like action potentials are known to be common to neural behavior, measures that are insensitive to non-linear relations between signals may not be desired.

Dimensionality

Connectivity metrics are traditionally bivariate; an association with one dimension is assessed between two signals. However, some metrics, such as the directed transfer function, allow for multi-dimensional associations between signals (Basti et al., 2020). Multi-dimensional connectivity measures are an advantage when the relationship between two regions cannot be captured along a single dimension. For example, if time series between two labels in a parcellation are considered, sources within the aggregate label may have differing connectivity from each other, leading to a situation where multi-dimensional connectivity estimates may more adequately capture complex dynamics between two labels.

Temporal Scale

Some connectivity measures are only sensitive to connectivity at a certain time scale, and temporal scale relevant to the task or behavior of interest must be considered when choosing a connectivity measure (Liuzzi et al., 2019). For example, amplitude envelope correlations measure slow fluctuations in the envelopes of the periodic components of the signals at a rate of 1 Hz or less (Godfrey & Singh, 2021). When measuring with amplitude envelope correlations, underlying connectivity states that are more transient in nature may be missed by such a metric. Static connectivity approaches assume that regional connections are stable over time, whereas dynamic connectivity approaches assume that functional regions of the brain flexibly reconfigure their networks given changing cognitive demands (Baker et al., 2014). One way to capture changes in connectivity is to calculate traditional connectivity metrics within a sliding window to estimate a temporal progression of connectivity between two or more regions. However, there are limitations to the resolution provided by this approach. Simulation work from Liuzzi et al showed that conventional connectivity metrics – specifically, coherence, imaginary part of coherence, phase locking value, phase lag index, and amplitude envelope correlations – are only able to estimate connectivity when the duration of the underlying connected state is of relatively long duration, i.e. 1 second or more (Liuzzi et al., 2019). When they tested transient states lasting only 200 ms, the authors found that conventional metrics performed poorly at detecting connectivity, even with relatively long window lengths. Other connectivity approaches, such as the instantaneous amplitude correlation, offer improved temporal resolution down to the order to 100 ms state durations (Tewarie, Liuzzi, et al., 2019). However, such approaches can be prohibitively computationally expensive, requiring either down-sampling by use of techniques such as recurrence plots to temporally window data around relevant states, or else by simply

limiting the data used for each subject. For some studies, such as resting state studies, slow connectivity estimates may be stable and useful for the desired connectivity estimates, but for rapid cognitive processes such as language processing, metrics that are sensitive to connectivity on a short time scale may be preferred.

Volume Conduction Sensitivity

Perhaps the most important consideration for successful connectivity estimation with M/EEG is the influence of volume conduction (Sakkalis, 2011; Schoffelen & Gross, 2009). Activity from a single current dipole is reflected in measurements of multiple sensors in a whole-head system. For electrical potential, differing conductivities of the pial and dural surfaces, CSF, skull, and skin cause spatial smearing of potential at the surface of the head where electrodes are located, while for MEG, magnetometers and gradiometers detect a linear mixture of the flux changes from all sources with fields that project into the subspace to which the sensor is sensitive (Hari & Puce, 2023). Therefore, relationships between signals from individual sensors may not be considered to reflect underlying connectivity without controlling for the influence of field spread and volume conduction. Generally, there are two ways to control for volume conduction and field spread: first, metrics that inherently exclude volume conducted signal may be employed, or second, conduction effects can be remedied by a number of techniques such as source localization (i.e. the measured signal can be source localized and connectivity computed in source space) or signal orthogonalization (Bastos & Schoffelen, 2016). Even when techniques for limiting the effects of field spread have been employed, there can be residual imperfections in connectivity estimation; therefore, conclusions about source localized connectivity must be treated with appropriate caution (Palva et al., 2018).

Considerations for Connectivity in Source Space

When connectivity analyses are conducted in source space to combat the effects of volume conduction, the choice of inversion method may significantly affect the outcome of the estimation of connectivity (Hincapié et al., 2017). Commonly, measured signals from M/EEG are first inverted to generate time courses for specific voxels, cortical labels, or dipolar source locations from a chosen source space, and connectivity metrics are calculated after the inversion process. However, assumptions made during the inversion process impact connectivity estimation. For example, beamformers assume that sources are uncorrelated during the inversion step, whereas minimum norm solutions do not (Hillebrand & Barnes, 2005). For point-like sources, beamformers can successfully estimate connectivity, but for patch-like sources, the assumption of uncorrelation results in signal cancellation when using beamformers and underestimation of connectivity (Hincapié et al., 2017). On the other hand, when using MNE, connectivity may be overestimated due to spatial smoothing of the inverse, particularly for small adjacent labels (Tait et al., 2021). One way to help combat imperfections in the inversion process is to include a baseline connectivity state for comparison against experimental conditions (Bastos & Schoffelen, 2016)

Furthermore, the choice of source space for connectivity calculation significantly affects the estimation of connectivity in several ways. Limitations to the fundamental spatial resolution of EEG and MEG must be considered when choosing a source space. Spatial resolution of these devices is dependent on several factors, including the number of sensors, the type of measurement rendered by the sensor (scalar potential vs field gradients), and factors that affect SNR such as source depth and orientation (Hauk et al., 2011; Hauk & Stenroos, 2014; Lin et al., 2006). Even though some source localization methods are able to achieve very low localization

error values, on the order of 3 mm (Jaiswal et al., 2020), spatial diffuseness of sources must be taken into account when considering the resolution of M/EEG. Hauk et al. investigated the spatial resolution of commonly used inverse methods for M/EEG and found that measures of mean spatial deviation, calculated from point spread and cross talk functions describing signal leakage from nearby sources, bottomed out at 2.6 cm (Hauk et al., 2022). On the other hand, when more sources are used than sensors available in the measurement, the resulting inversion matrix is rank deficient, which prohibits some techniques for combatting volume conductions, such as symmetric orthogonalization (Tait et al., 2021). Additionally, SNR varies across cortical locations for MEG due to dependence of MEG on tangential currents and sensitivity to source depth (Bastos & Schoffelen, 2016). Small labels or single dipolar sources may significantly vary in SNR, which can confound connectivity estimation, particularly for measures that are fully or partially amplitude dependent. Therefore, parcellation schemes with very small labels may not be desired. On the other hand, activity estimates averaged over large labels that stretch across multiple gyri and sulci may be affected by signal cancellation (Khan et al., 2018). Therefore, labels also should not be too large. Tait et al proposed a variant of Human Connectome Project atlas published by Glasser et al. (Glasser et al., 2016) optimized for MEG by combining labels in regions with low SNR and low spatial resolution (Tait et al., 2021). Whether using this or other sources spaces, potential confounds in connectivity estimation must be checked.

Prediction and Classification: Meaningful Functional Networks

Classifying subjects based on connectivity measurements is a common goal for many researchers that requires sophistication above and beyond descriptive connectivity studies.

Reliability, Repeatability, Reproducibility

For subject classification studies, the reliability and repeatability of the metrics used for classification is important, and many connectivity metrics perform poorly in terms of repeatability. Colclough et al. tested a selection of phase and amplitude-based connectivity metrics including phase-lag index, weighted phase-lag index, phase-locking value, phase slope index, mutual information, coherence, imaginary coherence, partial coherence, imaginary partial coherence, partial directed coherence, amplitude envelope correlations, partial amplitude envelope correlations, and orthogonalized amplitude envelope correlations. The authors found that amplitude envelope correlations are the most reliable connectivity metric across measurement time points (Colclough et al., 2016). In particular, within-subject repeatability was poor for most metrics. For example, the edge strengths of networks derived from PLI, wPLI, and ImCoh from three repeated resting state measurements from the same subject varied greatly across measurements, such that the median correlation between edge strengths across measurements was rho=0.3. When connectivity estimates are unstable between measurement time points, the goal of subject classification may not be achievable. Repeated measures in pediatric or adolescent populations face additional challenges; changing head size, for example, can change the signal-to-noise ratio of cortical regions unequally across cortical regions in MEG (Hunt et al., 2019). Therefore, even stable connectivity measures may require additional checks to ensure that changes assessed across timepoints are not artifactual.

Discriminative Features of Networks

Furthermore, care must be exercised when differentiating which connections are important for classification studies. Often, connectivity studies focus on regions with strong connections or a high volume of connections, known as “hubs” (Khan et al., 2022; Youssofzadeh

et al., 2017; Youssofzadeh & Babajani-Feremi, 2019). Yet low values of statistical association in functional connectivity do not necessarily imply that the association is spurious or insignificant. In fact, some disease states of interest may be detectable via changes in weak connections rather than changes in strong connections (Bassett et al., 2012).

Sometimes, contrasts between groups may be reliable and discriminative, yet ultimately turn out to be spurious because of inadequate controls rather than actual functional network differences. There are several ways to accidentally wind up with spurious connectivity contrasts between groups. For example, if epoch counts are unequal between groups, signal-to-noise ratio may be unequal between the groups, and this will affect connectivity estimates since many connectivity measures are sensitive to added noise (van Diessen et al., 2015). If physiological artifacts are not properly addressed, this could also induce spurious connectivity contrasts, if for example, one group blinks more frequently than another, global functional connectivity estimates may be affected and network properties as well (Ghaderi et al., 2018). These are common challenges in clinical populations and developmental research, since age and disease effects introduce differences in protocol compliance, movement, and standard physiological artifacts that must be considered when computing connectivity. When contrasting groups, care must be exercised to ensure that differences in group estimates are not due to artifacts, noise differences, or other sources of variability that do not reflect neural connectivity.

Causal Mechanisms: Effective Connectivity and Modeling

Beyond description and prediction, connectivity research ultimately seeks to explain the mechanisms underlying cognition, and this goal requires the most sophistication in terms of experimental design and analysis.

Effective / Directed Connectivity

To go beyond descriptions of statistical association and explain how parts of the brain influence each other, researchers need to differentiate directions of influence, for example from one hemisphere to another, or from frontal or executive regions to sensory regions (Friston, 2011). For such analyses, researchers must choose connectivity measures that allow for indicating the direction of influence. Directed connectivity metrics like partial directed coherence were originally developed for use with implanted electrode arrays; later these metrics were adopted for use with whole-head imaging data (Schelter et al., 2006). However, there are multiple potential confounds for directional connectivity metrics that are commonly used in M/EEG, including directed partial coherence, Granger causality, and the directed transfer function. Granger causality, for example, is significantly affected by volume conduction and noise, and source localization is insufficient for alleviating the effects of signal leakage, which confounds the estimation of influence (Bastos & Schoffelen, 2016; Vinck et al., 2015). Some methods, such as directed phase-lag index, that are relatively insensitive to the effects of volume conduction, are problematized by an inability to estimate bi-directional influences in contexts where regions of interest may have mutual or alternating influence.

Models for Hypothesis Testing

Using M/EEG alone, researchers can alter the stimuli or task assigned during recording, but not the brain itself (Rossini et al., 2019). Without direct control of the networks being studied, causal inference can be made by constructing a model and predicting the outcomes of variations in model parameters, then testing whether the actual observed data matches the model's predictions (Battaglia & Brovelli, 2020). Models may be data-driven or based on theory (Bassett et al., 2018). Exploratory descriptive work laying a foundation for testable models is

fundamental for causal inference in connectivity studies. Once sufficient evidence has been collected to justify a model choice, then perturbations (changing experimental conditions or tasks) can be used to probe the correspondence between model predictions and observed data. Researchers must be cautious about drawing causal inference from studies that were designed to be descriptive beforehand.

Confounds to Causal Influence

An inevitable complicating factor in the estimation of causal influence from one region of the brain to another is that brainstem nuclei project to multiple cortical regions, yet signal from whole-head imaging instruments is most sensitive to nearby, i.e. cortical, regions (since signal decays according to the square of distance for EEG or the cube of distance for MEG). Brain activity from deep regions, even if not entirely parameterized out of activity estimation during source inversion, picks up more noise during measurement than cortical regions, and the differing SNR of deep and cortical sources confounds the estimation of influence, particularly for methods that are sensitive to the addition of noise (Bastos & Schoffelen, 2016). While statistical association between cortical regions is easy to demonstrate in a descriptive analysis, causal inference is quite difficult to nail down when brainstem modulation of multiple cortical areas is both highly plausible and highly tricky to capture in connectivity estimates.

Choosing an Approach: Key Factors for the Current Investigation

Connectivity methods for successfully detecting functional integration of the cortex during auditory statistical learning in adults and adolescents must overcome some key obstacles. First, techniques for FC investigation must be suitable for exploratory analysis. For this purpose, robust, non-directed FC methods with evidence of good reliability are preferred. Second, methods must be appropriate for a pediatric population. Children and adolescents move during

data acquisition, head sizes change over the course of development, and protocol compliance fluctuates more than in adults. Therefore, FC methods sensitive to SNR variation should not be employed; additionally, rank reduction due to movement compensation with Maxwell filtering must be acceptable. Third, connectivity calculation should be sensitive to modulations expected due to the time scale of the stimulus. Fourth, methods should be amenable to future clinical and translational work, or in other words, replicability of results is important. The two methods that best suit the above criteria are both amplitude-based measures. The first, amplitude envelope correlations (AEC) is a well-known technique with strong repeatability, good robusticity to inter-individual variability, and an established history of results for comparison. The second method, the instantaneous amplitude correlation, is a newer measure developed to be sensitive to short connectivity states. While reproducibility studies of IAC have not yet been published, this measure was chosen for improved sensitivity to rapid oscillatory changes.

Overview of the Current Investigation

Core Aims

This analysis explores techniques for estimating amplitude-based connectivity during auditory statistical learning to examine the effects of temporal resolution on network estimation and explore associations between network characteristics and response to transitional probability in a speech stream. There are essentially two fundamental questions that I am probing. The first is a question of description — what do functional networks during auditory statistical learning look like? More specifically, what networks emerge when connectivity metric sensitive to slow modulation are applied and averaged over the whole recording using a “static” network approach? How do these compare to networks derived using a high temporal resolution technique? The second question is one of association — do these networks have a relationship

with event-related neural adaptation to transitional probability in a speech stream? Do high-temporal resolution networks adapt to the predictability of stimuli like transient responses or do they remain relatively constant? And finally, do network features predict auditory statistical learning? The ultimate objective of this inquiry is to advance the validity, sensitivity, and precision of neuroimaging measures of basic learning mechanisms.

Research Questions and Hypotheses

1. **Is functional connectivity measured by amplitude envelope correlations related to auditory statistical learning?**
    a. Characterize connectivity using AECs and describe functional networks during auditory statistical learning.
    b. Use support vector regression to predict event-related adaptation to transitional probability, the N400 difference. Null hypothesis: There's no relationship between AEC network characteristics and event-related responses.
    c. Use support vector regression to predict learning using network characteristics. Null hypothesis: There's no relationship between AEC network characteristics and statistical learning.
2. **Is functional connectivity measured by the instantaneous amplitude correlation related to auditory statistical learning?**
    a. Characterize dynamic connectivity networks using instantaneous amplitude correlation and describe connectivity between onset and medial syllables. Characterize spatial and temporal characteristics of edge differences between transitional probability conditions.

b. Use support vector regression to predict event-related responses to transitional probability. Null hypothesis: There's no relationship between dynamic network characteristics and event-related responses.
c. Use support vector regression to predict learning using IAC networks. Null hypothesis: There's no relationship between dynamic network characteristics and statistical learning.

Summary of Exploratory Approach

Two methods of FC estimation, AEC and IAC, are applied to a pre-existing data set consisting of MEG recordings of 107 adolescents and 30 adults performing inattentive auditory statistical learning. MEG recordings are cleaned of environmental noise and physiological artifacts; movement-compensation is applied. Data are source localized using the eLORETA inverse method and band-pass filtered into canonical bands, theta (4-7 Hz), alpha (8-12 Hz), low beta (13-18 Hz), high beta (19-30 Hz), and low gamma (31-55 Hz). Following pairwise-orthogonalization, FC is estimated in source space within cortical parcels of the Desikan-Kiliany atlas. Weighted adjacency matrices representing functional networks for each method are derived from edge measures. Two nodal graph theory metrics, node strength and eigenvector centrality, are calculated from weighted networks. First-order statistics are calculated for mean edge strength by cortical label, group mean node strength for each cortical label, and group mean eigenvector centrality for each cortical label. Network hubs and strongest edges are reported for both adolescent and adult populations. Support vector machines are used to test associations between functional networks and two outcomes of interest: first, the amplitude of the difference between N400 event-related responses to onset and medial syllables; second, scores from behavioral testing of statistical learning in adolescents.

Chapter 2: The Gen-Z Study

MEG recordings of auditory statistical learning that form the basis for the current investigation were drawn from an existing dataset originally collected as part of a large adolescent neuroimaging study conducted by the Institute for Learning and Brain Sciences at the University of Washington. The Gen-Z study was an ambitious, multi-faceted study of adolescent learning and development that combined structural and functional neuroimaging measures with behavioral measures of social-emotional, affective, and learning outcomes. The subset of data used for my investigation primarily draws from MEG recordings of auditory statistical learning but also includes structural T1-weighted MRIs collected for adolescent participants.

MEG recordings obtained for the Genz study and included in my analysis come from two populations. Recordings from a group of adult subjects engaged in auditory statistical learning provide a pilot cohort for my analysis. With 30 high SNR recordings from mature learners, adult participant recordings establish a low noise test group with relative consistency across subjects due to low variation in age, but a smaller sample pool than desired for robust machine learning results. The adolescent participant pool is comparatively large, containing 107 successful data sets spread across age cohorts ranging from 9 to 17 years old. The size of the adolescent recording collection allows for the application of machine learning techniques to the pool with confidence but necessarily included high developmental variability between subjects due to progressing pubescence.

Because of the expense of acquiring both MEG and MRI imaging for participants, few neuroimaging studies have a sufficiently large sample size to conduct source space connectivity analysis with adequate power for ML techniques. The Gen-Z data set provides a rare and exceptional opportunity to conduct an FC inquiry.

Participants

The Gen-Z study was approved by the University of Washington Human Subjects Institutional Review Board and conducted in accordance with the Declaration of Helsinki. Written informed consent was obtained from all participants and from participant guardians in the case of adolescent participants.

Adult Participants

32 typically developing adult subjects (16 female) were recruited for the study and were administered the protocol. Inclusion criteria were that subjects must be monolingual, native English speakers, and right-handed as assessed by a score of 80% or more on the Edinburgh Handedness Scale. Subjects were excluded if they had a history of neurological, psychiatric, learning, or speech and hearing disorders, or had non-removable body metal such that they could not safely participate in an MRI. One data set was discarded due to excessive noise in the MEG recording, and one data set was excluded due to a technical malfunction during MEG data acquisition, leaving 30 successful data sets in the final analysis.

Adolescent Participants

167 adolescents (81 female) were originally recruited in five age cohorts with initial ages of 9, 11, 13, 15, and 17 years. Inclusion criteria were that subjects must be monolingual, native English speakers, and right-handed as assessed by a score of 80% or more on the Edinburgh Handedness Scale. Subjects were excluded if they had a history of neurological, psychiatric, learning, or speech and hearing disorders, or had non-removable body metal such that they could not safely participate in an MRI. 59 data sets were excluded from analysis overall; 38 data sets were excluded due to technical errors during acquisition; 13 data sets were excluded due to

excessive noise during the recording (typically from orthodontia); 8 data sets were excluded due to attrition either from subject drop out or non-participation in data acquisition, or from diagnosis of disqualifying conditions after recruitment. 107 data sets (54 female) were included in the final analysis.

Data Acquisition

MEG Data Acquisition

All recordings were collected inside a magnetically shielded room at the Institute for Learning and Brain Science (ILABS) at the University of Washington. For adolescent participants, data were recorded with a MEGIN (formerly Elekta Neuromag) 306-channel whole-head magnetoencephalography system (VectorView™, Elekta Neuromag Oy, Helsinki, Finland). For adult participants, data were recorded with a MEGIN Triux Neo™ 306-channel whole-head magnetoencephalography system (MEGIN Oy, Helsinki, Finland). Data were sampled at 1000 Hz with a high-pass filter at 0.03 Hz. Limb-lead ECG, as well as vertical and horizontal EOG, were collected throughout the recording. Five continuous head position indicator (cHPI) coils were affixed to each subject's head on the scalp near the hairline, and signal from the coils was used to continuously track each subject's head position throughout the recording. A Polhemus FastTrak™ 3D position monitoring system (Polhemus, Colchester, VT) was used to digitize coil positions, locations of fiducial points including the nasion as well as left and right auricular points, and additional points (200 additional points at minimum) covering the surface of the scalp.

Subjects were comfortably seated in an upright position throughout the recording. An MEG technician monitored all recordings during data collection for data noise and artifacts, manually indicating noisy or saturated channels detected via visual inspection of the data,

ensuring participant compliance with the resting state protocol, and monitoring SNR of the cHPI coils.

MRI Acquisition

For adult participants, individual source spaces were created by morphing a template brain (the Freesurfer "fsaverage" template) to fit the individual subject's digitized head geometry recorded prior to MEG data acquisition (Fischl, 2012).

For adolescent participants, individual whole-brain MRIs were acquired on a 3.0 T Philips Ingenia MRI system using a 32-channel head coil. A Pearltec Crania (Pearltec AG, Schlieren/Zurich Switzerland) head fixation system was used to minimize head motion. High resolution T1-weighted images of the head were acquired using a multi-echo MPRAGE sequence with FOV=240x240x200, acquisition voxel size 1.0x1.0x1.0mm3, reconstructed voxel size 0.5x0.5x0.5 mm3, TR/TI/TE1/TE2=13.6/1100/3.7/9.8 ms, shot interval 2200 ms, and flip angle (FA) = 12°. For adolescent participants, MRIs were segmented using Freesurfer (Fischl, 2012) to generate volumetric and cortical parcellations along with surfaces for the outer skin, skull, pial, grey and white matter.

For all subjects, individual single-layer boundary element models were constructed from the inner skull surface (Mosher et al., 1999). Individualized surface source spaces were created by evenly distributing 4098 candidate dipole locations per hemisphere along the grey-white matter boundary. Dipoles were constrained to be normal to the cortical surface. Manual co-registration of morphed template source space to the MEG coordinate space was performed using MNE-Python (Gramfort et al., 2013). Cortical parcels from the Desikan-Kiliany atlas were used for in-label source time course calculation (Desikan et al., 2006).

Experimental Protocol

Auditory Statistical Learning Task

A speech stream consisting of tri-syllabic pseudowords was played from a flat speaker inside the MSR positioned directly in front of the seated subjects at a distance of 6 ft. Stimuli were used in a previous study (Bosseler et al., 2016).

Each speech stream consisted of four pseudowords. The speech stream was statistically manipulated such that syllabic transitions within pseudowords were perfectly predictable, but transitions between pseudowords were equiprobable and unpredictable except that pseudowords were never immediately repeated. Transitions following the final syllable of a pseudoword had an equal probability of 33%, while transitions following the initial and medial syllables had probabilities of 100%. Pseudowords were constructed from Finnish syllables recorded from a female native Finnish speaker recorded in an anechoic chamber. Syllables lasted for 600 milliseconds with a consistent inter-stimulus interval of 150 ms in between. Syllables had a mean fundamental frequency of 191 Hz and were acoustically matched for intensity and loudness at 70 dB SPL.

Visual Stimuli for Adult Participants

In the adult experimental condition, subjects passively listened to an auditory statistical learning speech stream while viewing a video of aquarium fish to divert explicit attention from the speech stream. Participants were instructed to ignore the alien language playing over the speaker while relaxing and focusing on the fish.

Visual Stimuli for Adolescent Participants

Adolescent subjects were presented with a two-alternative forced-choice task resulting in exposure to social feedback during the learning period while also diverting explicit attention from the speech stream. In the two-alternative forced choice tasks, participants were presented with a black screen with a fixation cross in the middle and white question marks to the left and right. Participants selected a direction, either right or left, via button press using their left thumb. Following the selection, participants were shown a greyscale image of a face with either positive or negative emotional valance (smiling or frowning); valence of the feedback was randomized throughout. Participants were told that they would earn a quarter for each correct answer, while they would earn no money for incorrect answers. Each trial was preceded by a single fixation cross for 500 milliseconds. Question marks were displayed for 3 seconds; an arrow confirming the participant's direction choice was displayed for 1 second; feedback images were displayed for 1.5 seconds.

Behavioral Statistical Learning Testing for Adolescent Participants

Adolescents were tested on pseudoword learning via a 2-alternative forced choice task. Pseudowords were played, after which participants indicated via a button press whether they had heard the pseudoword during the training period. Three testing periods following three five-minute language exposure periods was completed by adolescents. D-prime, a measure of signal detection, was calculated from behavioral responses (Swets et al., 1961). D-prime accounts for correct answers as well as false alarm responses (novel test pseudowords reported as previously heard), which helps control for participant positive or negative answer bias. A d-prime value above zero indicates learning by the participant. The mean d-prime score for adolescent participants was 0.28 (SD = 0.51), which indicates low but above-chance learning for the group

with significant inter-individual variability. Low scores on behavioral measures of word learning are expected for implicit learning tasks, particularly when the exposure period is short (McNealy et al., 2006). Because the number of pseudowords presented to participants during the learning phase was also low, only 4 words in any given exposure period, there were few hit trials during the testing phase compared to the number of false alarm trials, resulting in low sensitivity for the measure.

Data Preprocessing

Data were preprocessed and analyzed using MNE-Python (Gramfort et al., 2013). Continuous head position coil frequencies and line noise were filtered with an iterative amplitude fitting method. Extended Signal Space Separation (Helle et al., 2021) with movement compensation was used to clean the data from movement artifacts, external noise fields, and vibration artifacts (eSSS uses the temporal extension of Maxwell filtering with an additional basis field derived from empty room recordings for noise cancellation). Window duration for eSSS was 20 seconds with a correlation limit of 0.98 for environmental noise rejection. Channels marked by the MEG technician as bad were reconstructed during the Maxwell filtering step. Using symmetric linear-phase finite impulse response filters with hamming windows and a filter length of 10 seconds, clean raw data were band-pass filtered from 0.03 to 80 Hz. Cardiac and blink artifacts were removed with Signal Space Projection (Nolte & Curio, 1999).
Noise covariance from empty room recordings were calculated using “shrunk” estimators (Engemann & Gramfort, 2015). A forward model was constructed for each participant from the individualized source space, and eLORETA was used to construct an inverse model from the whitened data and the forward model (Pascual-Marqui et al., 2011). Cleaned data was filtered into canonical bands theta (4-7 Hz), alpha (8-12 Hz), low beta (13-18 Hz), high beta (19-30 Hz)

and low gamma (31-55 Hz). Source time courses were estimated within labels from the Desikan-Killiany atlas morphed to fit the individual surfaces derived from each subject's MRI (Desikan et al., 2006). In-label source time courses provided the basis for connectivity calculation and calculation of N400 amplitude.

Event-Related N400 Amplitude Difference Calculation

N400 activity is traditionally assessed at the sensor level using global field power or individual sensor time courses, depending on the study. However, FC calculation for the current study was entirely conducted in source space, and therefore a source-space measure of N400 amplitude difference is more appropriate for comparison. N400 activity localized to the left superior temporal gyrus from onset and medial syllables was chosen for testing the relationship between connectivity and N400 amplitude difference. Left STG source time courses were trimmed from 400 to 600 milliseconds for onset and medial syllables from the last 48 pseudoword trials excluding the final trial (matching trials included in FC calculation for both AEC and IAC methods). Window timing from 400 to 600 ms after syllable onset matched the statistically significant difference window revealed by 2-sample permutations t-test clustering conducted during prior event-related analysis of the Gen-Z data.

Regions of Interest for Auditory Statistical Learning

While functional connections across the whole cortex are estimated by both connectivity measures, regions reported in prior literature as demonstrating activity during auditory statistical learning tasks were chosen for network testing (see Table 2.1). Because visual tasks differed between adults and adolescents, with social feedback incorporated for adolescent but not adult participants, whole brain networks offer low comparability between populations. However, speech stream tasks were identical between adolescents and adults, and therefore regions with

prior evidence indicating involvement in word segmentation ought to be engaged for both, maximizing overall comparability. Because of lateralization instability in younger populations, left and right hemispheric homologs were included for all regions of interest (for example, the left pars opercularis is known to strongly activate during word segmentation, so it is included in the region of interest list along with the right pars opercularis).

Region	***Prior Literature***
Transverse Temporal Gyrus	McNealy (2006); Orpella (2022)
Superior Temporal Gyrus (STG, Bank of STS)	McNealy (2006); Orpella (2022); Batterink (2019)
Middle Temporal Gyrus	McNealy (2006); Nastase (2015)
Insula	McNealy (2006); Oh (2014)
Pars Opercularis	McNealy (2006); Batterink (2019); Nastase (2015)
Pars Triangularis	McNealy (2006); Batterink (2019); Nastase (2015)
Inferior Parietal	McNealy (2006); Farthouat (2017)
Precentral Gyrus	McNealy (2006); Orpella (2022); Nastase (2015)
Anterior Cingulate (Rostral, Caudal)	McNealy (2006); Nastase (2015);

Table 2.1 List of anatomical regions targeted for network testing in the current study and studies supporting the significance of the region (in at least one hemisphere) for auditory statistical learning. Label names in parentheses indicate regions that are covered by more than one label in the Desikan-Kiliany atlas.

Discussion

The Gen-Z data set is a rare and valuable collection of data. The acquisition of individualized MRI's along with MEG recordings and the large number of participants provides an invaluable opportunity for high resolution source analysis with greater statistical power than is typical for expensive neuroimaging studies.

However, conclusions about the impact of development on functional connectivity cannot be drawn from comparisons between functional connectivity results from adult and adolescent participants. Age and developmental stage vary between the two populations, but also visual

tasks vary between the two subject pools. The social nature and reward implications of the visual task for adolescents ensures that social, emotional, and visual systems were differently engaged in adolescent participants than in adults. Therefore, differences in FC that result from developmental change remain a topic for future work, along with differences in FC resulting from the social engagement during implicit learning. Nevertheless, adolescent and adult networks differences are reported in following chapters and statistical testing for significant differences is performed for two reasons. While causal factors for network differences between adults and adolescents must be determined by future work, insights from the current results can help prioritize developmental questions to pursue. Secondly, network similarities between populations are strong candidates for task-related connectivity features, so evidence of replication between groups deserves note.

Chapter 3: AEC Functional Connectivity

One way to assess functional connections during auditory statistical learning is via amplitude envelope correlations. Amplitude envelope correlations (AECs) have been shown to be reliable, repeatable between subjects, and useful for classification of subjects in varying developmental stages and or disease states (Colclough et al., 2016; Godfrey & Singh, 2021; Hipp et al., 2011). This method has been commonly used with resting state M/EEG and has been shown to relate to development, identify individuals as a brain "fingerprint", and show alterations in disease states such as Alzheimer's and Parkinson's (O'Neill et al., 2015; Sareen et al., 2021; Schoonhoven et al., 2022). Amplitude envelope correlations are most sensitive to slow (1 Hz or less) fluctuations in the power of narrow-band frequencies, and traditionally AEC values are averaged over the course of the whole recording to obtain a snapshot of mean connectivity over time. When assessed in source space, this measure allows the researcher to examine which cortical regions remain highly connected to each other persistently throughout a recording. Previously, AEC connectivity in the alpha and beta bands has been shown to relate to the default mode network and BOLD connectivity as measured via fMRI (Brookes et al., 2011; Liu et al., 2010; Maldjian et al., 2014). Therefore, static AEC measures from an M/EEG recording may functional relationships among cortical regions that may result in measurable hemodynamic signal. Functional connectivity assessed via amplitude envelope correlation has been used both in resting state recordings and task-based recordings, and amplitude envelope connections have been shown to vary as a function of a task (Favaretto et al., 2021; O'Neill et al., 2017; Tewarie, Hunt, et al., 2019; Wei et al., 2021).

AEC Methods

Connectivity Estimation

Amplitude envelopes were calculated by extracting the analytic signal of band-pass filtered, epoched data. After applying the Hilbert transform, the inverse solution was applied to the data and in-label time courses were extracted using the "pca_flip" method, which extracts the first PCA component from all the source vertices within the label to derive a representative label time course. After time course extraction, "all-to-all" envelope correlations were run (O'Neill et al., 2015). Signals were pairwise orthogonalized during the correlation process to control for signal leakage between labels (Hipp et al., 2012). Amplitude envelope correlations were averaged over the final two minutes of the recording to produce a static connectivity matrix during the last 48 trials of pseudoword learning (matching the time over which IAC metrics were also calculated).

To preserve network information contained in the edge weights, we chose to keep the networks weighted and fully dense (no thresholding or sparsification techniques applied). This resulted in five AEC correlations matrices for each subject, one for each frequency band of interest. For each frequency, a group mean correlation matrix was derived by averaging matrices across subjects.

Graph Theory Measures

Two measures of network hubness were calculated for all labels: node strength and eigenvector centrality. Node strength for a weighted network is the sum of all edge weights for a given node; eigenvector centrality is proportionate to the sum of the centrality of a node's neighbors weighted by connection strength. These metrics are indicators of a region's influence within a network. Not all regions in the cortex can be hubs; rather, hubness should reflect which

regions have the most influence at the time of measurement. While AEC is a non-directed connectivity measure and cannot signify whether a given region is the sender or recipient of information transfer, high node strength and eigenvector centrality values are evidence that a region plays a central role in the network.

Node strength and eigenvector centrality are both measures of the connectedness of a region, but these measures have different implications for a region's role. A social analogy is perhaps the easiest way to conceptualize the difference between these two measures. People who are extraverted are likely to have many acquaintances, but their acquaintances may be comprised of many people who are introverted and not very socially connected themselves. The social connectedness of an extravert would be well described by high node strength – lots of connections with people of many types. In contrast, social connections of a celebrity like Kim Kardashian might be better described by high eigenvector centrality because a celebrity is highly connected to other celebrities who are highly connected. Cortical regions with high eigenvector centrality are the power couples of the neural network; they connect with other influencers. A society may go through periods of low social connection generally as, for example, during the COVID pandemic, and in the same way, neural networks may go through periods of greater or lesser connectedness (alterations in node strength). However, society tends to have a small number of celebrities relative to the general population, and this proportion does not change dramatically even when the overall socialization level undergoes changes; similarly, neural networks may have relatively constant distributions of eigenvector centrality with only a few nodes at the top of the pyramid at any given moment. Just as media coverage and popular attention shifts from celebrity to celebrity over time, high eigenvector centrality values may shift significantly from region to region, even if the total distribution of EC values remain

proportionately distributed in a consistent way between networks and conditions. In the context of this investigation, both the connectedness of individual regions and of the network as a whole are of interest, particularly in comparison between transitional probability conditions. The identification of regions that have key influence at any given moment, assessed by eigenvector centrality, is also important. More advanced graph theory measures, such as modular analysis of the network structure, are also of interest, but are deferred for future work since basic relevance of connectivity results to language learning is the current goal.

First Order Statistics for Functional Connectivity Measured by AEC

Mean Correlation by Band

Correlation matrices were averaged across subjects to produce a mean group correlation matrix. Mean amplitude envelope correlation decreases with increasing frequency, as is expected based on work from prior studies.

As shown in Figure 3.1, there is some variance between adult and adolescent distributions of mean AEC edge strengths. While adolescent mean edge strength decreases monotonically by frequency, adult mean edge strength for the alpha band is slightly higher than the mean edge strength for the theta band. Additionally, the adult distribution is more spread out for the alpha band with larger standard deviations compared to the higher frequency bands, which have very compact distributions with low standard deviations. In contrast, adolescent mean edges have similar standard deviations across frequency bands. This demonstrates that adolescent edges are more variable than adult edges when measured using AEC.

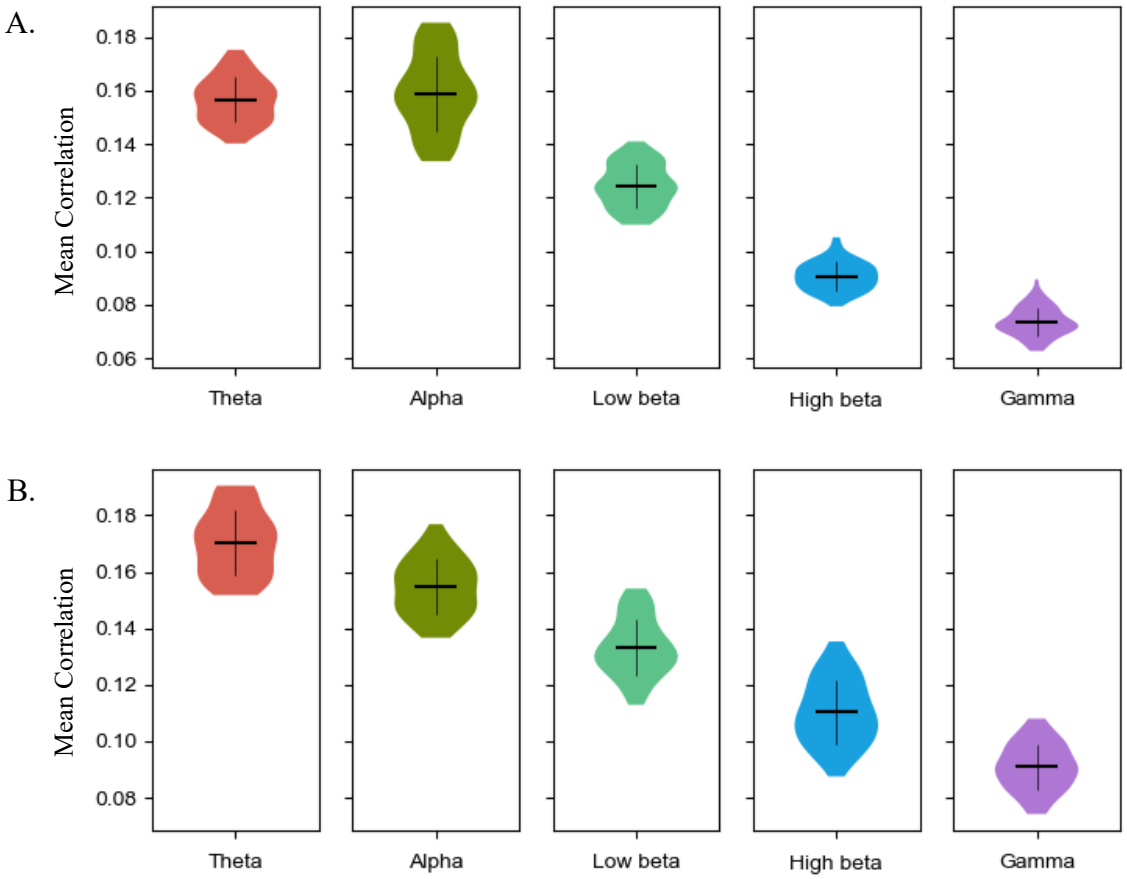

Figure 3.1 Mean AEC value distributions. Violins represent distribution of mean values for 68 labels in the Desikan-Kiliany atlas. Thick black horizontal bars indicate the mean, while vertical black bars indicate the standard deviation. A. Mean correlation distribution for adults. B. Mean correlation distribution for adolescents.

Node Strength by Frequency Band

Node strength for each label was calculated using networkx for each subject for each band and averaged over each subject pool to obtain the group mean (Hagberg et al., 2008). Node strength is a measure of node connectivity for weighted networks that represents the connectedness of a region when paths between regions are non-binary. Greater node strength values mean that a region is more highly connected. Node strength distributions across all the labels in the cortical atlas are shown in Figure 3.2.

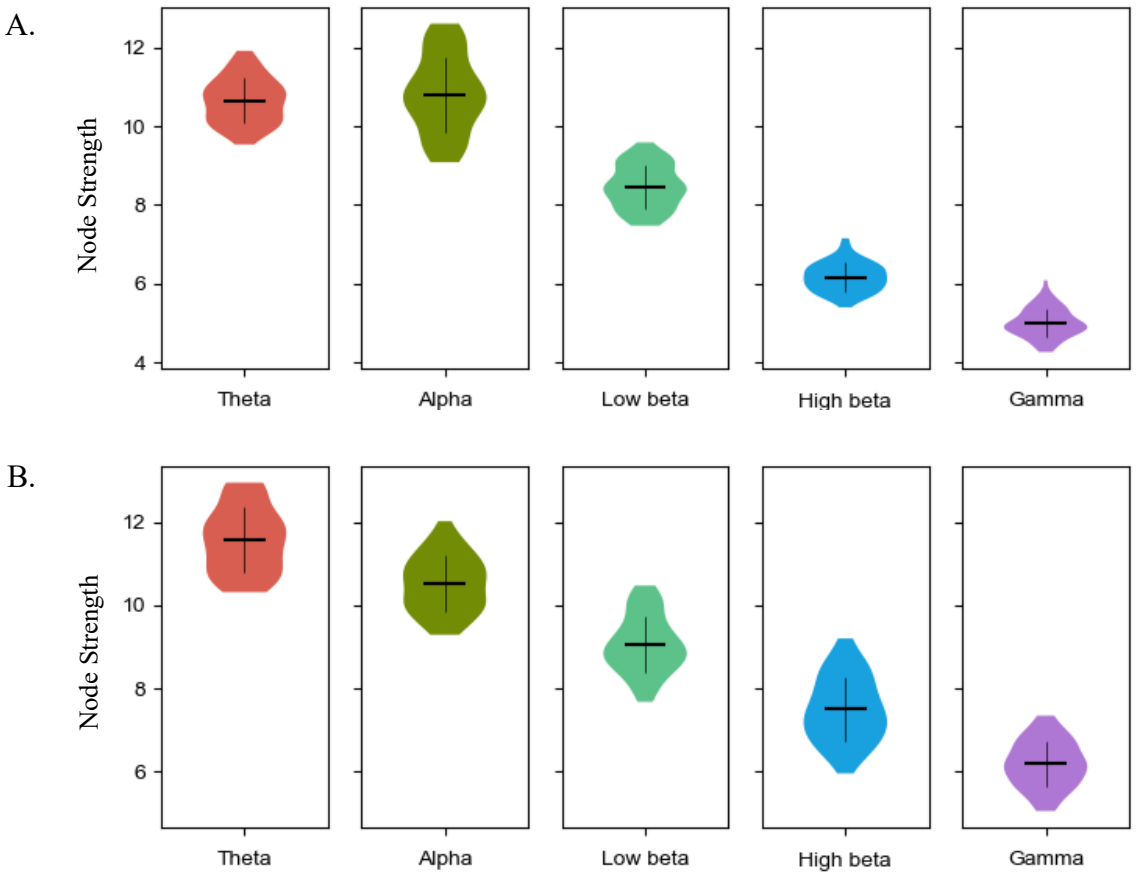

Figure 3.2 Node strength distributions. Violin plots represent the total distribution of node strengths over all 68 cortical labels in the atlas. Horizontal bars indicate the mean of the distribution and vertical black bars indicate standard deviation from the mean for the distribution.

Distributions appear similar at first glance between adolescents and adults, but Welch's 2-sample t-tests show that adults have lower node strength distributions than adolescents in all frequency bands except alpha, where adults have slightly higher connectivity (see Table 3.1). Adolescents have more variability in the node strength distribution, meaning that adolescent networks have more separation between highly connected and poorly connected nodes. In contrast, adults have more homogenous networks in most bands, with the alpha network alone

demonstrating greater standard deviations, indicating greater differentiation between the connectivity of different cortical nodes compared to adolescents.

	Adult Mean NS (SD)	***Adolescent Mean NS (SD)***	***Mean Difference (95% CI)***	***p-value***
Theta *	10.64 (0.58)	11.58 (0.78)	-0.93 (-1.16, -0.70)	1.15e-12
Alpha *	10.81 (0.96)	10.52 (0.68)	0.29 (0.006, 0.57)	0.045
Low beta *	8.46 (0.55)	9.06 (0.70)	-0.59 (-0.81, -0.38)	1.70e-07
High beta *	6.17 (0.37)	7.50 (0.79)	-1.33 (-1.54, -1.12)	< 2.2e-16
Gamma *	5.01 (0.67)	6.18 (0.57)	-1.17 (-1.33, -1.0)	< 2.2e-16

Table 3.1 Results of t-tests comparing node strength distributions between adults and adolescents. Bolded text indicates significant results. P-values are uncorrected for multiple comparisons. T-tests were implemented using base functions in R.

Eigenvector Centrality by Band

Like node strength, eigenvector centrality was calculated for all labels in all bands using networkx and averaged across subjects for a group mean. Higher values of eigenvector centrality indicate more influence of a region within a network. Unlike node strength, mean eigenvector centrality does not vary significantly between bands, nor does it vary between adults and adolescents (shown in Figure 3.3 and Table 3.2). However, distributions are more spread out, as evidenced by larger standard deviations, in the alpha and gamma bands; for adolescents, gamma and high beta bands have larger standard deviations.

At first glance the homogeneity of EC values may seem surprising; however, this is a direct consequence of preserving all of the edge weights in the construction of the network. Numerically, for weighted networks, contributions to EC values come from two primary sources: first, the number of non-zero connections for a given node, and second the strength of the present connections. The contribution stemming from the number of non-zero connections dominates the overall EC value for the node, so when the number of non-zero connections is equivalent for all

nodes in the network, as is the case for fully-weighted networks, this portion of the EC value does not vary between nodes and the distribution appears relatively homogenous. When the mean is subtracted from all EC values from fully dense networks, the remaining variance primarily reflects hubness differences due to variation in edge weights, which is the property of interest.

The construction of a 2-dimensional network for graph theory analysis from a 3-dimensional connectivity array necessarily involves dimensionality reduction, and the reduction process chosen may potentially obscure variance found in the higher dimensional object. For AEC and IAC methods, averaging connectivity matrices across different time points projects the three-dimensional connectivity array to the two-dimensional space, and potential impacts of this process should be acknowledged. For example, alternative methods of deriving a 2-dimensional adjacency matrix from FC calculations (for example, decomposition techniques such as non-negative matrix factorization) that tend to produce sparse representations may result in EC distributions with greater variance because they introduce zeros entries into the edge weights of the resulting adjacency matrix. For the purposes of this analysis, averaging was chosen for comparability to prior work with AECs, and non-zero edge weights were preserved, reflecting non-zero contributions from oscillatory neurons in all regions.

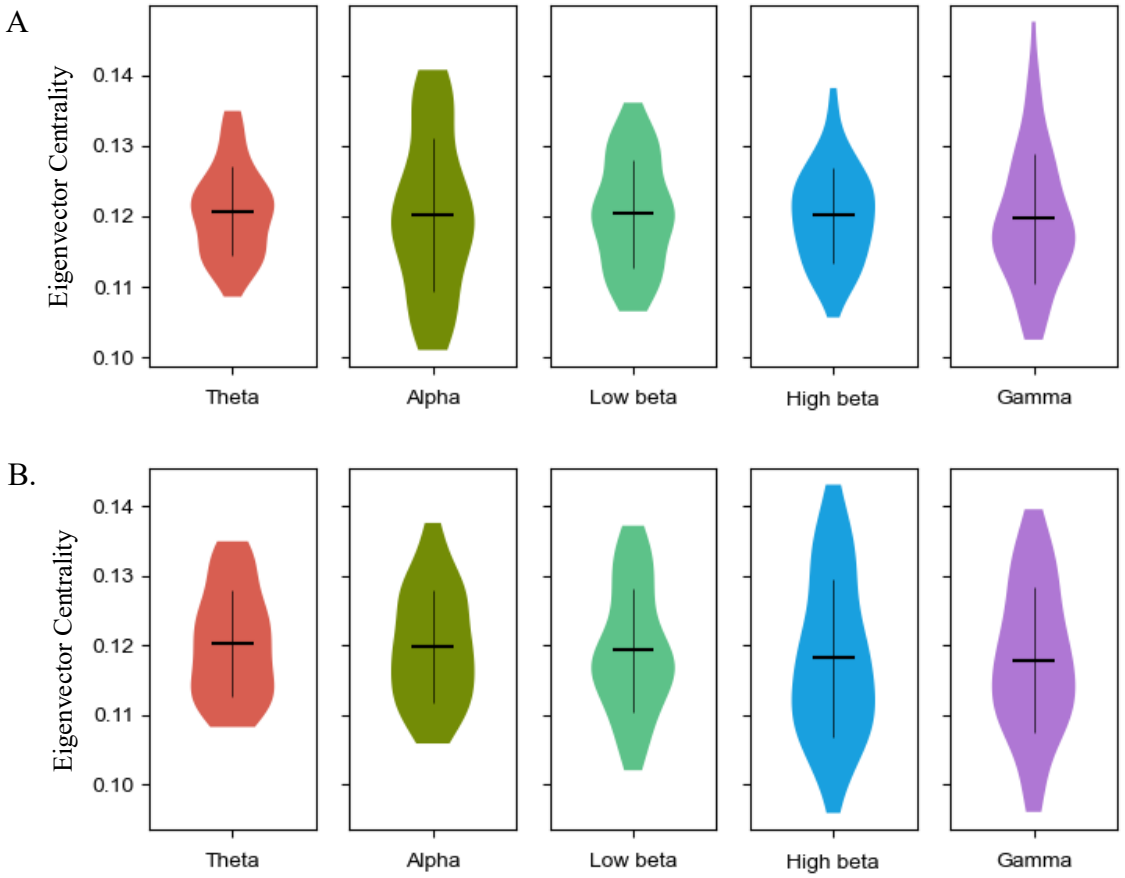

Figure 3.3 Eigenvector centrality distributions. Violin plots represent the total distribution of EC values over all 68 cortical labels in the atlas. Horizontal bars indicate the mean of the distribution and vertical black bars indicate standard deviation from the mean for the distribution. A. Distributions for adults. B. Distributions for adolescents.

	Adults	***Adolescents***	***Mean Difference (95% CI)***	***p-value***
Theta	0.1207 (0.006)	0.1203 (0.007)	0.0004 (-0.002, 0.002)	0.73
Alpha	0.1202 (0.01)	0.1199 (0.008)	0.0003 (-0.003, 0.003)	0.84
Low beta	0.1204 (0.007)	0.1193 (0.009)	0.001 (-0.002, 0.004)	0.44
High beta	0.1201 (0.007)	0.1182 (0.01)	0.002 (-0.001, 0.005)	0.22
Gamma	0.1197 (0.009)	0.1179 (0.01)	0.002 (-0.002, 0.005)	0.29

Table 3.2 Results of t-tests comparing adult to adolescent mean EC distributions. P-values are uncorrected for multiple comparisons. T-tests were implemented using base functions in R.

Hub Regions for AEC Networks

For both adults and adolescents, hubs in the theta, high beta, and gamma bands feature visual and frontal regions of interest, as shown in Figure 3.4. Notably, speech processing regions along the arcuate fasciculus are absent from high scoring hub regions, particularly in the theta, alpha, low beta bands. Middle temporal and inferior frontal gyri have positive mean z-scores across multiple bands but are not top scorers in any band except the gamma band for adolescents. In the higher frequency bands high beta and gamma, a few regions of interest for speech processing in the motor cortex, the pre- and post-central gyri, gain hubness in AEC networks. Conspicuously absent from AEC hubs are regions of the inferior frontal gyrus such as the pars opercularis and pars triangularis as well as primary auditory regions.

Instead of auditory and speech processing regions, top nodes in AEC networks include regions in the ventral visual stream along with higher order cognitive regions, like the rostral middle frontal area. Interestingly, key hubs seem to appear across multiple frequency bands. For example, the lateral occipital area features strong node strength in both theta, alpha, low beta, and high beta bands. Similarly, the right lateral orbitofrontal has high node strength for all bands except alpha. Top nodes are similar between hemispheres, which is unexpected given the left lateralization of language functions.

Regions in the visual system score strongly for both node strength and eigenvector centrality (see Figure 3.4 and Figure 3.5), but the primary visual cortex is not a strong hub for any frequency band network. Instead, peripheral visual regions like the lingual gyrus are implicated as hubs in AEC networks. Both adults and adolescents engaged in attentive viewing of scenes on a screen during auditory statistical learning. There is no doubt that the primary

visual cortex was engaged during the recording for both populations. However, as measured by the AEC method, functional connections from V1 to other regions were minimal.

Adolescent and adult populations share a lack of functional connections to primary auditory and visual regions – in other words, weak hubs are shared – but strong hubs are somewhat variable between the two groups. The superior frontal region is strongly connected in adolescents across multiple bands but exhibits mediocre connectivity for adults. Similarly, the inferior temporal gyrus is a much stronger hub for adolescents than adults. These population variances may reflect more effortful cognitive processing of visual stimuli from adolescents performing a 2AFC task.

Regions implicated as network hubs as measured by node strength are nearly identical to regions implicated by eigenvector centrality for the AEC measure. The strong overlap between these two measures means that in AEC networks, hubs tend to connect only to other strongly connected hubs. Overlaps of this sort occur in networks that qualify as threshold graphs (Oldham et al., 2019), in which the connections of one region are subsets of the connections belonging to a neighbor.

Top Regions by Z-Scored Node Strength

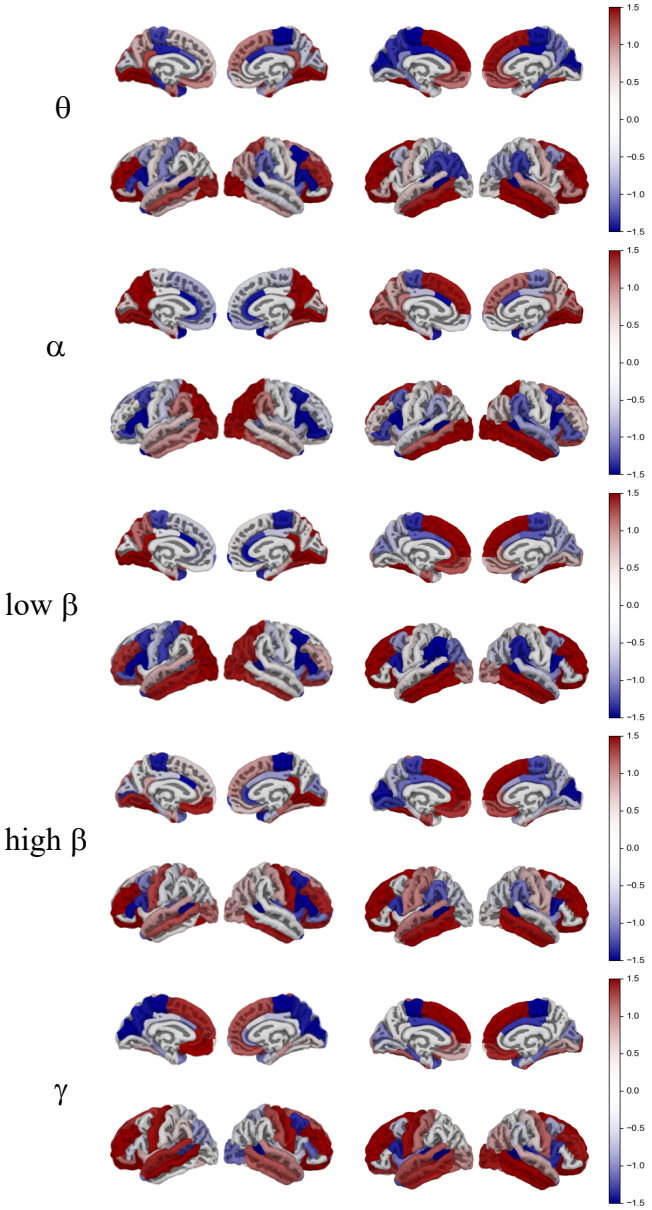

	C. Adults	D. Adolescents
θ	Rost. Mid. Frontal (L)	Sup. Frontal (L)
	Lat. Orbitofrontal (L)	Lat. Orbitofrontal (R)
	Lat. Orbitofrontal (R)	Lat. Orbitofrontal (L)
α	Sup. Parietal (R)	Fusiform (L)
	Isthmus Cing. (R)	Fusiform (R)
	Inf. Parietal (R)	Lat. Occipital (R)
low β	Fusiform (L)	Sup. Frontal (L)
	Lingual (R)	Sup. Frontal (R)
	Isthmus Cing. (R)	Fusiform (L)
high β	Rost. Mid. Frontal (L)	Sup. Frontal (R)
	Lat. Orbitofrontal (L)	Sup. Frontal (L)
	Lingual (R)	Lat. Orbitofrontal (R)
γ	Rost. Mid. Frontal (L)	Sup. Frontal (L)
	Med. Orbitofrontal (L)	Rost. Mid. Frontal (L)
	Lat. Orbitofrontal (R)	Mid. Temporal (R)

Figure 3.4 Z-scored node strength by frequency band. A. Top regions for adults. B. Top regions for adolescents. C. For adult participants, lists of the top three regions scoring highest for mean node strength for each frequency, starting with the top ranked region first (hemisphere for each label indicated within parentheses). D. Regions with highest mean node strength for adolescent participants.

Top Regions by Z-Scored Eigenvector Centrality

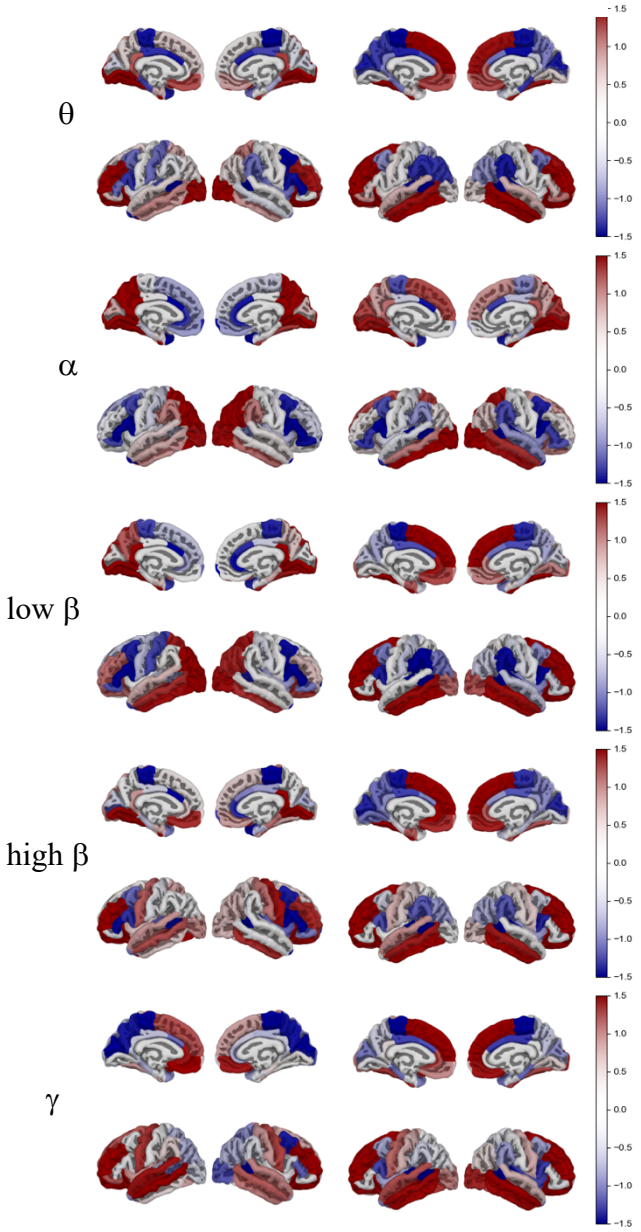

	C. Adults	D. Adolescents
θ	Rost. Mid. Frontal (L)	Lat. Orbitofrontal (L)
	Lat. Orbitofrontal (R)	Lat. Orbitofrontal (R)
	Lat. Orbitofrontal (L)	Rost. Mid. Frontal (R)
α	Sup. Parietal (R)	Fusiform (L)
	Isthmus Cing. (R)	Fusiform (R)
	Sup. Parietal (L)	Lat. Occipital (R)
low β	Fusiform (L)	Fusiform (L)
	Lingual (R)	Sup. Frontal (L)
	Isthmus Cing. (R)	Sup. Frontal (R)
high β	Rost. Mid. Frontal (L)	Sup. Frontal (L)
	Lat. Orbitofrontal (L)	Sup. Frontal (R)
	Lingual (R)	Rost. Mid. Frontal (L)
γ	Rost. Mid. Frontal (L)	Sup. Frontal (L)
	Lat. Orbitofrontal (R)	Rost. Mid. Frontal (L)
	Med. Orbitofrontal (L)	Lat. Orbitofrontal (R)

Figure 3.5 Z-scored eigenvector centrality by frequency band. A. Top regions for adults. B. Top regions for adolescents. C. For adult participants, lists of the top three regions scoring highest for mean node strength for each frequency, starting with the top ranked region first (hemisphere for each label indicated within parentheses). D. Regions with highest mean node strength for adolescent participants.

Strongest Edges by Frequency Band

Key edges for AEC connectivity do not include connections between the primary auditory cortex and the inferior frontal gyrus. Instead, in adults, connections between regions of the ventral visual stream return the highest connectivity values (Figure 3.6). In adolescents, prominent edges include some connections to temporal regions, but these are mostly connected to middle and inferior temporal areas. Again, visual regions feature prominently in strong edges across the lower frequency bands for adolescents. In both adults and adolescents, modulations in the gamma band deviate somewhat – connections within the motor cortex between pre- and post-central gyri score highly. Gamma band motor connections are strong in both adults and adolescents, which is remarkable because the adolescent visual task included periodic button presses whereas adults did not engage in any button presses or motor responses of any kind. Inter hemispheric connections are mostly in lower frequencies.

Edges in AEC networks have strong symmetry across the longitudinal fissure. Given that language networks, even in an adolescent population, tend to be left-lateralized at the group level, the symmetry of edge patterns in both adolescents and adults is surprising. Although there are some notable inter-hemispheric connections, they mostly appear to be connections between left and right analogs, such as the left and right lateral occipital regions. Overall, strong edges primarily connect regions within a single hemisphere.

Circle Plots of Edge Strength by Band

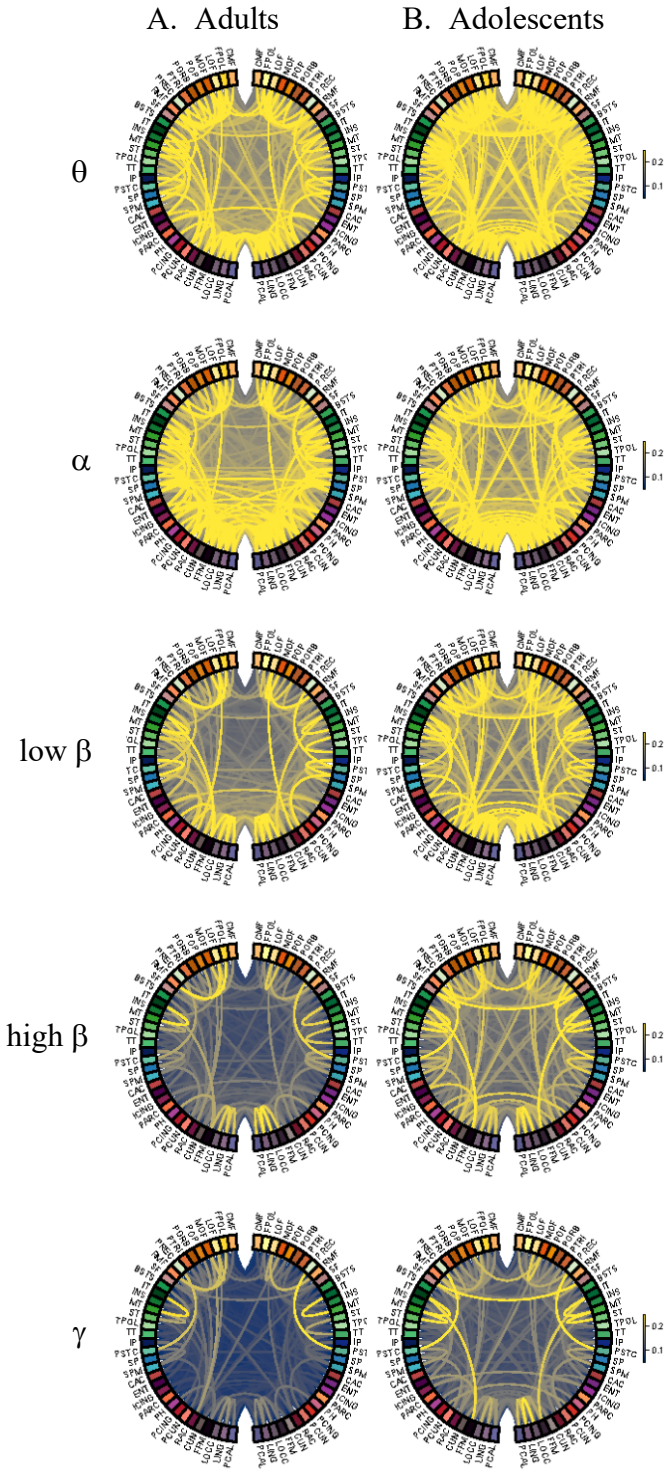

	C. Adults	D. Adolescents
θ	Lat. Occipital R to Lingual R	Inf. Temp. R to Mid. Temp. R
	Lingual L to Lat. Occipital L	Inf. Temp. L to Fusiform L
	Fusiform R to Lingual R	Inf. Temp. L to Mid. Temp. L
α	Lat. Occipital R to Lingual R	Inf. Temp. R to Mid. Temp. R
	Fusiform R to Lingual R	Lingual R to Lat. Occipital R
	Lingual L to Lat. Occipital L	Pericalcarine R to Lat. Occipital R
low β	Lingual R to Lat. Occipital R	Inf. Temp. R to Mid. Temp. R
	Lingual R to Fusiform R	Mid. Temp. L to Inf. Temp. L
	Lingual L to Lat. Occipital L	Lat. Occipital R to Lingual R
high β	Precentral R to Postcentral R	Sup. Temp. L to Mid. Temp. L
	Mid. Temp. R to Inf. Temp. R	Postcentral R to Precentral R
	Inf. Temp. L to Mid. Temp. L	Sup. Front. R to Sup. Front. L
γ	Rost. Mid. Front. L to Front. Pole L	Mid. Temp. L to Sup. Temp. L
	Lat. Occipital R to Lingual R	Inf. Temp. R to Mid. Temp. R
	Inf. Temp. L to Mid. Temp. L	Sup. Front. L to Sup. Front. R

Figure 3.6 Strongest edges by frequency band. A. Mean edge plots for adults. B. Mean edge plots for adolescents. C. Top three edges by frequency band (strongest edge listed first) for adult participants. D. Top three edges for each band in adolescents.

AEC Network Characteristics

AEC networks are dominated by visual and frontal hubs with strong intra-hemispheric connections.

The most surprising feature of AEC results is that, aside from links between the middle temporal and inferior temporal gyri, connections between speech regions barely appear in the network. Importantly, connections to the pars opercularis, the region most strongly implicated as important of auditory statistical learning from prior work, score poorly. A possible explanation for the absence of speech region connections is that they modulate too fast to be detected well by the AEC measure. AEC are sensitive to gradual changes in oscillatory amplitude at the rate of 0.1 Hz, whereas oscillatory power dynamics change within sub-second time frames. AEC have low temporal sensitivity to sub-second connectivity states. The temporal characteristics of the stimulus, with syllables occurring every 750 ms, shape the rate of oscillatory dynamics. An auditory statistical learning speech stream deviates from natural language in that larger probabilistic groupings are purposefully suppressed within the stream. Pseudo-words are intentionally prohibited from appearing in predictable groupings in order to carefully control syllable by syllable transitional probability. The temporal characteristics of the task in the current experiment, particularly the lack of slow rate structure inherent to language tasks like sentence processing, may render oscillatory coupling essentially invisible to the AEC measure. Introducing slower variations in stimulus characteristics might allow more effective detection of speech region connections by the AEC method, but in the context of the current experiment, AEC measures appear mismatched to the type of functional coupling occurring between speech regions.

Another possible explanation for the absence of speech region connections is that certain regions of the brain (for example, regions in the default mode network) natively gravitate to the slow rate coupling that the AEC measure is suited to detect. The visual system might have a consistent advantage over the auditory system for AEC measurement, which is suggested as an explanation because visual frontal connections were notable in both adults and adolescents despite the different character of the visual tasks given to the adult and teen subjects. On the other hand, visual trials for adolescents in the Gen-Z paradigm had a duration of 5 seconds, which gives the visual stimulus temporal properties that more closely align with modulations AEC detects well. Future work is needed to clarify whether stimulus timing, stimulus modality, or some combination of both factors is most important for successful connectivity measurement with AEC methods.

Chapter 4: AEC Networks and Learning

Significant obstacles confront the researcher interested in testing for relationships between functional connectivity properties and behavioral outcomes such as novel word learning. Functional connectivity data is inherently high dimensional in nature, and few neuroimaging studies are large enough to supply more subjects than features of interest. Machine learning techniques provide an avenue for testing associations between functional connectivity data and behavioral outcomes of interest. Support vector machines (SVM) are a machine learning technique suitable for high dimensional predictor data with a history of successful application to neuroimaging data. Support vector machines can be applied to classification tasks for predicting binary outcomes, and support vector regression is applicable when the outcome of interest is a continuous variable. Support vector machines apply a kernel function to map data into a higher dimensional space, then use training data to construct a hyperplane with maximum separation between binary classes for binary outcomes, or alternatively for regression tasks, to minimize error within a specified tolerance margin from the regression line. Because the number of edges between speech regions considerably exceeds the number of subjects in the current study, support vector techniques suited the needs of the investigation.

The primary question of interest is whether functional connectivity features predict statistical learning outcomes in adolescents, but to answer this question, it is important to test whether functional connectivity predicts N400 amplitude as well. Are functional connections tied to the event-related responses that have a known relationship to statistical learning, or is functional connectivity data independent? To answer this question, support vector techniques are applied to two primary tests of association: first, the association between patterns of speech region connectivity and the amplitude of the N400 difference in both adults and adolescents;

second, the association between patterns of speech region connectivity and D-prime scores in adolescents.

Testing Speech Region Connectivity and N400 Amplitude

Scikit-learn's implementation of SVR with a radial basis function kernel (C=0.1, gamma='scale', epsilon=0.1) was chosen to test associations between AEC networks in speech regions and the event-related N400 amplitude difference between onset and medial syllables (Pedregosa et al., n.d.). For adults, each training fold incorporated 24 of 30 subjects, leaving 6 out as testing sets, including for each subject a predictor vector of 231 edges between 22 regions of interest (the upper triangle of the square 22x22 connectivity matrix). For adolescents, each training fold incorporated 86 subjects with 231 predictor features, leaving 21 subjects for the test set. Standard scaling was applied to predictor and outcome vectors prior to fitting (training and testing data sets were scaled separately to avoid contamination between sets).

		Mean R^2 across 5-fold cross-validation
Theta	*Adults*	-0.13 (0.11)
	Adolescents	-0.01 (0.01)
Alpha	*Adults*	-0.13 (0.12)
	Adolescents	-0.01 (0.01)
Low beta	*Adults*	-0.11 (0.14)
	Adolescents	-0.01 (0.07)
High beta	*Adults*	-0.10 (0.88)
	Adolescents	-0.33 (0.38)
Gamma	*Adults*	-0.05 (0.46)
	Adolescents	-0.05 (0.03)

Table 4.1 Support vector regression predicting N400 amplitude difference in the superior temporal gyrus as a function of amplitude envelope correlation connectivity among speech regions.

In all bands, in both populations, mean R^2 values are negative, which indicates that there is no evidence of an association between AEC functional connectivity measures in speech regions and event-related N400 amplitude difference (Table 4.1).

Testing Speech Region Connectivity and D-prime Scores in Adolescents

To test associations between speech region connectivity and D-prime values in adolescents, SVR using a radial basis function kernel (C=0.11, gamma=" scale") with 5-fold cross validation was applied to the adolescent data set after standard scaling. As with the N400 run, each training fold incorporated 86 training and 21 test subjects with 231 predictor features. However, mean variance scores were negative across frequency bands for this test as well, indicating no evidence of association between speech region connectivity and adolescent pseudo-word learning (Table 4.2).

		Mean R^2 across 5-fold cross-validation
Theta	*Adolescents*	-0.02 (0.02)
Alpha	*Adolescents*	-0.02 (0.02)
Low beta	*Adolescents*	-0.15 (0.05)
High beta	*Adolescents*	-0.81 (0.80)
Gamma	*Adolescents*	-0.08 (0.12)

Table 4.2 Support vector regression predicting d-prime values as a function of amplitude envelope correlation connectivity among speech regions.

Additionally, I conducted a follow-up test using support vector classification to test if speech connectivity could classify whether subjects fall into the upper or lower half of a median split of the D-prime score (Table 4.3). Because of the noisy nature of D-prime scores as a metric in the context of our experiment, this follow up test examined if associations were more detectable with a simplified outcome. For AEC connectivity scores, however, classification did not succeed above chance in any band (ROC AUC scores of 0.5 represent at-chance levels, and

therefore scores must be greater than 0.5 with a standard deviation across folds not exceeding the difference between the mean ROC AUC score and 0.5).

		Mean ROC AUC across 5-fold cross-validation
Theta	*Adolescents*	0.54 (0.05)
Alpha	*Adolescents*	0.33 (0.06)
Low beta	*Adolescents*	0.52 (0.09)
High beta	*Adolescents*	0.57 (0.10)
Gamma	*Adolescents*	0.41 (0.09)

Table 4.3 Support vector classification categorizing high and low learners (median split of d-prime values) as a function of amplitude envelope correlation connectivity among speech regions.

Discussion

Support vector machine testing did not reveal any association between amplitude envelope connectivity in speech regions and any measure of participant learning. Given the characteristics of the hub regions and strong edges detected by amplitude envelope correlations, the outcome of SVM testing is not surprising.

Because prominent hubs in AEC networks include visual, frontal, and motor regions, and moreover AEC networks show no sign of association to speech outcomes, it is tempting to speculate that AEC measures are picking up on functional connections relating to participants' visual tasks. An analysis of the relationship between visual event-related responses and AEC network features is beyond the scope of this investigation, but observations from the current data set provide motivation to explore those associations in future work.

Chapter 5: IAC Functional Connectivity

Oscillatory activity in the cortex is known to adapt in response to language stimuli at sub-second rates. Because oscillations form the basis of the functional networks we wish to investigate, there is a clear motivation for measuring and assessing changes in functional connectivity at a sub-second level as well. Network adaptations, or dynamic functional connectivity, requires a metric that is sensitive to connectivity durations which are relatively short. Instantaneous amplitude correlation is a metric suited for this purpose. Like the amplitude envelope correlation, it is an amplitude-based measure of functional relationships between signals; however, fewer temporal smoothing steps are applied during the calculation of the metric, and this results in improved detection of short-duration connectivity states, albeit at the cost of increased noise. IAC allows researchers to examine how networks change within the time frame of linguistic stimuli, i.e. it allows the examination of network dynamics. If static network approaches allow the researcher to determine how a cortical network is generally organized and which connections predominate throughout the recording, dynamic network approaches allow the researcher to investigate fine-grained adjustments made by the cortex during the execution of cognitive tasks, both functional properties that may be reasonably related to the success of a participant's learning.

Methods

IAC Calculation

IAC calculation was performed on pairwise-orthogonalized in-label source time courses from all 68 labels in the Desikan-Kiliany atlas using functions implemented in python. Due to the computational and memory demands of the IAC method, the calculation of IAC connectivity was limited to approximately the last two minutes of the statistical learning task, including the

final 50 pseudoword trials, such that the measure captured connectivity when some degree of statistical learning had already taken place. This analysis resulted in continuous connectivity tensors over the final two minutes of statistical learning, such that connectivity values could be examined in relation to trial onsets.

Connectivity Matrices

A primary research question for high temporal resolution connectivity measures is whether functional networks adapt to differing transitional probability conditions. Therefore, IAC networks were derived by collapsing IAC values over experimental conditions to examine condition contrasts, averaging IAC values from each trial of a given syllable type to capture mean connectivity for each syllable separately. Fully dense, weighted networks were chosen for graph analysis to avoid throwing away fine detail in the networks. As with AEC networks, graph theory metrics compatible with weighted networks, node strength and eigenvector centrality, implemented in the python package networkx, were utilized in subsequent analyses to compare regional roles in IAC networks (Hagberg et al., 2008).

Condition Difference Tensors

Because IAC produces connectivity tensors with continuous values for each edge over the full course of all trials, connectivity between cortical regions can be examined with respect to the onset of stimuli. Trimming IAC tensors from the start of the baseline period to the end of each syllable and averaging trials by condition makes connectivity modulations in response to stimulus conditions observable. To create difference tensors, we created epochs in our edge tensors by trimming IAC values from 150 seconds prior to syllable onset to 600 seconds after syllable onset for all syllables, preserving the baseline window in case of anticipatory effects. Then for each edge and each subject, IAC tensors from 48 medial syllable trials were subtracted

from the IAC tensors for matching onset syllables (discarding the first and last trial of the set of 50 trials over which IAC was calculated to avoid edge artifacting from IAC calculation) to create difference tensors for each trial. Finally, syllable differences were averaged for each subject.

Subtracting medial from onset mean produces condition difference tensors, which reveal modulations in connectivity between expected and unexpected syllables. Difference tensors from difference frequency bands exhibit obvious variance in the timing of connectivity modulations (see Fig 5.1).

Permutations T-Tests with Temporal Clustering

Because connections in different frequency bands modulate at different times, a method for quantifying adaptation timing was required. Comparing IAC connectivity networks to AEC networks necessitates capturing a representative "still" of the network so that graph theory metrics for both FC methods can be calculated on a 2-dimensional adjacency matrix. While averaging IAC values over the full trial of conditions does reveal differences between syllables, condition differences are contaminated by noise when matrices are formed by averaging the full trial, but the timing of modulations is limited to specific temporal windows within the trial course. The goal for high temporal resolution connectivity is to capture networks dynamics, and to do that, capturing network structure during modulation is essential. Since different frequencies diverge in modulation timing, a data-driven technique for determining when temporal windows of interest for deriving networks provides adequate SNR for comparing network features between conditions.

One-sample permutations t-testing with temporal clustering is a data-driven method that captures statistically significant deviations from zero in difference time series, such as IAC condition difference tensors. To examine temporal windows when differences emerge between

high and low probability syllables, we took the difference in IAC tensors between medial and onset syllables and used one sample temporal clustering with permutations to assess time periods when mean difference time courses between syllables were significantly different from zero (see Figure 5.1). For each edge tensor, clustering was applied across subjects using 10,000 permutations.

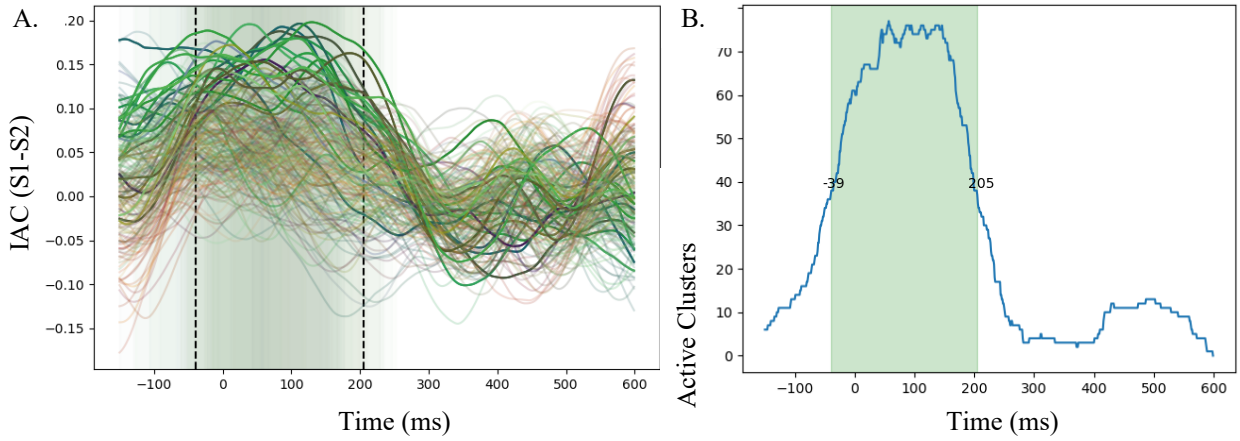

Figure 5.1 Example of temporal window of interest for difference tensors between speech regions in the alpha band. A. Each edge in the plot represents the group mean tensor averaged across subjects. Bold lines indicate edges with significant peaks. Shaded areas indicate cluster durations of significant clusters. Dotted black lines enclose the temporal window of interest during which speech regions modulate between onset and medial syllables. B. Count of active clusters in alpha band edges over the course of the trial.

Temporal Windows of Interest: Aggregate Cluster Timing

To quantify temporal windows when the most edges showed significant clustering within each band, we summed the number of edges with an active temporal cluster at each millisecond of the trial time course, then took the sample with the maximum number of active clusters, extending a temporal window on either side of the peak sample until either we hit the end of the trial or the number of active clusters dropped below half of the maximum cluster number at its peak (Table 5.1).

Band	*Number of Significant Clusters*	*Timepoint with Maximum Active Clusters*	*Window Start (First Half-Max)*	*Window End (Last Half-Max)*	*Window Length*
Theta	110	489 ms	431 ms	600 ms (trial end)	169 ms
Alpha	124	57 ms	-39 ms	205 ms	244 ms
Low Beta	88	61 ms	13 ms	135 ms	122 ms
High Beta	24	263 ms	233 ms	275 ms	42 ms
Gamma	31	255 ms	221 ms	284 ms	63 ms

Table 5.1 Data-driven temporal windows of maximum edge adaptation by frequency band.

First Order Statistics for Functional Connectivity Measured by IAC

For IAC connections, first order statistics were calculated separately for onset syllables and medial syllables. IAC values were averaged over temporal windows of interest for each frequency band, which equates the number of samples averaged for each syllable within frequency bands, but keeps averaging windows proportionate to the underlying oscillatory frequency across frequency bands. Mean correlation matrices were calculated by averaging matrices for each syllable and frequency across subjects.

Mean Correlation by Band and Syllable

In both adults and adolescents, clear dynamics related to syllable type are apparent in overall connectivity measured by IAC. Adolescent distributions vary between syllables similarly to adult distributions through with less pronounced syllabic differentiation.

In contrast to AEC measures, IAC edge strength does not vary systematically across frequency bands, as shown in Figure 5.2. Unlike connectivity measured by AEC, IAC connections are stronger in adults than in adolescents. During onset syllables, adults have higher IAC mean values compared to adolescents in all bands except gamma where adolescent connections are stronger. In contrast, during medial syllables, adults have significantly higher mean IAC values in the gamma band. In adolescents, edges in the low beta band have greater

relative strength compared to edges in other bands, whereas onset syllable theta edge strength is the highest for adults.

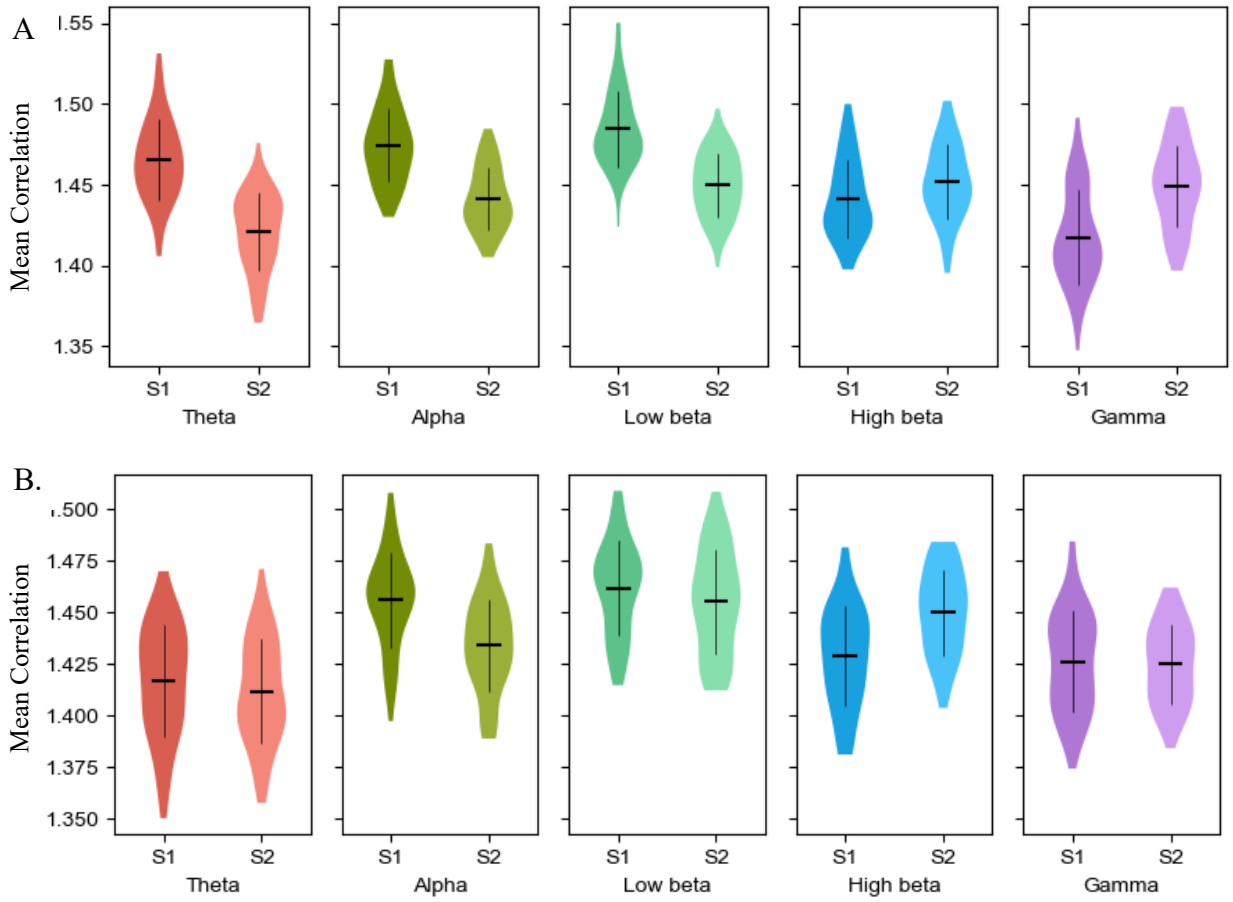

Figure 5.2 Mean IAC value distributions. Violins represent distribution of mean values for 68 labels in the Desikan-Kiliany atlas. Thick black horizontal bars indicate the mean, while vertical black bars indicate the standard deviation. A. Mean correlation distribution for adults. B. Mean correlation distribution for adolescents.

Correlation matrices from temporal windows of interest were the basis for graph theory measure calculation, since network structure changes between probability conditions is of interest. Both node strength and eigenvector centrality were calculated for each subject individually using networkx, then averaged across subjects to produce group mean distributions.

Node Strength by Frequency Band and Syllable Type

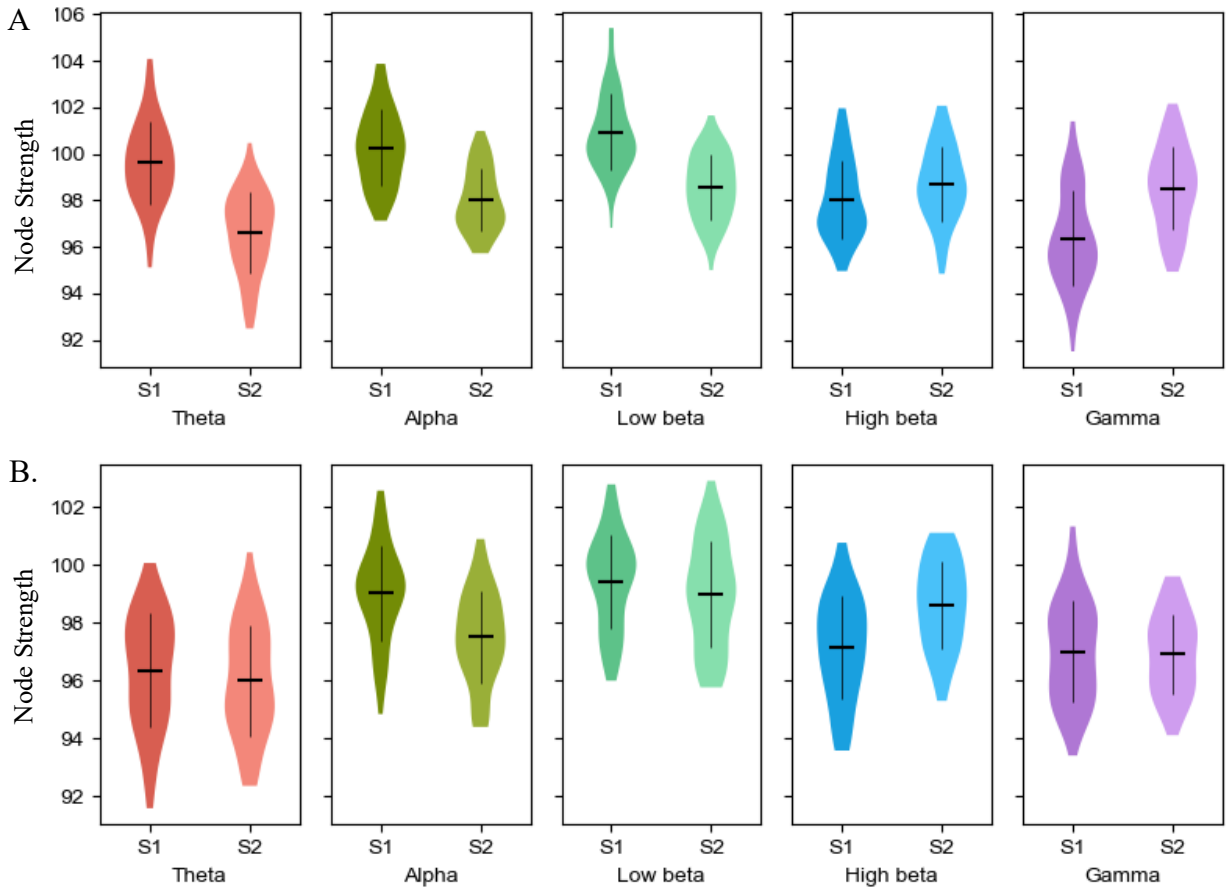

Figure 5.3 Mean node strength distributions. Violins represent distribution of mean node strength values for 68 labels in the Desikan-Kiliany atlas. Thick black horizontal bars indicate the mean, while vertical black bars indicate the standard deviation. A. Mean correlation distributions for adults. B. Mean correlation distributions for adolescents.

Distributions differ significantly between onset and medial syllables in all bands for adult participants (Figure 5.3). For adults, the direction that node strength trends across frequency bands changes between onset and medial syllables. In onset syllables, node strength decreases with increasing frequency; in medial syllables, edge strength increases with increasing frequency (Table 5.2). In adolescents, a similar tradeoff occurs from onset to medial syllables, except that low beta node strength is persistently elevated for adolescents.

	S1	***S2***	***Mean diff (95% CI)***	***p-value***
Theta ***	99.6 (1.8)	96.6 (1.8)	3.0 (2.4, 3.6)	< 2.2e-16
Alpha ***	100.3 (1.6)	97.9 (1.4)	2.3 (1.8, 2.8)	8.30e-15
Low beta ***	100.9 (1.7)	98.6 (1.4)	2.4 (1.8, 2.9))	3.87e-15
High beta *	98.0 (1.7)	98.7 (1.6)	-0.7 (-1.3, -0.1)	0.01463
Gamma ***	96.4 (2.1)	98.5 (1.8)	-2.2 (-2.8, -1.5)	1.08e-09

Table 5.2 Results of t-tests comparing node strength distributions between onset and medial syllables in adult participants. P-values are uncorrected for multiple comparisons.

In adolescent participants, node strength distributions differ significantly in alpha and high beta bands across syllables. Similarly to adults, node strength is greater for low frequency bands during onsets, whereas the high beta band increases for medial syllables (Table 5.3).

	S1	***S2***	***Mean diff (95% CI)***	***p-value***
Theta	96.4 (2.0)	96.0 (1.9)	0.4 (-0.3, 1.0)	0.2806
Alpha ***	99.0 (1.7)	97.5 (1.6)	1.5 (0.95, 2.1)	3.08e-07
Low beta	99.4 (1.6)	99.0 (1.9)	0.5 (-0.1, 1.1)	0.1301
High beta ***	97.1 (1.8)	98.6 (1.5)	-1.5 (-2.0, -0.9)	9.47e-07
Gamma	97.0 (1.8)	96.9 (1.4)	0.1 (-0.5, 0.6)	0.7513

Table 5.3 Results of t-tests comparing node strength distributions between onset and medial syllables in adolescent participants. P-values are uncorrected for multiple comparisons.

Between adolescents and adults, node strength is higher for adults in most bands except in the gamma band during onset syllables (Table 5.4).

	Adult	***Adolescent***	***Mean diff (95% CI)***	***p-value***
Theta ***	99.6 (1.8)	96.4 (2.0)	3.3 (2.6, 3.9)	< 2.2e-16
Alpha ***	100.3 (1.6)	99.0 (1.7)	1.3 (0.7, 1.8)	1.8e-05
Low beta ***	100.9 (1.7)	99.4 (1.6)	1.5 (0.9, 2.1)	4.2e-07
High beta **	98.0 (1.7)	97.1 (1.8)	0.9 (0.3, 1.4)	0.004
Gamma	96.4 (2.1)	97.0 (1.8)	-0.6 (-1.3, 0.0)	0.06

Table 5.4 Results of t-tests comparing node strength distributions between adult and adolescent populations for onset syllables.

	Adult	*Adolescent*	*Mean diff (95% CI)*	*p-value*
Theta *	96.6 (1.8)	96.0 (1.9)	0.6 (-0.0, 1.2)	0.05
Alpha *	97.9 (1.4)	97.5 (1.6)	0.5 (0.0, 1.0)	0.05
Low beta	98.6 (1.4)	99.0 (1.9)	-0.4 (-0.9, 0.2)	0.17
High beta	98.7 (1.6)	98.6 (1.5)	0.1 (-0.4, 0.6)	0.70
Gamma ***	98.5 (1.8)	96.9 (1.4)	1.6 (1.1, 2.2)	3.0e-08

Table 5.5 Results of t-tests comparing node strength distributions between adult and adolescent populations for medial syllables.

In medial syllables, the margin between adult and adolescent node strength decreases (Table 5.5). The gamma band alone differs strongly between adults and adolescents in medial syllables, demonstrating significantly higher mean connectivity for adults, reflecting the much stronger medial syllable connectivity bump for adults compared to adolescents.

Overall, adolescent patterns of connectivity largely recapitulate patterns in adult connectivity except that adolescent syllable adaptation is less pronounced. While adolescents do have stronger low frequency connectivity for onset syllables, the adaptation is less pronounced, particularly in the theta band where the medial syllable connectivity suppression is modest. Similarly, while high beta band node strength increases for medial syllables in both populations, the high frequency bump for medial syllables does not extend into the gamma band for adolescents. This is indicative of less connective flexibility for adolescent learners. Because adolescents have lower mean node strength values, particularly during onset syllables, it suggests that adolescents mobilize cortical connections during high entropy moments less powerfully than adults. Muted adaptations for the adolescent population are suggestive of a developmental difference, but it is also possible that adolescent learners might demonstrate less refined IAC adaptation between syllables because of greater cognitive resources allocated to the social feedback task they performed.

Eigenvector Centrality by Frequency Band and Syllable Type

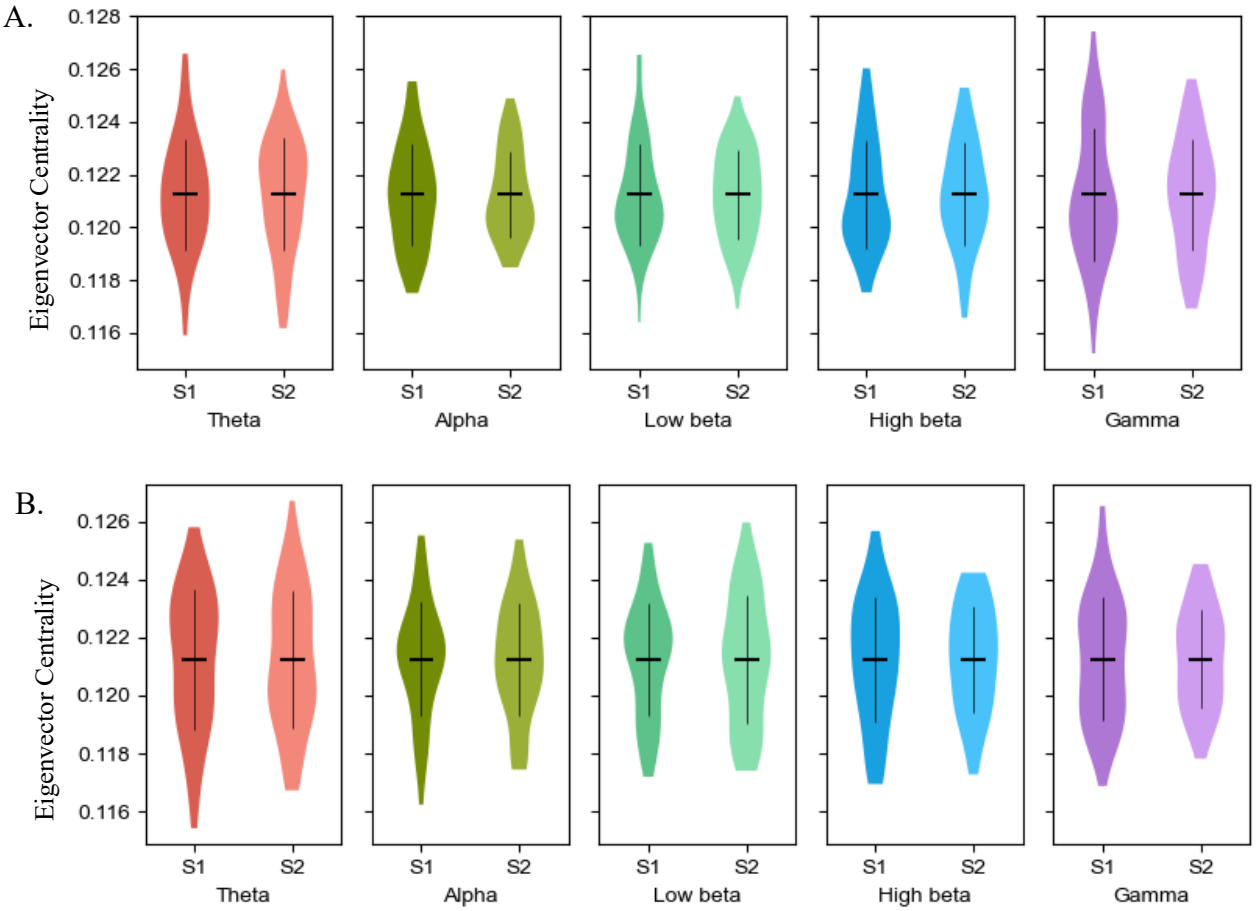

Figure 5.4 Mean eigenvector centrality distributions. Violins represent distribution of mean EC values for 68 labels in the Desikan-Kiliany atlas. Thick black horizontal bars indicate the mean, while vertical black bars indicate the standard deviation. A. Mean correlation distributions for adults. B. Mean correlation distributions for adolescents.

Comparing distributions between onset and medial syllables, eigenvector centrality distributions remain constant across syllables in all frequency bands and in both adult and adolescent populations as shown in Figure 5.4. As previously discussed, constancy of the overall EC distribution across cortical labels is expected given the preservation of edge weights. Onset syllables for theta and gamma bands have the strongest tendency to exhibit tails in the distribution, a few regions peaking as influencers, a few regions losing influencer status.

	S1	***S2***	***Mean diff (95 CI)***	***p-value***
Theta	0.1212 (0.0021)	0.1212 (0.0021)	0.0 (0.0, 0.0)	1
Alpha	0.1213 (0.0019)	0.1213 (0.0016)	0.0 (0.0, 0.0)	0.99
Low beta	0.1213 (0.0020)	0.1213 (0.0017)	0.0 (0.0, 0.0)	0.99
High beta	0.1213 (0.0020)	0.1213 (0.0020)	0.0 (0.0, 0.0)	1
Gamma	0.1212 (0.0025)	0.1212 (0.0021)	0.0 (0.0, 0.0)	0.99

Table 5.6 Results of t-tests comparing eigenvector centrality distributions between onset and medial syllables for adult participants.

	S1	***S2***	***Mean diff (95 CI)***	***p-value***
Theta	0.1212 (0.0024)	0.1212 (0.0024)	0.0 (0.0, 0.0)	1
Alpha	0.1213 (0.0020)	0.1213 (0.0019)	0.0 (0.0, 0.0)	1
Low beta	0.1213 (0.0020)	0.1212 (0.0024)	0.0 (0.0, 0.0)	0.99
High beta	0.1212 (0.0022)	0.1213 (0.0018)	0.0 (0.0, 0.0)	0.99
Gamma	0.1212 (0.0021)	0.1213 (0.0017)	0.0 (0.0, 0.0)	0.98

Table 5.7 Results of t-tests comparing eigenvector centrality distributions between onset and medial syllables for adolescent participants.

Comparing EC distributions between adult and adolescent participants as shown in Table 5.6 and Table 5.7, EC distributions do not vary between populations in either onset or medial syllables. Homogeneity of EC scores across nodes is a natural consequence of choosing weighted fully dense networks, as the resulting networks are highly interconnected, but it is worth noting that functional connections are sufficiently dense in an adolescent subject pool replete with young subjects to replicate the adult trends.

	Adult	***Adolescent***	***Mean diff (95% CI)***	***p-value***
Theta	0.1212 (0.0021)	0.1212 (0.0024)	0 (0.0, 0.0)	0.98
Alpha	0.1213 (0.0019)	0.1213 (0.0019)	0 (0.0, 0.0)	0.99
Low beta	0.1213 (0.0020)	0.1213 (0.0019)	0 (0.0, 0.0)	0.99
High beta	0.1213 (0.0020)	0.1212 (0.0022)	0 (0.0, 0.0)	0.99
Gamma	0.1212 (0.0025)	0.1212 (0.0021)	0 (0.0, 0.0)	0.98

Table 5.8 Results of t-tests comparing eigenvector centrality distributions between adult and adolescent participants for onset syllables.

	Adult	***Adolescent***	***Mean diff (95% CI)***	***p-value***
Theta	0.1212 (0.0022)	0.1212 (0.0024)	0 (0.0, 0.0)	0.99
Alpha	0.1213 (0.0016)	0.1213 (0.0019)	0 (0.0, 0.0)	0.99
Low beta	0.1213 (0.0017)	0.1212 (0.0022)	0 (0.0, 0.0)	0.98
High beta	0.1213 (0.0019)	0.1213 (0.0018)	0 (0.0, 0.0)	0.99
Gamma	0.1212 (0.0021)	0.1213 (0.0017)	0 (0.0, 0.0)	0.98

Table 5.9 Results of t-tests comparing eigenvector centrality distributions between adult and adolescent participants for medial syllables.

As expected, eigenvector centrality distributions over the cortex remain constant between syllables and populations (Table 5.8 and Table 5.9).

Although EC scores are numerically close together because of fundamental network characteristics like the interconnectedness of the matrices and the number of nodes, z-scoring graph theory metrics allows key differences in regional hubness to be observable. For IAC graph theory measures, z-scoring is performed within each frequency band but across syllables for each population, so that hubness across syllables can be compared. Syllable differences are z-scored separately. While significant network dynamism is evidenced by overall network distributions compared between syllables, plots of z-scored regions make network dynamics even more apparent between onset and medial syllables, as shown by Figure 5.5. While certain regions appear repeatedly across frequency bands, such as the left superior temporal sulcus (Table 5.10), almost all regions vary in connectedness between syllables, exhibiting low connectedness stability across syllables. In contrast, more regions retain high eigenvector centrality between syllables; in other words, despite retaining a more modest set of connections for medial syllables than for onsets, regions like the left inferior parietal play a strong influencer role in the network consistently.

Regions by Z-Scored Node Strength

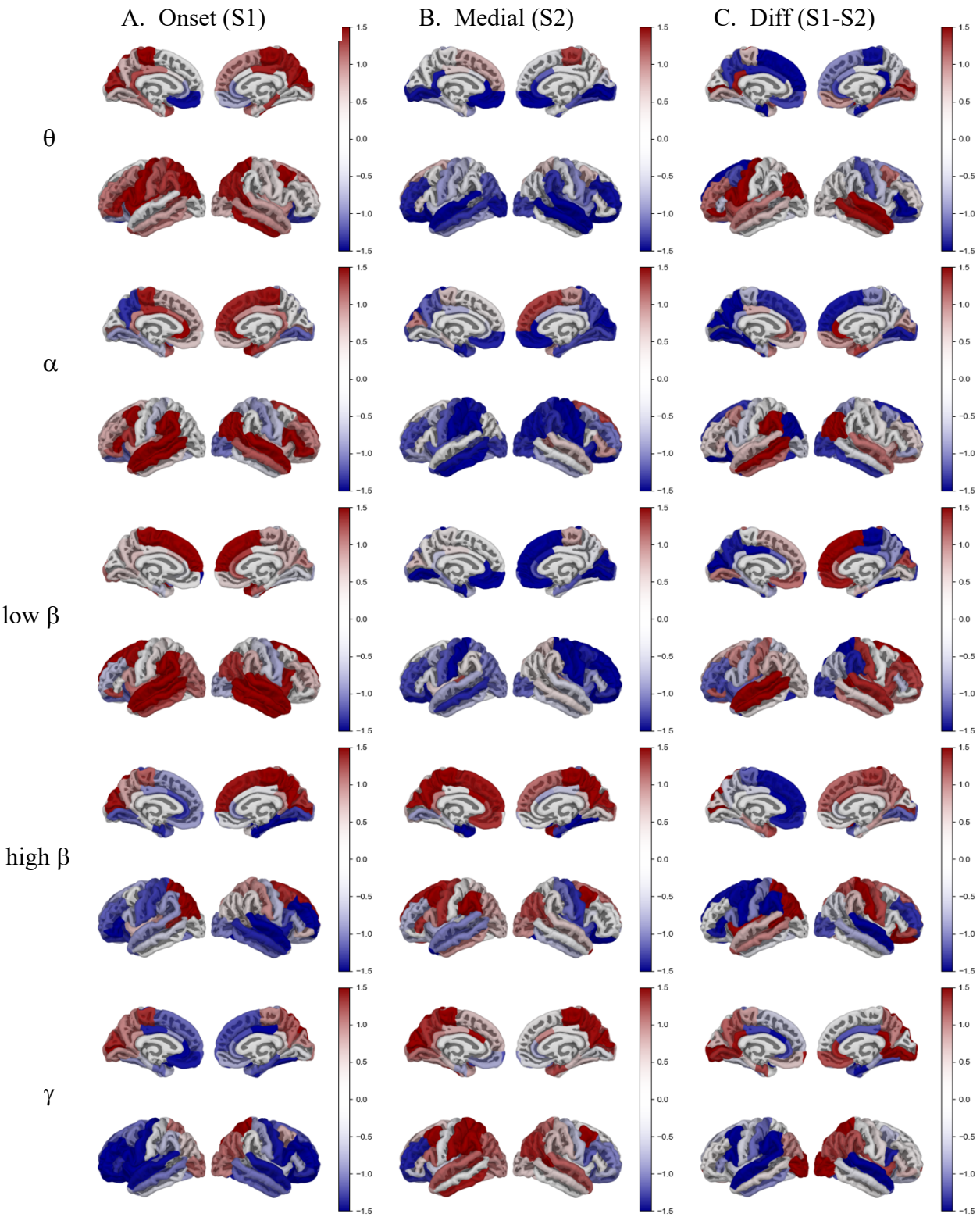

Figure 5.5 Z-scored node strength for adult participants plotted on the inflated template cortical surface across bands and syllables. A. Onset syllables. B. Medial syllables. C. Syllable differences.

	Onset (S1)	***Medial (S2)***	***Difference (S1-S2)***
Theta	Inf. Parietal (L) Caud. Mid. Frontal (R) Pars Op. (L)	Paracentral (R) Sup. Frontal (L) Caud. Mid. Frontal (R)	Inf. Parietal (L) Precentral (L) Sup. Temporal (R)
Alpha	Bank STS (L) Temp. Pole (R) Mid. Temporal (L)	Sup. Frontal (R) Cuneus (L) Bank STS (R)	Mid. Temporal (L) Bank STS (L) Supramarginal (L)
Low beta	Bank STS (L) Bank STS (R) Trans. Temporal (L)	Trans. Temporal (L) Trans. Temporal (R) Paracentral (R)	Bank STS (L) Mid. Temporal (L) Sup. Frontal (R)
High beta	Paracentral (R) Sup. Parietal (L) Inf. Parietal (L)	Supramarginal (L) Paracentral (L) Caud. Ant. Cing (L)	Sup. Parietal (L) Bank STS (L) Post Central (R)
Gamma	Sup. Parietal (R) Pericalcarine (L) Cuneus (L)	Supramarginal (L) Bank STS (R) Caud. Mid. Frontal (R)	Sup. Parietal (R) Lat. Occipital (R) Lat. Occipital (L)

Table 5.10 Top three regions with the strongest node strength by band and syllable in adult participants.

Highly connected regions in adult participants feature core auditory and speech processing regions like the left pars opercularis, the bank of the left superior temporal sulcus, and the left inferior parietal region (Table 5.10). Regions that show the strongest adaptation between syllables differ somewhat from regions with highest node strength. Strong adaptors are primarily temporal and parietal but include motor regions like the pre- and post-central gyri, as well as frontal areas such as the superior frontal gyrus. Notably, highly connected regions show more variability across frequencies when connectivity is assessed via IAC compared to AEC.

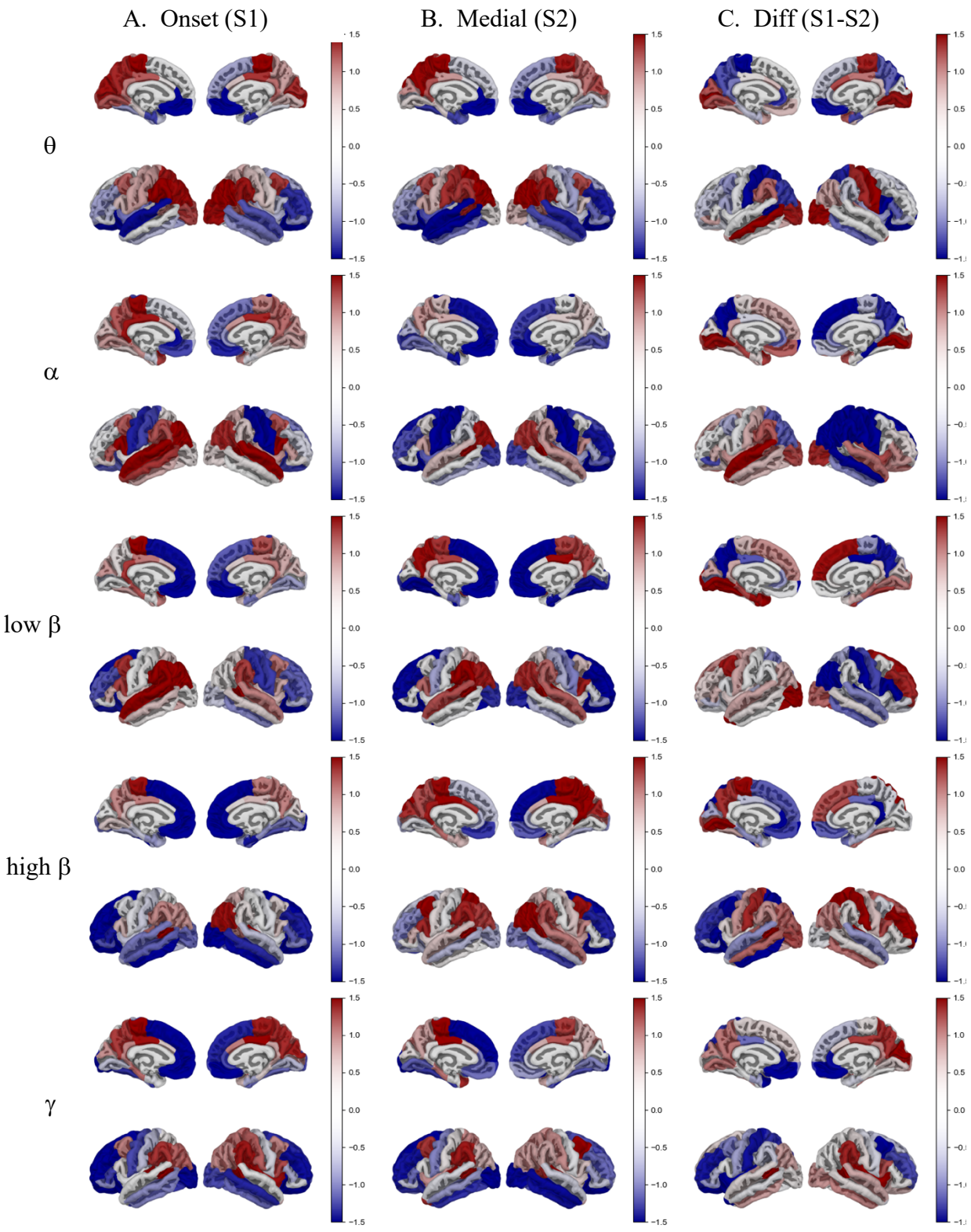

Figure 5.6 Z-scored node strength for adolescent participants plotted on the inflated template cortical surface across bands and syllables. A. Onset syllables. B. Medial syllables. C. Syllable differences.

	Onset (S1)	***Medial (S2)***	***Difference (S1-S2)***
Theta	Inf. Parietal (R) Paracentral (R) Paracentral (L)	Paracentral (L) Sup. Parietal (L) Inf. Parietal (L)	Mid. Temporal (L) Pericalcarine (L) Precentral (R)
Alpha	Bank STS (L) Bank STS (R) Trans. Temporal (L)	Bank STS (R) Bank STS (L) Inf. Parietal (L)	Trans. Temporal (L) Pericalcarine (L) Sup. Temporal (L)
Low beta	Supramarginal (L) Bank STS (L) Inf. Parietal (L)	Trans. Temporal (R) Supramarginal (L) Trans. Temporal (L)	Fusiform (L) Lingual (L) Lat. Occipital (L)
High beta	Bank STS (L) Trans. Temporal (R) Inf. Parietal (R)	Post. Cing. (L) Inf. Parietal (R) Post. Cing. (R)	Lingual (L) Trans. Temporal (R) Bank STS (L)
Gamma	Trans. Temporal (R) Bank STS (L) Bank STS (R)	Post. Cingulate (L) Paracentral (L) Caud. Mid. Frontal (R)	Trans. Temporal (R) Bank STS (L) Cuneus (R)

Table 5.11 Top three regions with the strongest node strength by band and syllable in adolescent participants.

Like connectivity in the adult population, highly connected regions for adolescents feature auditory and speech processing regions (Figure 5.6). Inferior frontal gyral regions like the pars opercularis have less pronounced hubness for adolescents compared to adults, not appearing in any of the top three hubs for any band (Table 5.11). A trend unique to adolescent participants is that visual regions do not score as highly for medial or onset syllables, but in all bands, at least one visual region scores among the strongest adaptors between syllables. Visual trials for adolescents did not align with auditory trials in timing, which means that visual region dynamics generated by visual trials are averaged out. Therefore, connection dynamics for visual regions must relate to auditory trials.

Regions by Z-Scored Eigenvector Centrality by Band and Syllable

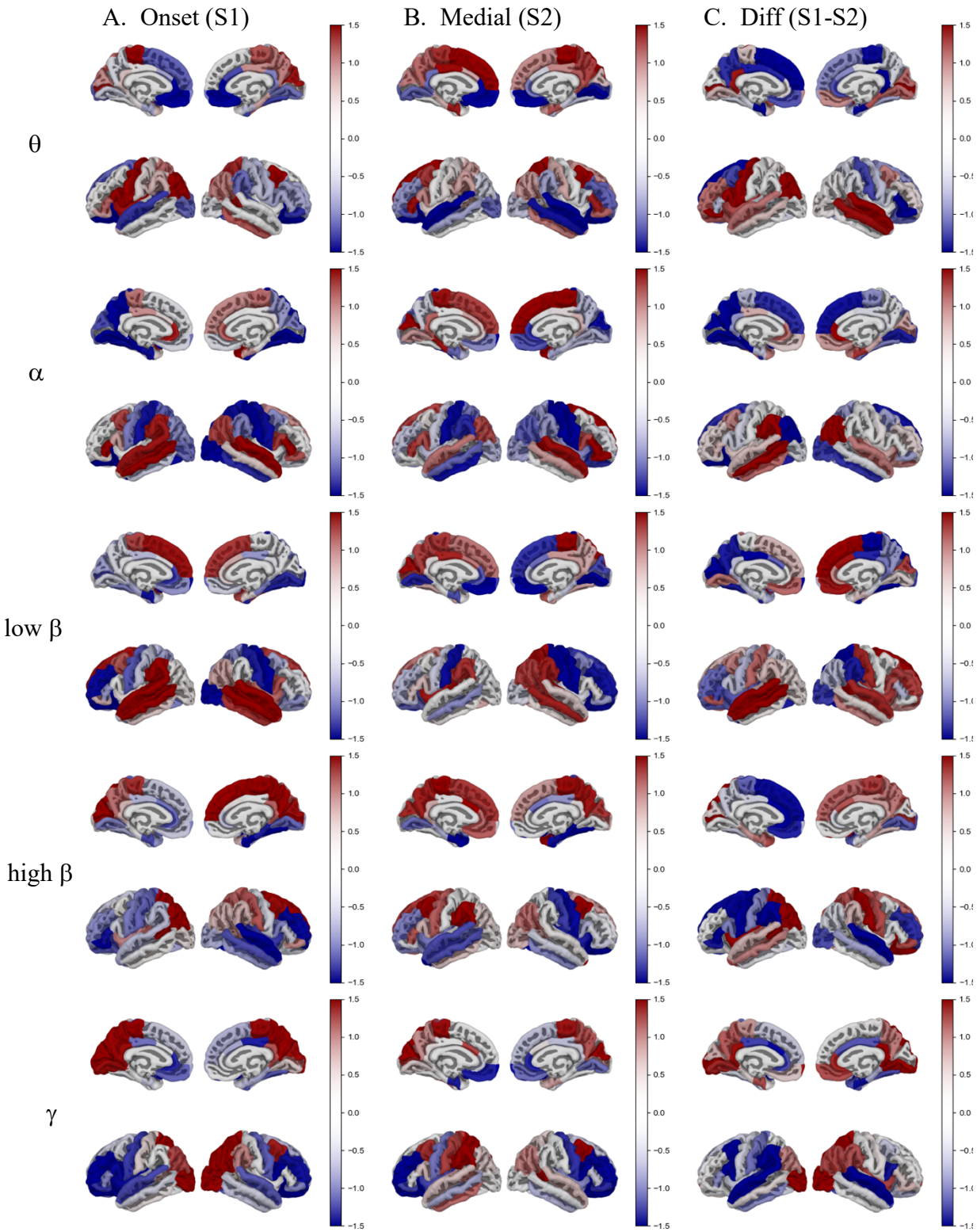

Figure 5.7 Z-scored eigenvector centrality for adult participants plotted on the inflated template cortical surface across bands and syllables. A. Onset syllables. B. Medial syllables. C. Syllable differences.

	Onset (S1)	***Medial (S2)***	***Difference (S1-S2)***
Theta	Inf. Parietal (L) Pars Op. (L) Caud. Mid. Frontal (R)	Paracentral (R) Sup. Frontal (L) Post. Cing. (L)	Inf. Parietal (L) Sup. Temporal (R) Precentral (L)
Alpha	Bank STS (L) Temp. Pole (R) Mid. Temporal (L)	Sup. Frontal (R) Cuneus (L) Bank STS (R)	Mid. Temporal (L) Bank STS (L) Supramarginal (L)
Low beta	Bank STS (L) Bank STS (R) Trans. Temporal (L)	Trans. Temporal (L) Trans. Temporal (R) Paracentral (R)	Bank STS (L) Mid. Temporal (L) Sup. Frontal (R)
High beta	Paracentral (R) Sup. Parietal (L) Precuneus (R)	Paracentral (L) Supramarginal (L) Caud. Ant. Cing (L)	Bank STS (L) Sup. Parietal (L) Post Central (R)
Gamma	Sup. Parietal (R) Pericalcarine (L) Cuneus (L)	Supramarginal (L) Caud. Mid. Frontal (R) Bank STS (R)	Sup. Parietal (R) Lat. Occipital (R) Pericalcarine (L)

Table 5.12 Top three regions with the strongest eigenvector centrality by band and syllable in adult participants.

When assessed with eigenvector centrality, strong hubs for adults look very similar to strong hubs identified by node strength (see Figure 5.7), but regions like the left pars opercularis and left posterior cingulate rank more highly as network influencers (Table 5.12). Overall, hubs scoring highly in EC for adults are strongly concentrated in speech regions with additions from cingulate areas, except in the gamma band where a few select visual regions are strongly connected to network hubs, notably the left pericalcarine (left V1).

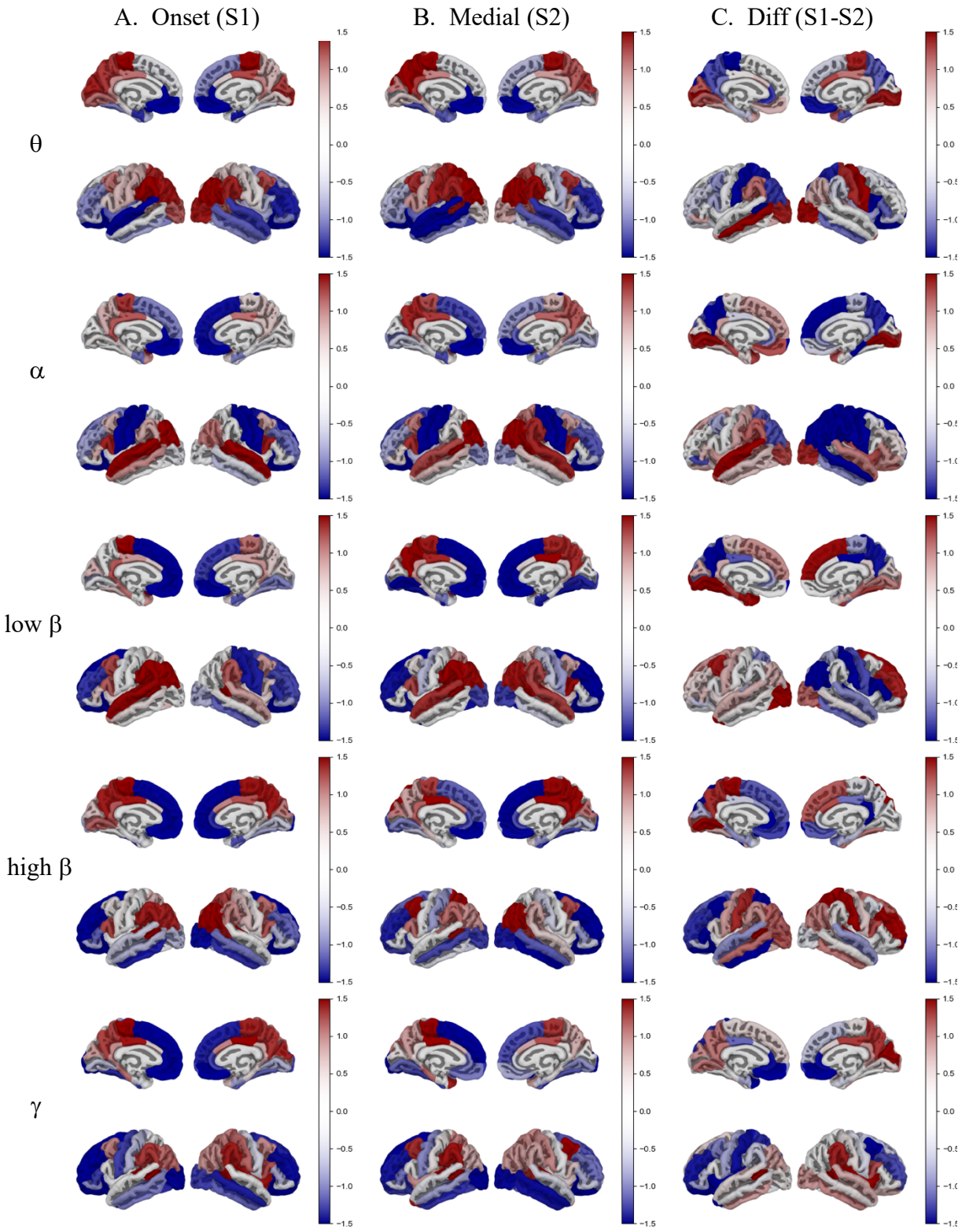

Figure 5.8 Z-scored eigenvector centrality for adolescents plotted on the inflated template cortical surface across bands and syllables. A. Onset syllables. B. Medial syllables. C. Syllable differences.

	Onset (S1)	***Medial (S2)***	***Difference (S1-S2)***
Theta	Paracentral (R) Inf. Parietal (R) Paracentral (L)	Paracentral (L) Inf. Parietal (R) Inf. Parietal (L)	Mid. Temporal (L) Pericalcarine (L) Paracentral (R)
Alpha	Bank STS (L) Bank STS (R) Trans. Temporal (L)	Bank STS (R) Bank STS (L) Inf. Parietal (L)	Pericalcarine (L) Trans. Temporal (L) Sup. Temporal (L)
Low beta	Supramarginal (L) Bank STS (L) Inf. Parietal (L)	Trans. Temporal (R) Supramarginal (L) Bank STS (L)	Fusiform (L) Lingual (L) Lat. Occipital (L)
High beta	Bank STS (L) Trans. Temporal (R) Paracentral (L)	Post. Cingulate (L) Inf. Parietal (R) Precuneus (R)	Lingual (L) Trans. Temporal (R) Bank STS (R)
Gamma	Trans. Temporal (R) Bank STS (L) Bank STS (R)	Paracentral (L) Post. Cingulate (L) Caud. Mid. Frontal (R)	Trans. Temporal (R) Cuneus (R) Bank STS (L)

Table 5.13 Top three regions with the strongest eigenvector centrality by band and syllable in adolescent participants.

For adolescents, regions with high EC largely repeat hubs scoring highly for node strength, but as with adults, a few regions are more influential than connected, namely the left bank of the superior temporal sulcus and the right inferior parietal region (Figure 5.8). The trend of adolescent visual connections exhibiting strong adaptation between onset and medial syllables is reflected in EC measures as well as node strength (Table 5.13). The degree of adaptation is not marginal or ambiguous for visual regions; for example, left V1 node strength adaptation from onset to medial syllables is double the value of the next highest adaptor. While this trend may not immediately seem a natural consequence of the auditory task, it is interpretable from the vantage point of predictive coding as an evolutionary survival mechanism. Onset syllables are characterized by high entropy (in other words, subjects can't predict what's coming). The

establishment of strong connections from auditory regions to other sensory modalities like the visual system during moments of uncertainty could provide a survival advantage. Primed cross-modal connections might allow for rapid bottom-up cues to pass from the auditory system to the visual system in the event that incoming auditory stimuli signal danger during a high entropy moment. Entropy-responsive connections like this may be more persistent in adolescent populations than in adults.

Top Edges in Adult Participants

Top edges for adult participants vary across frequency and feature diverse regions (Figure 5.9). Theta, high beta, and gamma bands feature strong parietal connections to temporal and inferior frontal gyral areas for onset syllables. For medial syllables, cingulate connections take center stage, along with connections to parahippocampal and entorhinal areas. Circle plots in Figure 5.9 clearly show that edges formed during onset syllables are stronger than edges formed during medial syllables in theta, alpha, and low beta bands. In the upper frequency bands, edges are stronger for medial syllables.

IAC networks feature many more strong inter-hemispheric connections than AEC networks, especially in the low beta network. Overall, patterns of connection vary significantly across frequency bands, as well as between syllables within a frequency band. A notable exception is that high beta and gamma networks during medial syllables share multiple similarities. Both feature strong connections from the right bank of the superior temporal sulcus to left hemispheric speech regions, along with a few other key hubs like the caudal middle frontal region and the left supramarginal gyrus (Table 5.14). Unlike AEC networks, strong visual connections are limited to the high frequency bands.

Edge Strength Circle Plots by Frequency and Syllable Type for Adults

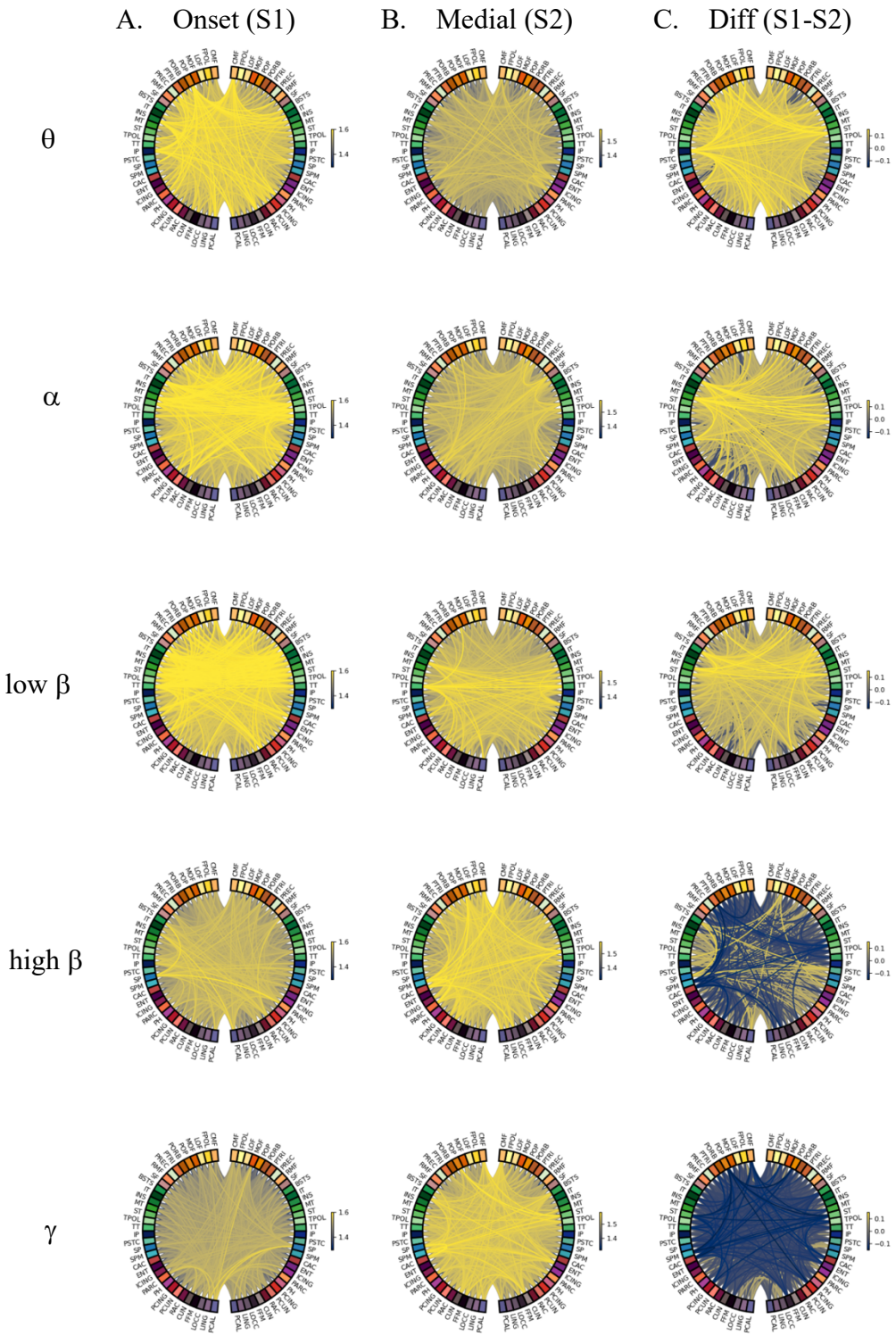

Figure 5.9 Strongest edges by frequency band and syllable type. Regions are generally organized spatially; frontal regions on top, occipital on the bottom, temporal regions in the middle. A. Onset syllables. B. Medial syllables. C. Syllable differences.

	Onset (S1)	***Medial (S2)***	***Difference (S1-S2)***
Theta	Pars Opercularis L to Inf. Parietal L	Entorhinal L to Pars Orbitalis R	Pars Opercularis L to Inf. Parietal L
	Insula L to Inf. Parietal L	Entorhinal L to Caud. Mid. Front. R	Pars Orbitalis L to Inf. Parietal L
	Caud. Mid. Front. R to Insula L	Isthmus Cing. R to Paracentral R	Pericalcarine R to Inf. Parietal L
Alpha	Sup. Temp. R to Bank of STS L	Parahippocampal L to Sup. Front. R	Insula R to Mid. Temp. L
	Mid. Temp. L to Trans. Temp. R	Sup. Front. R to Pars Orbitalis R	Trans. Temp. R to Mid. Temp. L
	Temp. Pole R to Bank of STS L	Sup. Front. R to Sup. Temp. R	Sup. Temp. R to Bank of STS L
Low beta	Bank Of STS L to Sup. Temp. R	Trans. Temp. R to Trans. Temp. L	Bank Of STS L to Mid. Temp. L
	Mid. Temp. R to Bank of STS L	Insula L to Trans. Temp. R	Sup. Temp. R to Bank of STS L
	Sup. Temp. R to Sup. Temp. L	Trans. Temp. R to Insula L	Sup. Temp. R to Pars Orbitalis L
High beta	Sup. Parietal L to Paracentral R	Supramarginal L to Caud. Ant. Cing. L	Bank Of STS L to Sup. Parietal L
	Bank Of STS L to Sup. Parietal L	Lat. Occipital R to Caud. Ant. Cing. L	Lat. Orbitofront. R to Trans. Temp. L
	Pericalcarine R to Insula L	Paracentral L to Pericalcarine R	Pericalcarine L to Lat. Occipital L
Gamma	Pericalcarine L to Sup. Parietal R	Supramarginal L to Caud. Ant. Cing. L	Pericalcarine L to Sup. Parietal R
	Sup. Parietal R to Lingual L	Caud. Mid. Front. L to Caud. Ant. Cing. R	Sup. Parietal R to Pericalcarine L
	Med. Orbitofront. R to Pericalcarine L	Sup. Temp. R to Pars Opercularis L	Entorhinal L to Sup. Parietal R

Table 5.14 Top three strongest edges by band and syllable in adult participants.

Edge Strength Circle Plots by Frequency and Syllable Type for Adolescents

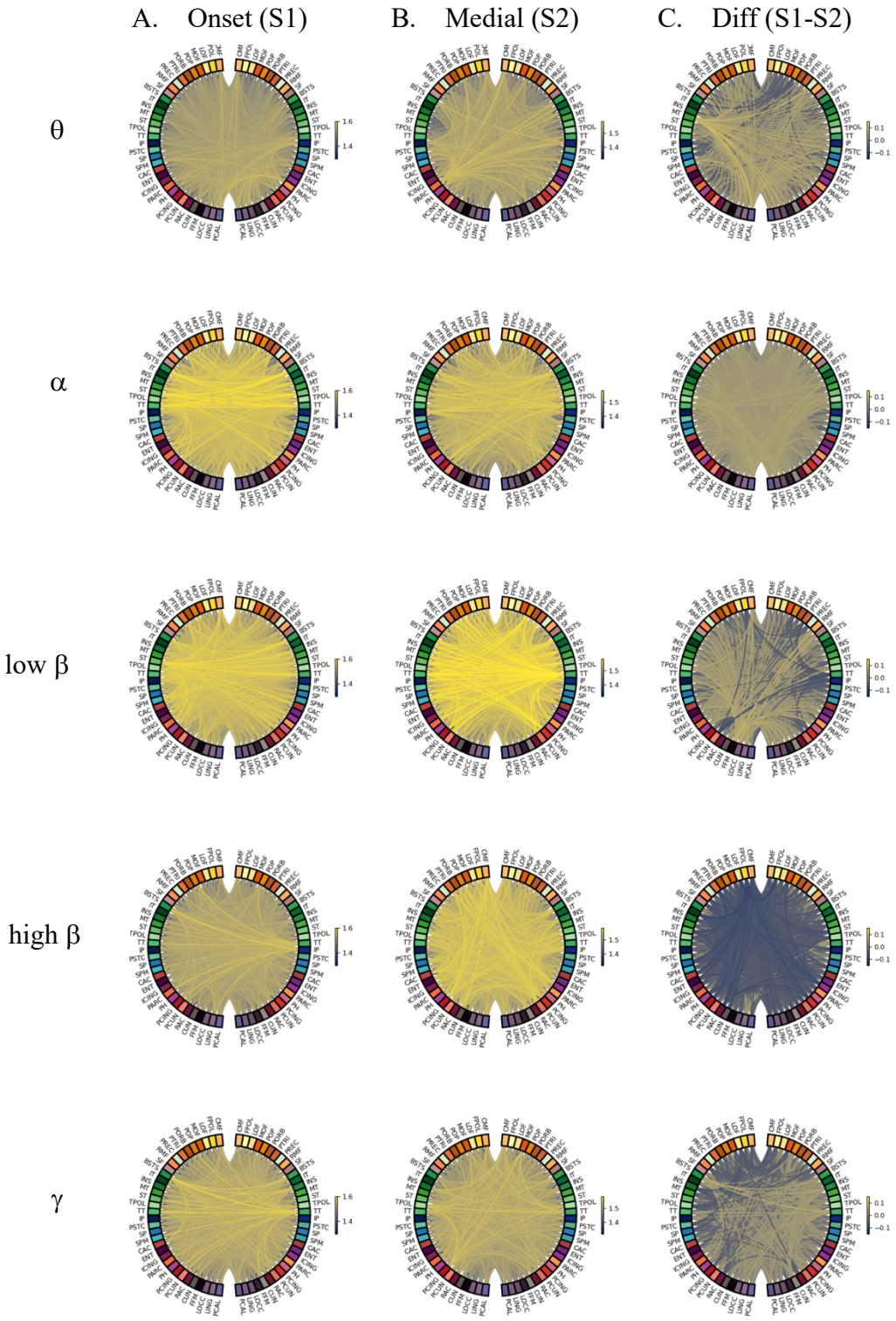

Figure 5.10 Strongest edges by frequency band and syllable type for adolescents. Regions are generally organized spatially; frontal regions on top, occipital on the bottom, temporal regions in the middle. A. Onset syllables. B. Medial syllables. C. Syllable differences.

	Onset (S1)	***Medial (S2)***	***Difference (S1-S2)***
Theta	Paracentral R to Lingual L	Paracentral L to Inf. Temp. R	Mid. Temp. L to Pericalcarine L
	Paracentral R to Pericalcarine L	Caud. Mid. Front. R to Paracentral L	Lingual R to Mid. Temp. L
	Paracentral R to Lat. Occipital R	Paracentral L to Parahippocampal R	Mid. Temp. L to Lingual L
Alpha	Bank Of STS R to Sup. Temp. L	Bank Of STS R to Sup. Temp. L	Trans. Temp. L to Parahippocampal L
	Bank Of STS L to Sup. Temp. R	Trans. Temp. R to Inf. Parietal L	Lingual R to Sup. Temp. L
	Sup. Temp. L to Trans. Temp. R	Trans. Temp. R to Sup. Temp. L	Sup. Temp. L to Lingual R
Low beta	Bank Of STS R to Sup. Temp. L	Trans. Temp. R to Sup. Temp. L	Fusiform L to Lat. Occipital L
	Trans. Temp. R to Sup. Temp. L	Sup. Temp. L to Trans. Temp. R	Rost. Mid. Front. R to Fusiform L
	Sup. Temp. L to Insula R	Supramarginal L to Trans. Temp. R	Fusiform L to Rost. Mid. Front. R
High beta	Bank Of STS L to Inf. Parietal R	Post. Cing. L to Sup. Temp. R	Lingual L to Trans. Temp. R
	Bank Of STS L to Trans. Temp. R	Caud. Mid. Front. L to Parahippocampal L	Cuneus R to Lingual L
	Trans. Temp. R to Pars Opercularis L	Front. Pole L to Post. Cing. L	Trans. Temp. R to Postcentral R
Gamma	Bank Of STS L to Trans. Temp. R	Post. Cing. L to Med. Orbitofront. R	Bank Of STS L to Trans. Temp. R
	Trans. Temp. R to Trans. Temp. L	Temp. Pole L to Post. Cing. L	Bank Of STS L to Insula R
	Bank Of STS L to Insula R	Insula L to Caud. Mid. Front. R	Bank Of STS L to Bank of STS R

Table 5.15 Top three strongest edges by band and syllable in adolescent participants.

Compared to adult connections, adolescent edges feature stronger right hemispheric connections across bands as shown in Figure 5.10. Also, adolescent edges notably feature less adaptation between syllables, evidenced by the more muted colors on the S1-S2 plots (adult and adolescent circle plots have fixed color bar limits to facilitate comparison across syllables and populations). Like adults, parahippocampal connections rank among the strongest edges for adolescents during medial syllables, but in theta and high beta bands rather than the alpha band.

In high frequency bands, note the strong role of the right transverse temporal region, featured much more prominently in adolescent networks compared to adult networks in these bands. Bilateral transverse temporal regions appear to share strong connections for adolescents in multiple bands, including alpha, low beta, high beta and gamma (Table 5.15).

Key Characteristics of IAC Networks

Overall, IAC networks feature regions of interest for language processing tasks in general and regions of interest for statistical learning specifically. Moreover, IAC connectivity responds to transitional probability of syllables in a speech stream. IAC values clearly modulate between expected and unexpected syllables, whether assessed over the full duration of the stimulus trial or within more limited temporal windows within the trial. IAC FC offers a robust basis for rejection of the null hypothesis of network equivalence between transitional probability conditions. Furthermore, connections in different carrier frequencies modulate in different temporal window with respect to stimulus onset.

Chapter 6: IAC Networks and Learning

Support vector machines provide an appropriate approach for testing the same questions of association with IAC networks as were tested for AEC networks, namely whether speech region connectivity predicts the N400 difference across subjects, and whether speech region connectivity predicts word learning in adolescents. In addition, because IAC connectivity measures can be contrasted between transitional probability conditions, more detailed examination is possible. Specifically, SVC is used to test whether speech network connections classify syllable type above chance.

Testing Transitional Probability Classification from IAC Connectivity

As with AEC connectivity metrics, support vector machine classification with five-fold cross-validation was chosen to test the relationship between speech networks and transitional probability condition because of the viability of the technique for high dimensional predictor data. Networks providing the features for testing were derived by collapsing IAC values for each edge over the data-driven temporal window of interest for each syllable as well as for each frequency band, and 231 connections between speech regions of interest were chosen as predictor vectors, consistent with testing for AEC networks. Predictor features and outcomes were scaled separately for training and testing data sets prior to fitting. Scikit-learn's implementation of SVC with a radial basis function kernel (C=0.11, gamma='scale') was applied to both adult and adolescent data sets (Pedregosa et al., n.d.). Five-fold cross-validation across subjects was performed using an 80-20 split (for adolescents, 86 subjects as training data and 21 subjects as test data, and for adults, 24 subjects as training data and 6 subjects as test). ROC AUC scores were averaged across folds to evaluate performance.

Band	***Mean ROC AUC***	***St. Dev.***
Theta	**0.64**	**0.13**
Alpha	**0.70**	**0.17**
Low Beta	**0.70**	**0.17**
High Beta	**0.63**	**0.06**
Gamma	0.41	0.09

Table 6.1 Syllable classification results in adults using support vector machine classification on band-limited networks derived from IAC values averaged during temporal windows of interest.

For adults, classification succeeds above chance in all bands except the gamma band (Table 6.1). Classification results indicate that patterns of connectivity among speech regions respond to transitional probability across subjects. In other words, networks respond strongly to whether an incoming stimulus is predictable or not.

Band	***Mean ROC AUC***	***St. Dev.***
Theta	**0.59**	**0.08**
Alpha	0.55	0.07
Low Beta	0.47	0.06
High Beta	0.51	0.06
Gamma	**0.58**	**0.08**

Table 6.2 Syllable classification results in adolescents using support vector machine classification on band-limited networks derived from IAC values averaged during temporal windows of interest.

In adolescents, classification is less robust than in adults, but still successful above chance in the theta band and in the gamma band (Table 6.2). Overall, results provide evidence that connectivity measured by IAC modulates according to transitional probability for both adults and adolescents, although only classification in the theta band is shared across both populations.

Testing N400 Difference Prediction from IAC Connectivity

Support vector regression methods for testing the association between IAC connectivity and the N400 difference are mostly consistent with methods for testing AEC connectivity, except that for IAC, condition differences were used as features rather than connection strength over time. Using condition differences as features tests the hypothesis that network adaptation, not just connection strength, predicts event-related adaptation, matching outcome and predictor characteristics more closely. Condition difference tensors for 231 edges of interest were averaged over the temporal windows of interest for each band, and 5-fold cross-validation was used to test the association between network differences and N400 differences in all bands.

		Mean R^2 across 5-fold cross-validation (SD)
Theta	*Adults*	-0.13 (0.12)
	T1	-0.01 (0.01)
Alpha	*Adults*	-0.19 (0.17)
	T1	0.01 (0.05)
Low beta l	*Adults*	-0.15 (0.14)
	T1	0.01 (0.02)
High beta	*Adults*	-0.13 (0.12)
	T1	-0.01 (0.01)
Gamma	*Adults*	-0.04 (0.07)
	T1	-0.01 (0.02)

Table 6.3 Support vector regression results predicting N400 difference in the superior temporal gyrus as a function of IAC connectivity in speech regions using 5-fold cross-validation across subjects.

Regression does not succeed above chance in any band for any population (Table 6.3). While mean R^2 values in the alpha and low beta bands are positive, standard deviations exceed the difference between the mean and zero. Evidence from regression indicates that connectivity assessed with IAC does not have a significant association with event-related neural adaptation.

Testing D-prime Prediction from IAC Connectivity in Adolescents

As with testing for AEC connectivity, SVR tests for association between IAC condition differences and D-prime scores as a continuous outcome. As a follow-up, SVC tests for association between IAC network adaptation and whether the subject is a strong learner (operationally defined as whether the subject's D-prime score falls in the upper half of the median split of D-prime values).

		Mean R^2 across 5-fold cross-validation (SD)
Theta	*T1*	-0.02 (0.02)
Alpha	*T1*	-0.14 (0.1)
Low beta	*T1*	-0.05 (0.03)
High beta	*T1*	-0.02 (0.02)
Gamma	*T1*	-0.031 (0.08)

Table 6.4 Support vector regression results predicting d-prime values as a function of IAC connectivity in speech regions in adolescents.

Testing D-prime scores as a continuous outcome, regression does not succeed above chance in any band (Table 6.4).

		Mean ROC AUC across 5-fold cross-validation (SD)
Theta	*T1*	**0.65 (0.15)**
Alpha	*T1*	0.41 (0.06)
Low beta	*T1*	0.45 (0.14)
High beta	*T1*	**0.60 (0.08)**
Gamma	*T1*	0.52 (0.17)

Table 6.5 Support vector classification predicting median split d-prime values as a function of IAC connectivity among speech regions in adolescents.

IAC connectivity in the theta band does succeed above chance in classifying subjects as strong learners (Table 6.5). This concords with successful syllable type classification by connectivity in the theta band for adolescents. Unlike syllable classification, the high beta band appears to be more predictive than the gamma band for the outcome of interest. As was shown in

Chapter 5, gamma band and high beta band networks have a number of similarities, but one of the limits of SVM as a technique is that it is not possible to tell whether similar edges (like connections to the right bank of the superior temporal sulcus) differentiate syllables and learners.

Altogether, SVM testing reveals evidence of association between connectivity measured with IAC and auditory statistical learning. While results vary somewhat in higher frequency bands, theta networks seem to respond to transitional probability and offer predictive value for pseudo-word learning in both adults and adolescents.

Chapter 7: Auditory Statistical Learning and Cortical Integration

The core research questions for this investigation have two-fold aims: to characterize networks detected by two measures of functional connectivity, and to determine if networks features predict measures of statistical learning in our populations. The over-arching goal of the investigation, however, is to critically examine results of connectivity estimation to evaluate the claim that connections evidence functional integration of the cortex, not artifacts of the recording, phenomena resulting from noise or SNR variation, or information redundant to event-related measures of neural adaptation.

Connectivity results representing genuine evidence of functional integration during statistical learning should align with prior knowledge in multiple core domains. First, as reviewed in Chapter 1, the connectivity methods employed should avoid major confounds and pitfalls known to affect estimation. Methods for this investigation were chosen for adequate control of signal leakage, relative robustness to SNR variability across cortical regions (compared to phase-based measures), compatibility with noise-control measures like movement compensation required for pediatric imaging, and suitability for first-pass exploratory investigations. Appropriate inversion methods, acceptable sizes for cortical parcels, and controls for between-condition SNR equivalence all justify high confidence that connectivity measures in this investigation are detecting real relationships between cortical regions and real condition contrasts, not noise or recording artifacts.

Next, to evidence functional integration in a useful way, connectivity measures should reveal links between regions known to be relevant to the task, e.g. motor-auditory integration for speech processing must be evidenced by motor-auditory connections. For this study, strong connections should involve the speech regions introduced in Chapter 2; in particular, connections

should relate left inferior frontal and superior temporal regions to each other and other parts of the cortex. Certainly, any exploratory investigation must leave room for surprising or unexpected nuance, but generally the spatial distribution of strong connections detected by the connectivity measure should concord with what is already known about regional participation in word segmentation[1].

If connections detected by the measure vary across carrier frequencies, the frequency characteristics of the connection should make sense in light of prior knowledge about oscillatory activity during speech processing. For example, the theta band, particularly in the left hemisphere, is strongly associated with word learning as well as visual statistical learning (Elmer et al., 2018; Spaak & Lange, 2020; Tóth et al., 2017), which makes theta band functional connections in the left hemisphere a strong candidate for relationship to transitional probability and predictive value for pseudo-word learning. In contrast, while gamma band power has been shown to related to word learning and prediction during language processing (Fitzgibbon et al., 2004; Gou et al., 2011; L. Wang et al., 2018), gamma may be a stronger candidate for local (within label) rather than long-distance connections .

The temporal sensitivity of the IAC method adds additional factors to consider when evaluating the likelihood that IAC edges reflect functionally relevant cortical coupling. Because IAC connectivity varies across the time course of each trial, an added constraint for IAC connections is that edge dynamics should make sense given the known properties of the event-

[1] See Bassett et al for a discussion of the significance of weak connections in a network (Bassett et al., 2012). Here, I do not mean to imply that weak network connections are insignificant, but rather, when choosing between different connectivity measures, the savvy researcher should opt for metrics that highlight the connections of interest.

related response to transitional probability. For example, results indicating that the primary auditory cortex forms strong alpha band connections with other speech regions in the left hemisphere during the N100 might reasonably provoke doubt. Similarly, results suggesting strong beta band connections from left hemispheric regions to the superior temporal gyrus during the N400 window during predictable medial syllables would not easily reconcile with prior knowledge, whereas theta connections indicating multi-region theta power during the late processing window in onset syllables would align well. Even if speech networks do not predict N400 amplitude difference, suggesting that different neural adaptations are tracked by FC and event-related analyses, FC results should accommodate event-related activity.

Moreover, IAC connectivity contrasts between transitional probability conditions should have interpretive value within a predictive coding framework. Successful pseudo-word learning from a speech stream results in listener expectation activation by pseudoword onsets. Theoretically, this should result in feedback signals propagating gain control from higher order language processing centers such as the inferior frontal gyrus to lower order auditory processing regions such as the transverse temporal gyrus.

I review connectivity results for the AEC method and the IAC method in light of the above considerations, but before beginning this evaluation, I report results of one additional analysis comparing group mean hubness for cortical labels in AEC networks to group mean hubness of cortical labels in IAC networks. Relatedness of AEC and IAC measures informs the final discussion.

AEC and IAC Hubness Tend Toward Inverse Correlation

An important sanity check for comparing the value of AEC and IAC connectivity measures is testing whether connectivity values of one measure predict connectivity values of the

other. The association between IAC and AEC connectivity can be examined by regressing AEC node strength and eigenvector centrality values against IAC values for each label in each frequency band for both adult and adolescent participants.

Linear regression was implemented in R using the "rigr" package for general linear modeling. Robust standard errors were calculated using sandwich estimators. Because the modeling is exploratory, not confirmatory in nature, p-values are uncorrected for multiple comparisons.

	Adult ***β (95% CI)***	***Adult*** ***Adjusted R^2 (p-val)***	***Adolescent*** ***β (95% CI)***	***Adolescent*** ***Adjusted R^2 (p-val)***
Theta (S1)	**-0.11 (-0.18, -0.05)**	**0.11 (0.002)**	**-0.29 (-0.34, -0.23)**	**0.53 (4.581e-16)**
Alpha (S1)	**-0.26 (-0.39, -0.13)**	**0.19 (0.0002)**	**-0.15 (-0.22, -0.07)**	**0.12 (0.0002)**
Low beta (S1)	-0.05 (-0.12, 0.01)	0.01 (0.11)	**-0.30 (-0.36, -0.23)**	**0.49 (3.318e-13)**
High beta (S1)	**-0.05 (-0.10, 0)**	**0.04 (0.03)**	**-0.35 (-0.41, -0.30))**	**0.65 (< 2.2e-16)**
Gamma (S1)	**-0.12, (-0.16, -0.07)**	**0.41 (4.628e-07)**	**-0.26 (-0.30, -0.21)**	**0.62 (< 2.2e-16)**
Theta (S2)	**-0.14 (-0.21, -0.07)**	**0.17 (0.0001)**	**-0.29 (-0.34, -0.24)**	**0.51 (< 2.2e-16)**
Alpha (S2)	**-0.17 (-0.33, -0.01)**	**0.04 (0.03)**	**-0.16 (-0.244, -0.08)**	**0.13 (0.0003)**
Low beta (S2)	-0.03 (-0.10, 0.05)	0.0 (0.47)	**-0.31 (-0.35, -0.26)**	**0.66 (< 2.2e-16)**
High beta (S2)	**-0.07 (-0.11, -0.03)**	**0.08 (0.002)**	**-0.39 (-0.47, -0.32)**	**0.58 (1.948e-15)**
Gamma (S2)	**-0.13 (-0.18, -0.08)**	**0.39 (1.639e-06)**	**-0.32 (-0.38, -0.27)**	**0.64 (< 2.2e-16)**

Table 7.1 Results of linear modeling regressing AEC node strength values against IAC node strength values. Bolded text indicates significant results. P-values are uncorrected for multiple comparisons.

All beta coefficients are negative, indicating that regions that are highly connected as assessed with IAC are much less connected when assessed with AEC (Table 7.1). In adults, the variance in AEC node strength explained by IAC node strength ranges from less than one percent to a little over forty percent, but in adolescents, IAC node strength explains over fifty percent of the variance in AEC node strength in all bands except alpha. Using eigenvector centrality as the measured of hubness, regression results are even more pronounced.

	Adult ***β (95% CI)***	***Adult*** ***Adjusted R^2 (p-val)***	***Adolescent*** ***β (95% CI)***	***Adolescent*** ***Adjusted R^2 (p-val)***
Theta (S1)	**-1.18 (-1.82, -0.55)**	**0.15 (0.0004)**	**-2.39 (-2.81, -1.96)**	**0.56 (< 2.2e-16)**
Alpha (S1)	**-2.55 (-3.79, -1.31)**	**0.20 (0.0001)**	**-1.31 (-2.08, -0.53)**	**0.09 (0.001)**
Low beta (S1)	-0.27 (-1.16, 0.61)	0.01 (0.10)	**-3.2 (-3.94, -2.54)**	**0.49 (1.456e-13)**
High beta (S1)	**-0.76 (-1.45, -0.07)**	**0.04 (0.03)**	**-4.5 (-5.1, -3.9)**	**0.73 (< 2.2e-16)**
Gamma (S1)	**-2.53 (-3.37, -1.7)**	**0.46 (7.272e-08)**	**-4.2 (-4.81, -3.66)**	**0.73 (< 2.2e-16)**
Theta (S2)	**-1.5 (-2.08, -0.87)**	**0.24 (7.617e-06)**	**-2.45 (-2.85, -2.04)**	**0.56 (< 2.2e-16)**
Alpha (S2)	**-1.57 (-3.017, -0.1149)**	**0.04 (0.03)**	**-1.4 (-2.24, -0.60)**	**0.10 (0.001)**
Low beta (S2)	-0.28 (-1.16, 0.61)	0.0 (0.53)	**-3.38 (-3.85, -2.92)**	**0.68 (< 2.2e-16)**
High beta (S2)	**-1.12 (-1.79, -0.45)**	**0.09 (0.001)**	**-5.02 (-5.87, -4.19)**	**0.65 (< 2.2e-16)**
Gamma (S2)	**-2.9 (-3.91, 1.88)**	**0.43 (3.534e-07)**	**-5.2 (-6.1, -4.4)**	**0.73 (< 2.2e-16)**

Table 7.2 Results of linear modeling regressing AEC eigenvector centrality values against IAC eigenvector centrality values. Bolded text indicates significant results. P-values are uncorrected for multiple comparisons.

Regression results reported in Table 7.2 show that AEC and IAC measures of connection tend toward inverse correlation, and strong antagonism between AEC and IAC hubness is evident in high frequency bands. Inverse correlation is not a fundamental property of the mathematics of the two metrics, as is made clear by the variation across frequencies, across populations, and across syllable types. In adults, the low beta band has no significant inverse relationship between slow and fast modulations, but in adolescents, the low beta band is highly antagonistic between slow and fast modulations. Adolescents exhibit the lowest antagonism between IAC and AEC metrics in the alpha band in terms of beta coefficient values, explained variance, and significance, while in adults, the beta coefficient in the alpha band is the highest of all the frequencies. In adults, beta coefficients, adjusted R^2 values, and significance levels vary between syllables, but in adolescents, the same variables respond to frequency but remain relatively consistent across syllable types.

The pattern of inverse correlation demonstrated by regressions results raises intriguing questions.

What explains the tendency of connected regions to gravitate either to slow or fast modulations? Rapid modulations in connectivity state, producing high IAC connectivity values, would not be represented well in AEC measures, so the lack of AEC strength exhibited by regions of high IAC hubness is not surprising. But rapid modulations could be nested within slower modulations suited to detection by the AEC measure. Generally, our data set show that regions tend to be hubs in one or the other. One potential explanation is suggested by the fact that AEC hubs tend to be visual and frontal regions, whereas IAC hubs tend to be temporal and parietal: perhaps temporal characteristics of the stimulus processed by a region dictates the temporal characteristics of the connections formed with other regions. Visual stimuli in our experiment were presented over the course of multiple seconds. Slow presentation of visual stimuli, contrasting with rapid temporal progression of the speech stream, might explain hub selection between the two measures.

What conditions produce a state in which slow and fast modulations are not opposed, as in the low beta band in the adult population? It is well known that phase-amplitude coupling, commonly between low frequencies like theta and high frequencies like gamma, is produced by language processing tasks within a single cortical region in which neurons in layers of cortical columns regulate each other, but this type of relationship has not been demonstrated in a connection between distant regions. Moreover, low antagonism (indicated by least negative beta coefficients) between slow and fast modulations occurs in the alpha and low-beta bands, not the higher frequency bands like high-beta and gamma. Regions with both strong AEC and IAC node strength in the low beta band include the left superior temporal gyrus, left inferior parietal, and

left and right isthmus cingulate regions, regions that play a role in multi-sensory integration. Might the low beta band serve as a carrier frequency for multisensory integration in mature learners? Results from the data set in the current investigation cannot answer this question, but it certainly deserves attention in future work.

Our data does make one thing clear: AEC and IAC measures of functional connectivity are tied together, most noticeably in theta and gamma bands. Results from the current experiment suggest that the two measures are mutually responsive to dynamic properties of the cortex, but in opposite directions, which shapes their subsequent utility for investigating language learning.

Speech Regions Are Hubs in IAC, but not AEC, Networks

Across bands, speech regions do not exhibit strong connectivity as assessed by AEC. When assessed by the IAC measure, speech regions vary in hubness across frequencies and syllables but score strongly overall. The left pars opercularis is a good example. AEC node strength (z-scored across cortical labels) for the pars opercularis scores is consistently negative, with scores below -1 for all bands except the gamma band (z-score of -0.26). For IAC node strength, the left pars opercularis scores above 2 in the theta band and above 1 in the alpha band, only returning negative z-scores (low hubness relative to other cortical labels) for onset syllables in the high beta and gamma bands. Pars opercularis scores are even more exaggerated for eigenvector centrality. As another illustration of this tendency, none of the speech regions of interest named in Chapter 2 appear on the list of top hubs for AEC hubs with the sole exception of the right inferior parietal region, which is listed in third place for high node strength in the beta band for adults. In contrast, more than half of the IAC hubs in the top three lists for all band appear in the speech regions list, a proportion that holds true for both node strength and

eigenvector centrality in adults. Overall, results from this data set strongly implicate the IAC measure as the more successful metric for detecting edges of interest.

IAC Connectivity Outperforms AEC for Predicting Statistical Learning

IAC connectivity in speech regions classifies the transitional probability of syllables above chance, and in the theta band, classifies adolescent participants as strong learners. Evaluated in the light of previous work on predictive coding in the cortex, the current results suggest that high temporal resolution connectivity may mark feed-forward and feedback signals facilitating functional integration of the cortex. IAC data shows that connections in the lower frequency bands are more powerful in onset relative to medial syllables, a finding that aligns well with a model in which low frequency signals convey predictions about the stimuli. The onset of a pseudoword should prompt predictions about what will follow in subjects who have successfully learned the statistical patterns in the speech stream. Current results suggest that word onsets elicit prediction signals starting very early in the trial in the alpha and beta bands, beginning in anticipation of the syllable for alpha connections. In the theta band, connections form strongly for onset and medial syllables, but theta connections subside more rapidly in medial syllables, which produces the late window contrast with onset connections. Greater neural recruitment for processing unpredictable or incongruent stimuli has been commonly reported in language processing paradigms, and IAC results, showing that low frequency mean node strength increases during low transitional probability syllables, concord with these findings.

In contrast, node strength and eigenvector centrality in the high beta and gamma bands peak during medial syllables. This behavior evident in the data aligns with a model in which auditory regions contribute to word learning by conveying error signals generated when learner expectations about medial syllables are violated after this initial acoustical processing of the

medial syllable has taken place (i.e. post-N100). In the gamma band, extra connectivity between 200 ms to 300 ms after medial syllable onset is driven by the right bank of the superior temporal sulcus, characteristics that share some regional and frequency overlap with prior work investigation prediction error signaling using audio-visual speech paradigms (Arnal et al., 2011). Right hemispheric involvement could be due to participant age, or it might contribute during early stages of language learning (Prat et al., 2023; Sharma et al., 2023). Further elucidation of the high frequency connectivity during medial syllables requires future work.

Overall, IAC connectivity appears to integrate well with a predictive coding framework.

FC Relates to Learning but not the N400

IAC connectivity predicts learning measured by D-prime, but not N400 differences. Similarly, AEC networks do not predict N400 amplitude difference. This shows that functional connectivity data has predictive value independent of event-related measures of learning, explaining variance in participant learning that event-related neural measures cannot explain. If event-related and functional connectivity learning measures are not predictive of each other but both matter for learning outcomes, then deficits in functional connectivity might explain learning difficulties in subjects when event-related measures appear intact. That makes connectivity an exciting area of investigation for developmental, cognitive, and language researchers.

Foundations for Future Hypotheses: Key Observations and Associations

1. Both AEC and IAC measures respond to cortical dynamics, but IAC measures are preferred for language learning investigations.
2. AEC measures may respond to connections resulting from stimuli with slower timing, or AEC measures may respond preferentially to connections from the visual and default mode systems.

3. IAC connectivity differentiates between transitional probability conditions and predicts word learning.
4. Neither measure predicts event-related responses.

Testable hypotheses for IAC connectivity suggested by this work include:

1. *Theta adaptation between onset and medial syllables relates to the entropy of the syllable, not the correctness of the prediction.* This can be tested by introducing violation trials to a speech stream after a suitable exposure phase, then contrasting high entropy syllable networks to violation syllable networks.
2. *Initial power and subsequent decay of right hemispheric connections is predictive of strong learning.* This can be tested by breaking exposure phases into blocks and performing response-based testing between blocks such that decay in RH connection strength can be related to improvement in learning scores.
3. *Mid-syllable connections from the left hemispheric speech regions to the right bank of the superior temporal sulcus signify error feedback*. This can be tested by comparing violation trial networks to networks from "hit" trials during a test block and networks from novelty pseudo-words.

Testable hypotheses for AEC connectivity suggested by this work include:

1. *AEC metrics preferentially track modality-related connections characterized by slow modulations, regardless of the temporal characteristics of the stimulus.* This could be tested by deriving AEC connectivity over a four-block experimental design comparing slow and fast-paced auditory stimuli to slow and fast-paced visual stimuli.

Chapter 8: Conclusion

Limitations and Future Directions

The most immediate limitation, and clearest future direction, is simply that this study is an exploratory effort that requires replication to confirm the current observations. With foundational connectivity information from this investigation in hand, the hypotheses detailed above are also ready for confirmatory analyses in future.

The current study, while an exciting first step, was not without limitations. Limitations of support vector machine learning as a tool for exploring associations between FC data and learning outcomes are manifold. A primary limitation is that features chosen by the model for predictive value do not have physiological interpretability. Support vectors that allow classification do not reveal information about the comparative value of edges or submodules of the networks tested. Another limitation highlighted by the current work is poor classification consistency across cross-validation folds, evidenced by high standard deviations of the scoring metrics for the functions. High standard deviations across validation folds indicate that classification models are sensitive to inter-subject variability; while some subjects are easy to classify, others confound the model. These two limitations together mean that models used in this study prove that significant subject variability exists but cannot provide useful information about the sources of variance. For future work, testing methods with better interpretability should be chosen.

A limitation previously discussed but worth mentioning again is that developmental effects on connectivity cannot be assessed from the current study. Because machine learning methods require a starting sample size of 50 subjects or more, the population of adolescents was not sufficiently powered for developmental investigation, and visual task variation between

adults and adolescents makes between-population comparisons interesting but inconclusive. While conclusions about developmental differences cannot be drawn from this study's results, observations from the current study offer helpful guidance for future work. First, machine learning methods are not robust to inter-subject variability, and this makes ML techniques a poor choice for developmental investigation. Pediatric and adolescent subjects tend to have very high individual variability; therefore, alternative methods suitable for high dimensional predictor data but more tolerant of variance should be selected. Examining individual learning trajectories across time points in comparison to network change might be a viable alternative.

Another limitation to the current methods is that network effects on word learning and N400 amplitude have been examined in isolation by frequency band. Multi-band effects have not been investigated. This is potentially an area of interest since oscillations in different frequency bands are known to interact like, for example, during phase-amplitude coupling. It is possible that inter-frequency dynamics might relate to event-related amplitude. For example, might the ratio of alpha to theta connectivity of the superior temporal gyrus influence the amplitude of the N400 in the superior temporal gyrus? So far, interaction between connections in different frequencies are unexplored and require future work.

Additionally, several open questions raised by this investigation warrant future investigation. The timeline for emergence of network adaptations is a major question that needs future work. How soon after starting exposure to a speech stream do network adaptations emerge? How do network adaptations change over the course of learning? So far, this is unknown. Another major area of investigation relates to individual differences in learning. Strong learners may exhibit multiple network configurations that appear dissimilar but equally result in robust statistical learning. What types of network variation represent functionally

equivalent alternatives? What variation is tied to poor learning? This question leads to perhaps the most important future direction: investigating the relationship between functional connectivity for statistical learning and clinical conditions such as dyslexia or specific language impairment.

Conclusion

Results from this investigation support the value of connectivity investigations. Current data support the validity of connectivity measurement using the IAC method by demonstrating alignment between IAC network properties and prior knowledge about word segmentation. Evidence from the current analysis illustrates the impact of temporal resolution of FC methodology, helping future researchers choose more sensitive measures. Identification of key ASL network hubs, edges, and temporal windows of adaptation for functional connections increase the specificity of future hypotheses. While many questions lie ahead, the rich relationship between auditory statistical learning and high temporal resolution functional connectivity in the current data affirms the potential of network analysis to aid our understanding of how the brain adapts and learns, particularly in the context of language paradigms where rapid multi-modal processing streams are the norm. Leveraging network approaches alongside classic event-related and oscillatory pipelines will allow researchers deeper insight into mechanisms supporting outcomes of interest and thereby expand the opportunity for neuroimaging research to facilitate learning, growth, and health for all.

References

Abla, D., Katahira, K., & Okanoya, K. (2008). On-line Assessment of Statistical Learning by Event-related Potentials. *Journal of Cognitive Neuroscience*, *20*(6), 952–964. https://doi.org/10.1162/jocn.2008.20058

Ahveninen, J., Jääskeläinen, I. P., Raij, T., Bonmassar, G., Devore, S., Hämäläinen, M., Levänen, S., Lin, F.-H., Sams, M., Shinn-Cunningham, B. G., Witzel, T., & Belliveau, J. W. (2006). Task-modulated "what" and "where" pathways in human auditory cortex. *Proceedings of the National Academy of Sciences*, *103*(39), 14608–14613. https://doi.org/10.1073/pnas.0510480103

Altamura, M., Carver, F. W., Elvevåg, B., Weinberger, D. R., & Coppola, R. (2014). Dynamic cortical involvement in implicit anticipation during statistical learning. *Neuroscience Letters*, *558*, 73–77. https://doi.org/10.1016/j.neulet.2013.09.043

Andrade-Talavera, Y., Fisahn, A., & Rodríguez-Moreno, A. (2023). Timing to be precise? An overview of spike timing-dependent plasticity, brain rhythmicity, and glial cells interplay within neuronal circuits. *Molecular Psychiatry*, *28*(6), 2177–2188. https://doi.org/10.1038/s41380-023-02027-w

Armeni, K., Willems, R. M., van den Bosch, A., & Schoffelen, J.-M. (2019). Frequency-specific brain dynamics related to prediction during language comprehension. *NeuroImage*, *198*, 283–295. https://doi.org/10.1016/j.neuroimage.2019.04.083

Arnal, L. H., Wyart, V., & Giraud, A.-L. (2011). Transitions in neural oscillations reflect prediction errors generated in audiovisual speech. *Nature Neuroscience*, *14*(6), 797–801. https://doi.org/10.1038/nn.2810

Atallah, B. V., & Scanziani, M. (2009). Instantaneous Modulation of Gamma Oscillation Frequency by Balancing Excitation with Inhibition. *Neuron*, *62*(4), 566–577. https://doi.org/10.1016/j.neuron.2009.04.027

Attaheri, A., Choisdealbha, Á. N., Di Liberto, G. M., Rocha, S., Brusini, P., Mead, N., Olawole-Scott, H., Boutris, P., Gibbon, S., Williams, I., Grey, C., Flanagan, S., & Goswami, U. (2022). Delta- and theta-band cortical tracking and phase-amplitude coupling to sung speech by infants. *NeuroImage*, *247*, 118698. https://doi.org/10.1016/j.neuroimage.2021.118698

Baker, A. P., Brookes, M. J., Rezek, I. A., Smith, S. M., Behrens, T., Probert Smith, P. J., & Woolrich, M. (2014). Fast transient networks in spontaneous human brain activity. *eLife*, *3*, e01867. https://doi.org/10.7554/eLife.01867

Bakker-Marshall, I., Takashima, A., Schoffelen, J.-M., van Hell, J. G., Janzen, G., & McQueen, J. M. (2018). Theta-band Oscillations in the Middle Temporal Gyrus Reflect Novel Word Consolidation. *Journal of Cognitive Neuroscience*, *30*(5), 621–633. https://doi.org/10.1162/jocn_a_01240

Bassett, D. S., Nelson, B. G., Mueller, B. A., Camchong, J., & Lim, K. O. (2012). Altered resting state complexity in schizophrenia. *NeuroImage*, *59*(3), 2196–2207. https://doi.org/10.1016/j.neuroimage.2011.10.002

Bassett, D. S., Zurn, P., & Gold, J. I. (2018). On the nature and use of models in network neuroscience. *Nature Reviews Neuroscience*, *19*(9), Article 9. https://doi.org/10.1038/s41583-018-0038-8

Basti, A., Nili, H., Hauk, O., Marzetti, L., & Henson, R. N. (2020). Multi-dimensional connectivity: A conceptual and mathematical review. *NeuroImage*, *221*, 117179. https://doi.org/10.1016/j.neuroimage.2020.117179

Bastiaansen, M., & Hagoort, P. (2006). Oscillatory neuronal dynamics during language comprehension. In *Progress in Brain Research* (Vol. 159, pp. 179–196). Elsevier. https://doi.org/10.1016/S0079-6123(06)59012-0

Bastiaansen, M., & Hagoort, P. (2015). Frequency-based Segregation of Syntactic and Semantic Unification during Online Sentence Level Language Comprehension. *Journal of Cognitive Neuroscience*, *27*(11), 2095–2107. https://doi.org/10.1162/jocn_a_00829

Bastiaansen, M., Magyari, L., & Hagoort, P. (2010). Syntactic Unification Operations Are Reflected in Oscillatory Dynamics during On-line Sentence Comprehension. *Journal of Cognitive Neuroscience*, *22*(7), 1333–1347. https://doi.org/10.1162/jocn.2009.21283

Bastos, A. M., & Schoffelen, J.-M. (2016). A Tutorial Review of Functional Connectivity Analysis Methods and Their Interpretational Pitfalls. *Frontiers in Systems Neuroscience*, *9*. https://www.frontiersin.org/articles/10.3389/fnsys.2015.00175

Bastos, A. M., Usrey, W. M., Adams, R. A., Mangun, G. R., Fries, P., & Friston, K. J. (2012). Canonical Microcircuits for Predictive Coding. *Neuron*, *76*(4), 695–711. https://doi.org/10.1016/j.neuron.2012.10.038

Battaglia, D., & Brovelli, A. (2020). Functional Connectivity and Neuronal Dynamics: Insights from Computational Methods. In D. Poeppel, G. R. Mangun, & M. S. Gazzaniga (Eds.), *The Cognitive Neurosciences* (6th ed., pp. 739–748). The MIT Press. https://doi.org/10.7551/mitpress/11442.003.0080

Batterink, L. (2020). Syllables in Sync Form a Link: Neural Phase-locking Reflects Word Knowledge during Language Learning. *Journal of Cognitive Neuroscience*, *32*(9), 1735–1748. https://doi.org/10.1162/jocn_a_01581

Batterink, L. J., Paller, K. A., & Reber, P. J. (2019). Understanding the Neural Bases of Implicit and Statistical Learning. *Topics in Cognitive Science*, *11*(3), 482–503. https://doi.org/10.1111/tops.12420

Betti, V., Della Penna, S., de Pasquale, F., & Corbetta, M. (2021). Spontaneous Beta Band Rhythms in the Predictive Coding of Natural Stimuli. *The Neuroscientist*, *27*(2), 184–201. https://doi.org/10.1177/1073858420928988

Bogaerts, L., Richter, C. G., Landau, A. N., & Frost, R. (2020). Beta-Band Activity Is a Signature of Statistical Learning. *Journal of Neuroscience*, *40*(39), 7523–7530. https://doi.org/10.1523/JNEUROSCI.0771-20.2020

Bosseler, A. N., Teinonen, T., Tervaniemi, M., & Huotilainen, M. (2016). Infant Directed Speech Enhances Statistical Learning in Newborn Infants: An ERP Study. *PLOS ONE*, *11*(9), e0162177. https://doi.org/10.1371/journal.pone.0162177

Brookes, M. J., Woolrich, M., Luckhoo, H., Price, D., Hale, J. R., Stephenson, M. C., Barnes, G. R., Smith, S. M., & Morris, P. G. (2011). Investigating the electrophysiological basis of resting state networks using magnetoencephalography. *Proceedings of the National Academy of Sciences*, *108*(40), 16783–16788. https://doi.org/10.1073/pnas.1112685108

Buzsáki, G., & Wang, X.-J. (2012). Mechanisms of Gamma Oscillations. *Annual Review of Neuroscience*, *35*(Volume 35, 2012), 203–225. https://doi.org/10.1146/annurev-neuro-062111-150444

Colclough, G. L., Woolrich, M. W., Tewarie, P. K., Brookes, M. J., Quinn, A. J., & Smith, S. M. (2016). How reliable are MEG resting-state connectivity metrics? *NeuroImage*, *138*, 284–293. https://doi.org/10.1016/j.neuroimage.2016.05.070

Cunillera, T., Càmara, E., Toro, J. M., Marco-Pallares, J., Sebastián-Galles, N., Ortiz, H., Pujol, J., & Rodríguez-Fornells, A. (2009). Time course and functional neuroanatomy of speech segmentation in adults. *NeuroImage*, *48*(3), 541–553. https://doi.org/10.1016/j.neuroimage.2009.06.069

Daikoku, T. (2018). Neurophysiological Markers of Statistical Learning in Music and Language: Hierarchy, Entropy and Uncertainty. *Brain Sciences*, *8*(6), Article 6. https://doi.org/10.3390/brainsci8060114

Daikoku, T., Yatomi, Y., & Yumoto, M. (2017). Statistical learning of an auditory sequence and reorganization of acquired knowledge: A time course of word segmentation and ordering. *Neuropsychologia*, *95*, 1–10. https://doi.org/10.1016/j.neuropsychologia.2016.12.006

Daltrozzo, J., Emerson, S. N., Deocampo, J., Singh, S., Freggens, M., Branum-Martin, L., & Conway, C. M. (2017). Visual statistical learning is related to natural language ability in adults: An ERP study. *Brain and Language*, *166*, 40–51. https://doi.org/10.1016/j.bandl.2016.12.005

Davidson, D. J., & Indefrey, P. (2007). An inverse relation between event-related and time–frequency violation responses in sentence processing. *Brain Research*, *1158*, 81–92. https://doi.org/10.1016/j.brainres.2007.04.082

Desikan, R. S., Ségonne, F., Fischl, B., Quinn, B. T., Dickerson, B. C., Blacker, D., Buckner, R. L., Dale, A. M., Maguire, R. P., Hyman, B. T., Albert, M. S., & Killiany, R. J. (2006). An automated labeling system for subdividing the human cerebral cortex on MRI scans into

gyral based regions of interest. *NeuroImage*, *31*(3), 968–980. https://doi.org/10.1016/j.neuroimage.2006.01.021

Doesburg, S. M., Tingling, K., MacDonald, M. J., & Pang, E. W. (2016). Development of Network Synchronization Predicts Language Abilities. *Journal of Cognitive Neuroscience*, *28*(1), 55–68. https://doi.org/10.1162/jocn_a_00879

Elmer, S., Albrecht, J., Valizadeh, S. A., François, C., & Rodríguez-Fornells, A. (2018). Theta Coherence Asymmetry in the Dorsal Stream of Musicians Facilitates Word Learning. *Scientific Reports*, *8*(1), 4565. https://doi.org/10.1038/s41598-018-22942-1

Engel, A. K., & Fries, P. (2010). Beta-band oscillations—Signalling the status quo? *Current Opinion in Neurobiology*, *20*(2), 156–165.

Engel, A. K., Fries, P., & Singer, W. (2001). Dynamic predictions: Oscillations and synchrony in top–down processing. *Nature Reviews Neuroscience*, *2*(10), 704–716.

Engemann, D. A., & Gramfort, A. (2015). Automated model selection in covariance estimation and spatial whitening of MEG and EEG signals. *NeuroImage*, *108*, 328–342. https://doi.org/10.1016/j.neuroimage.2014.12.040

Erickson, L. C., & Thiessen, E. D. (2015). Statistical learning of language: Theory, validity, and predictions of a statistical learning account of language acquisition. *Developmental Review*, *37*, 66–108. https://doi.org/10.1016/j.dr.2015.05.002

Fan, T., Decker, W., & Schneider, J. (2024). The Domain-Specific Neural Basis of Auditory Statistical Learning in 5–7-Year-Old Children. *Neurobiology of Language*, *5*(4), 981–1007. https://doi.org/10.1162/nol_a_00156

Farthouat, J., Franco, A., Mary, A., Delpouve, J., Wens, V., Op de Beeck, M., De Tiège, X., & Peigneux, P. (2017). Auditory Magnetoencephalographic Frequency-Tagged Responses

Mirror the Ongoing Segmentation Processes Underlying Statistical Learning. *Brain Topography*, *30*(2), 220–232. https://doi.org/10.1007/s10548-016-0518-y

Favaretto, C., Spadone, S., Sestieri, C., Betti, V., Cenedese, A., Della Penna, S., & Corbetta, M. (2021). Multi-band MEG signatures of BOLD connectivity reorganization during visuospatial attention. *NeuroImage*, *230*, 117781. https://doi.org/10.1016/j.neuroimage.2021.117781

Fischl, B. (2012). FreeSurfer. *NeuroImage, 20 YEARS OF fMRI*, *62*(2), 774–781. https://doi.org/10.1016/j.neuroimage.2012.01.021

Fitzgibbon, S. P., Pope, K. J., Mackenzie, L., Clark, C. R., & Willoughby, J. O. (2004). Cognitive tasks augment gamma EEG power. *Clinical Neurophysiology*, *115*(8), 1802–1809. https://doi.org/10.1016/j.clinph.2004.03.009

Foxe, J., & Snyder, A. (2011). The Role of Alpha-Band Brain Oscillations as a Sensory Suppression Mechanism during Selective Attention. *Frontiers in Psychology*, *2*, 154. https://doi.org/10.3389/fpsyg.2011.00154

Fries, P. (2015). Rhythms for Cognition: Communication through Coherence. *Neuron*, *88*(1), 220–235. https://doi.org/10.1016/j.neuron.2015.09.034

Friston, K. J. (2011). Functional and Effective Connectivity: A Review. *Brain Connectivity*, *1*(1), 13–36. https://doi.org/10.1089/brain.2011.0008

Friston, K. J., Bastos, A. M., Pinotsis, D., & Litvak, V. (2015). LFP and oscillations—What do they tell us? *Current Opinion in Neurobiology, SI: Brain Rhythms and Dynamic Coordination*, *31*, 1–6. https://doi.org/10.1016/j.conb.2014.05.004

Frost, R., Armstrong, B. C., & Christiansen, M. H. (2019). Statistical learning research: A critical review and possible new directions. *Psychological Bulletin*, *145*, 1128–1153. https://doi.org/10.1037/bul0000210

Frost, R., Siegelman, N., Narkiss, A., & Afek, L. (2013). What Predicts Successful Literacy Acquisition in a Second Language? *Psychological Science*, *24*(7), 1243–1252. https://doi.org/10.1177/0956797612472207

Gabay, Y., Thiessen, E. D., & Holt, L. L. (2015). Impaired Statistical Learning in Developmental Dyslexia. *Journal of Speech, Language, and Hearing Research*, *58*(3), 934–945. https://doi.org/10.1044/2015_JSLHR-L-14-0324

Gastaldon, S., Arcara, G., Navarrete, E., & Peressotti, F. (2020). Commonalities in alpha and beta neural desynchronizations during prediction in language comprehension and production. *Cortex*, *133*, 328–345. https://doi.org/10.1016/j.cortex.2020.09.026

Gaudet, I., Hüsser, A., Vannasing, P., & Gallagher, A. (2020). Functional Brain Connectivity of Language Functions in Children Revealed by EEG and MEG: A Systematic Review. *Frontiers in Human Neuroscience*, *14*. https://doi.org/10.3389/fnhum.2020.00062

Ghaderi, A. H., Andevari, M. N., & Sowman, P. F. (2018). Evidence for a Resting State Network Abnormality in Adults Who Stutter. *Frontiers in Integrative Neuroscience*, *12*. https://www.frontiersin.org/article/10.3389/fnint.2018.00016

Giraud, A.-L., & Poeppel, D. (2012). Cortical oscillations and speech processing: Emerging computational principles and operations. *Nature Neuroscience*, *15*(4), Article 4. https://doi.org/10.1038/nn.3063

Glasser, M. F., Coalson, T. S., Robinson, E. C., Hacker, C. D., Harwell, J., Yacoub, E., Ugurbil, K., Andersson, J., Beckmann, C. F., Jenkinson, M., Smith, S. M., & Van Essen, D. C.

(2016). A multi-modal parcellation of human cerebral cortex. *Nature*, *536*(7615), 171–178. https://doi.org/10.1038/nature18933

Godfrey, M., & Singh, K. D. (2021). Measuring robust functional connectivity from resting-state MEG using amplitude and entropy correlation across frequency bands and temporal scales. *NeuroImage*, *226*, 117551. https://doi.org/10.1016/j.neuroimage.2020.117551

Gou, Z., Choudhury, N., & Benasich, A. A. (2011). Resting frontal gamma power at 16, 24 and 36 months predicts individual differences in language and cognition at 4 and 5 years. *Behavioural Brain Research*, *220*(2), 263–270. https://doi.org/10.1016/j.bbr.2011.01.048

Gramfort, A., Luessi, M., Larson, E., Engemann, D., Strohmeier, D., Brodbeck, C., Goj, R., Jas, M., Brooks, T., Parkkonen, L., & Hämäläinen, M. (2013). MEG and EEG data analysis with MNE-Python. *Frontiers in Neuroscience*, *7*, 267. https://doi.org/10.3389/fnins.2013.00267

Gross, J., Hoogenboom, N., Thut, G., Schyns, P., Panzeri, S., Belin, P., & Garrod, S. (2013). Speech Rhythms and Multiplexed Oscillatory Sensory Coding in the Human Brain. *PLOS Biology*, *11*(12), e1001752. https://doi.org/10.1371/journal.pbio.1001752

Hagberg, A., Swart, P., & S Chult, D. (2008). *Exploring network structure, dynamics, and function using networkx* (LA-UR-08-05495; LA-UR-08-5495). Los Alamos National Lab. (LANL), Los Alamos, NM (United States). https://www.osti.gov/biblio/960616

Hanslmayr, S., Staudigl, T., & Fellner, M.-C. (2012). Oscillatory power decreases and long-term memory: The information via desynchronization hypothesis. *Frontiers in Human Neuroscience*, *6*. https://doi.org/10.3389/fnhum.2012.00074

Hari, R., & Puce, A. (2023). *MEG-EEG Primer*. Oxford University Press.

Hauk, O., & Stenroos, M. (2014). A framework for the design of flexible cross-talk functions for spatial filtering of EEG/MEG data: DeFleCT. *Human Brain Mapping*, *35*(4), 1642–1653. https://doi.org/10.1002/hbm.22279

Hauk, O., Stenroos, M., & Treder, M. S. (2022). Towards an objective evaluation of EEG/MEG source estimation methods – The linear approach. *NeuroImage*, *255*, 119177. https://doi.org/10.1016/j.neuroimage.2022.119177

Hauk, O., Wakeman, D. G., & Henson, R. (2011). Comparison of noise-normalized minimum norm estimates for MEG analysis using multiple resolution metrics. *NeuroImage*, *54*(3), 1966–1974. https://doi.org/10.1016/j.neuroimage.2010.09.053

Helle, L., Nenonen, J., Larson, E., Simola, J., Parkkonen, L., & Taulu, S. (2021). Extended Signal-Space Separation Method for Improved Interference Suppression in MEG. *IEEE Transactions on Biomedical Engineering*, *68*(7), 2211–2221. IEEE Transactions on Biomedical Engineering. https://doi.org/10.1109/TBME.2020.3040373

Hillebrand, A., & Barnes, G. R. (2005). Beamformer Analysis of MEG Data. In *International Review of Neurobiology* (Vol. 68, pp. 149–171). Academic Press. https://doi.org/10.1016/S0074-7742(05)68006-3

Hincapié, A.-S., Kujala, J., Mattout, J., Pascarella, A., Daligault, S., Delpuech, C., Mery, D., Cosmelli, D., & Jerbi, K. (2017). The impact of MEG source reconstruction method on source-space connectivity estimation: A comparison between minimum-norm solution and beamforming. *NeuroImage*, *156*, 29–42. https://doi.org/10.1016/j.neuroimage.2017.04.038

Hipp, J. F., Engel, A. K., & Siegel, M. (2011). Oscillatory Synchronization in Large-Scale Cortical Networks Predicts Perception. *Neuron*, *69*(2), 387–396. https://doi.org/10.1016/j.neuron.2010.12.027

Hunt, B. A. E., Wong, S. M., Vandewouw, M. M., Brookes, M. J., Dunkley, B. T., & Taylor, M. J. (2019). Spatial and spectral trajectories in typical neurodevelopment from childhood to middle age. *Network Neuroscience*, *3*(2), 497–520. https://doi.org/10.1162/netn_a_00077

Jaiswal, A., Nenonen, J., Stenroos, M., Gramfort, A., Dalal, S. S., Westner, B. U., Litvak, V., Mosher, J. C., Schoffelen, J.-M., Witton, C., Oostenveld, R., & Parkkonen, L. (2020). Comparison of beamformer implementations for MEG source localization. *NeuroImage*, *216*, 116797. https://doi.org/10.1016/j.neuroimage.2020.116797

Kabdebon, C., Pena, M., Buiatti, M., & Dehaene-Lambertz, G. (2015). Electrophysiological evidence of statistical learning of long-distance dependencies in 8-month-old preterm and full-term infants. *Brain and Language, The Electrophysiology of Speech, Language, and Its Precursors*, *148*, 25–36. https://doi.org/10.1016/j.bandl.2015.03.005

Karuza, E. A., Newport, E. L., Aslin, R. N., Starling, S. J., Tivarus, M. E., & Bavelier, D. (2013). The neural correlates of statistical learning in a word segmentation task: An fMRI study. *Brain and Language*, *127*(1), 46–54. https://doi.org/10.1016/j.bandl.2012.11.007

Khan, S., Hashmi, J. A., Mamashli, F., Hämäläinen, M. S., & Kenet, T. (2022). Functional Significance of Human Resting-State Networks Hubs Identified Using MEG During the Transition From Childhood to Adulthood. *Frontiers in Neurology*, *13*. https://doi.org/10.3389/fneur.2022.814940

Khan, S., Hashmi, J. A., Mamashli, F., Michmizos, K., Kitzbichler, M. G., Bharadwaj, H., Bekhti, Y., Ganesan, S., Garel, K.-L. A., Whitfield-Gabrieli, S., Gollub, R. L., Kong, J.,

Vaina, L. M., Rana, K. D., Stufflebeam, S. M., Hämäläinen, M. S., & Kenet, T. (2018). Maturation trajectories of cortical resting-state networks depend on the mediating frequency band. *NeuroImage*, *174*, 57–68. https://doi.org/10.1016/j.neuroimage.2018.02.018

Kielar, A., Meltzer, J. A., Moreno, S., Alain, C., & Bialystok, E. (2014). Oscillatory Responses to Semantic and Syntactic Violations. *Journal of Cognitive Neuroscience*, *26*(12), 2840–2862. https://doi.org/10.1162/jocn_a_00670

Klimesch, W. (1999). EEG alpha and theta oscillations reflect cognitive and memory performance: A review and analysis. *Brain Research Reviews*, *29*(2), 169–195. https://doi.org/10.1016/S0165-0173(98)00056-3

Klimesch, W. (2012). Alpha-band oscillations, attention, and controlled access to stored information. *Trends in Cognitive Sciences*, *16*(12), 606–617. https://doi.org/10.1016/j.tics.2012.10.007

Kok, P., Rahnev, D., Jehee, J. F. M., Lau, H. C., & de Lange, F. P. (2012). Attention Reverses the Effect of Prediction in Silencing Sensory Signals. *Cerebral Cortex*, *22*(9), 2197–2206. https://doi.org/10.1093/cercor/bhr310

Kuhl, P. K. (2004). Early language acquisition: Cracking the speech code. *Nature Reviews Neuroscience*, *5*(11), Article 11. https://doi.org/10.1038/nrn1533

Kuhl, P. K. (2010). Brain Mechanisms in Early Language Acquisition. *Neuron*, *67*(5), 713–727. https://doi.org/10.1016/j.neuron.2010.08.038

Kuhl, P. K., Conboy, B. T., Padden, D., Nelson, T., & Pruitt, J. (2005). Early Speech Perception and Later Language Development: Implications for the “Critical Period.” *Language*

Learning and Development, *1*(3–4), 237–264. https://doi.org/10.1080/15475441.2005.9671948

La Vaque, T. J. (1999). The History of EEG Hans Berger: Psychophysiologist. A Historical Vignette. *Journal of Neurotherapy*, *3*(2), 1–9. https://doi.org/10.1300/J184v03n02_01

Lam, N. H. L., Schoffelen, J.-M., Uddén, J., Hultén, A., & Hagoort, P. (2016). Neural activity during sentence processing as reflected in theta, alpha, beta, and gamma oscillations. *NeuroImage*, *142*, 43–54. https://doi.org/10.1016/j.neuroimage.2016.03.007

Lau, E. F., Phillips, C., & Poeppel, D. (2008). A cortical network for semantics: (De)constructing the N400. *Nature Reviews Neuroscience*, *9*(12), 920–933. https://doi.org/10.1038/nrn2532

Lewis, A. G., Schoffelen, J.-M., Schriefers, H., & Bastiaansen, M. (2016). A Predictive Coding Perspective on Beta Oscillations during Sentence-Level Language Comprehension. *Frontiers in Human Neuroscience*, *10*. https://doi.org/10.3389/fnhum.2016.00085

Lin, F.-H., Witzel, T., Ahlfors, S. P., Stufflebeam, S. M., Belliveau, J. W., & Hämäläinen, M. S. (2006). Assessing and improving the spatial accuracy in MEG source localization by depth-weighted minimum-norm estimates. *NeuroImage*, *31*(1), 160–171. https://doi.org/10.1016/j.neuroimage.2005.11.054

Liu, Z., Fukunaga, M., de Zwart, J. A., & Duyn, J. H. (2010). Large-scale spontaneous fluctuations and correlations in brain electrical activity observed with magnetoencephalography. *NeuroImage*, *51*(1), 102–111. https://doi.org/10.1016/j.neuroimage.2010.01.092

Liuzzi, L., Quinn, A. J., O'Neill, G. C., Woolrich, M. W., Brookes, M. J., Hillebrand, A., & Tewarie, P. (2019). How Sensitive Are Conventional MEG Functional Connectivity

Metrics With Sliding Windows to Detect Genuine Fluctuations in Dynamic Functional Connectivity? *Frontiers in Neuroscience*, *13*. https://www.frontiersin.org/articles/10.3389/fnins.2019.00797

Lizarazu, M., Carreiras, M., Bourguignon, M., Zarraga, A., & Molinaro, N. (2021). Language Proficiency Entails Tuning Cortical Activity to Second Language Speech. *Cerebral Cortex*, *31*(8), 3820–3831. https://doi.org/10.1093/cercor/bhab051

Lozano-Soldevilla, D., ter Huurne, N., Cools, R., & Jensen, O. (2014). GABAergic Modulation of Visual Gamma and Alpha Oscillations and Its Consequences for Working Memory Performance. *Current Biology*, *24*(24), 2878–2887. https://doi.org/10.1016/j.cub.2014.10.017

Luo, Y., Zhang, Y., Feng, X., & Zhou, X. (2010). Electroencephalogram oscillations differentiate semantic and prosodic processes during sentence reading. *Neuroscience*, *169*(2), 654–664. https://doi.org/10.1016/j.neuroscience.2010.05.032

Maldjian, J. A., Davenport, E. M., & Whitlow, C. T. (2014). Graph theoretical analysis of resting-state MEG data: Identifying interhemispheric connectivity and the default mode. *NeuroImage*, *96*, 88–94. https://doi.org/10.1016/j.neuroimage.2014.03.065

Marzetti, L., Basti, A., Chella, F., D'Andrea, A., Syrjälä, J., & Pizzella, V. (2019). Brain Functional Connectivity Through Phase Coupling of Neuronal Oscillations: A Perspective From Magnetoencephalography. *Frontiers in Neuroscience*, *13*. https://www.frontiersin.org/articles/10.3389/fnins.2019.00964

McNealy, K., Mazziotta, J. C., & Dapretto, M. (2006). Cracking the Language Code: Neural Mechanisms Underlying Speech Parsing. *The Journal of Neuroscience*, *26*(29), 7629–7639. https://doi.org/10.1523/JNEUROSCI.5501-05.2006

Meindertsma, T., Kloosterman, N. A., Engel, A. K., Wagenmakers, E.-J., & Donner, T. H. (2018). Surprise About Sensory Event Timing Drives Cortical Transients in the Beta Frequency Band. *Journal of Neuroscience*, *38*(35), 7600–7610. https://doi.org/10.1523/JNEUROSCI.0307-18.2018

Molinaro, N., Monsalve, I. F., & Lizarazu, M. (2016). Is there a common oscillatory brain mechanism for producing and predicting language? *Language, Cognition and Neuroscience*, *31*(1), 145–158. https://doi.org/10.1080/23273798.2015.1077978

Mosher, J. C., Leahy, R. M., & Lewis, P. S. (1999). EEG and MEG: Forward solutions for inverse methods. *IEEE Transactions on Biomedical Engineering*, *46*(3), 245–259. IEEE Transactions on Biomedical Engineering. https://doi.org/10.1109/10.748978

Muller, A. M., & Meyer, M. (2014). Language in the brain at rest: New insights from resting state data and graph theoretical analysis. *Frontiers in Human Neuroscience*, *8*. https://www.frontiersin.org/article/10.3389/fnhum.2014.00228

Nastase, S. A., Iacovella, V., Davis, B., & Hasson, U. (2015). Connectivity in the human brain dissociates entropy and complexity of auditory inputs. *NeuroImage*, *108*, 292–300. https://doi.org/10.1016/j.neuroimage.2014.12.048

Nolte, G., & Curio, G. (1999). The effect of artifact rejection by signal-space projection on source localization accuracy in MEG measurements. *IEEE Transactions on Biomedical Engineering*, *46*(4), 400–408. IEEE Transactions on Biomedical Engineering. https://doi.org/10.1109/10.752937

Oh, A., Duerden, E. G., & Pang, E. W. (2014). The role of the insula in speech and language processing. *Brain and Language*, *135*, 96–103. https://doi.org/10.1016/j.bandl.2014.06.003

Oldham, S., Fulcher, B., Parkes, L., Arnatkevičiūtė, A., Suo, C., & Fornito, A. (2019). Consistency and differences between centrality measures across distinct classes of networks. *PLoS ONE*, *14*(7), e0220061. https://doi.org/10.1371/journal.pone.0220061

O'Neill, G. C., Barratt, E. L., Hunt, B. A. E., Tewarie, P. K., & Brookes, M. J. (2015). Measuring electrophysiological connectivity by power envelope correlation: A technical review on MEG methods. *Physics in Medicine & Biology*, *60*(21), R271. https://doi.org/10.1088/0031-9155/60/21/R271

O'Neill, G. C., Tewarie, P. K., Colclough, G. L., Gascoyne, L. E., Hunt, B. A. E., Morris, P. G., Woolrich, M. W., & Brookes, M. J. (2017). Measurement of dynamic task related functional networks using MEG. *NeuroImage*, *146*, 667–678. https://doi.org/10.1016/j.neuroimage.2016.08.061

Orpella, J., Assaneo, M. F., Ripollés, P., Noejovich, L., López-Barroso, D., Diego-Balaguer, R. de, & Poeppel, D. (2022). Differential activation of a frontoparietal network explains population-level differences in statistical learning from speech. *PLOS Biology*, *20*(7), e3001712. https://doi.org/10.1371/journal.pbio.3001712

Palva, J. M., Wang, S. H., Palva, S., Zhigalov, A., Monto, S., Brookes, M. J., Schoffelen, J.-M., & Jerbi, K. (2018). Ghost interactions in MEG/EEG source space: A note of caution on inter-areal coupling measures. *NeuroImage*, *173*, 632–643. https://doi.org/10.1016/j.neuroimage.2018.02.032

Paraskevopoulos, E., Chalas, N., & Bamidis, P. (2017). Functional connectivity of the cortical network supporting statistical learning in musicians and non-musicians: An MEG study. *Scientific Reports*, *7*(1), 16268. https://doi.org/10.1038/s41598-017-16592-y

Pascual-Marqui, R. D., Lehmann, D., Koukkou, M., Kochi, K., Anderer, P., Saletu, B., Tanaka, H., Hirata, K., John, E. R., Prichep, L., Biscay-Lirio, R., & Kinoshita, T. (2011). Assessing interactions in the brain with exact low-resolution electromagnetic tomography. *Philosophical Transactions of the Royal Society A: Mathematical, Physical and Engineering Sciences*, *369*(1952), 3768–3784. https://doi.org/10.1098/rsta.2011.0081

Pavlidou, E. V., Louise Kelly, M., & Williams, J. M. (2010). Do children with developmental dyslexia have impairments in implicit learning? *Dyslexia*, *16*(2), 143–161. https://doi.org/10.1002/dys.400

Pedregosa, F., Varoquaux, G., Gramfort, A., Michel, V., Thirion, B., Grisel, O., Blondel, M., Prettenhofer, P., Weiss, R., Dubourg, V., Vanderplas, J., Passos, A., & Cournapeau, D. (n.d.). Scikit-learn: Machine Learning in Python. *MACHINE LEARNING IN PYTHON*.

Pfurtscheller, G., & Lopes da Silva, F. H. (1999). Event-related EEG/MEG synchronization and desynchronization: Basic principles. *Clinical Neurophysiology*, *110*(11), 1842–1857. https://doi.org/10.1016/S1388-2457(99)00141-8

Prat, C. S., Gallée, J., & Yamasaki, B. L. (2023). Getting language right: Relating individual differences in right hemisphere contributions to language learning and relearning. *Brain and Language*, *239*, 105242. https://doi.org/10.1016/j.bandl.2023.105242

Price, C. J. (2000). The anatomy of language: Contributions from functional neuroimaging. *The Journal of Anatomy*, *197*(3), 335–359. https://doi.org/10.1046/j.1469-7580.2000.19730335.x

Pu, Y., Cheyne, D., Sun, Y., & Johnson, B. W. (2020). Theta oscillations support the interface between language and memory. *NeuroImage*, *215*, 116782. https://doi.org/10.1016/j.neuroimage.2020.116782

Roehe, M. A., Kluger, D. S., Schroeder, S. C. Y., Schliephake, L. M., Boelte, J., Jacobsen, T., & Schubotz, R. I. (2021). Early alpha/beta oscillations reflect the formation of face-related expectations in the brain. *PLOS ONE*, *16*(7), e0255116. https://doi.org/10.1371/journal.pone.0255116

Ross, B., Tremblay, K. L., & Alain, C. (2020). Simultaneous EEG and MEG recordings reveal vocal pitch elicited cortical gamma oscillations in young and older adults. *NeuroImage*, *204*, 116253. https://doi.org/10.1016/j.neuroimage.2019.116253

Rossini, P. M., Di Iorio, R., Bentivoglio, M., Bertini, G., Ferreri, F., Gerloff, C., Ilmoniemi, R. J., Miraglia, F., Nitsche, M. A., Pestilli, F., Rosanova, M., Shirota, Y., Tesoriero, C., Ugawa, Y., Vecchio, F., Ziemann, U., & Hallett, M. (2019). Methods for analysis of brain connectivity: An IFCN-sponsored review. *Clinical Neurophysiology*, *130*(10), 1833–1858. https://doi.org/10.1016/j.clinph.2019.06.006

Saffran, J. R., Aslin, R. N., & Newport, E. L. (1996). Statistical Learning by 8-Month-Old Infants. *Science*, *274*(5294), 1926–1928. https://doi.org/10.1126/science.274.5294.1926

Sakkalis, V. (2011). Review of advanced techniques for the estimation of brain connectivity measured with EEG/MEG. *Computers in Biology and Medicine, Special Issue on Techniques for Measuring Brain Connectivity*, *41*(12), 1110–1117. https://doi.org/10.1016/j.compbiomed.2011.06.020

Sanders, L. D., Newport, E. L., & Neville, H. J. (2002). Segmenting nonsense: An event-related potential index of perceived onsets in continuous speech. *Nature Neuroscience*, *5*(7), 700–703. https://doi.org/10.1038/nn873

Sareen, E., Zahar, S., Ville, D. V. D., Gupta, A., Griffa, A., & Amico, E. (2021). Exploring MEG brain fingerprints: Evaluation, pitfalls, and interpretations. *NeuroImage*, *240*, 118331. https://doi.org/10.1016/j.neuroimage.2021.118331

Schelter, B., Winterhalder, M., & Timmer, J. (2006). Handbook of Time Series Analysis: Introduction and Overview. In *Handbook of Time Series Analysis* (pp. 1–4). John Wiley & Sons, Ltd. https://doi.org/10.1002/9783527609970.ch1

Schoffelen, J.-M., & Gross, J. (2009). Source connectivity analysis with MEG and EEG. *Human Brain Mapping*, *30*(6), 1857–1865. https://doi.org/10.1002/hbm.20745

Schoffelen, J.-M., Hultén, A., Lam, N., Marquand, A. F., Uddén, J., & Hagoort, P. (2017). Frequency-specific directed interactions in the human brain network for language. *Proceedings of the National Academy of Sciences*, *114*(30), 8083–8088. https://doi.org/10.1073/pnas.1703155114

Schoonhoven, D. N., Briels, C. T., Hillebrand, A., Scheltens, P., Stam, C. J., & Gouw, A. A. (2022). Sensitive and reproducible MEG resting-state metrics of functional connectivity in Alzheimer's disease. *Alzheimer's Research & Therapy*, *14*(1), 38. https://doi.org/10.1186/s13195-022-00970-4

Sharma, V. V., Vannest, J., & Kadis, D. S. (2023). Asymmetric information flow in brain networks supporting expressive language in childhood. *Human Brain Mapping*, *44*(3), 1062–1069. https://doi.org/10.1002/hbm.26136

Sherman, B. E., Graves, K. N., & Turk-Browne, N. B. (2020). The prevalence and importance of statistical learning in human cognition and behavior. *Current Opinion in Behavioral Sciences, Understanding Memory: Which Level of Analysis?*, *32*, 15–20. https://doi.org/10.1016/j.cobeha.2020.01.015

Siegel, M., Donner, T. H., & Engel, A. K. (2012). Spectral fingerprints of large-scale neuronal interactions. *Nature Reviews Neuroscience*, *13*(2), Article 2. https://doi.org/10.1038/nrn3137

Siegel, M., Körding, K. P., & König, P. (2000). Integrating Top-Down and Bottom-Up Sensory Processing by Somato-Dendritic Interactions. *Journal of Computational Neuroscience*, *8*(2), 161–173. https://doi.org/10.1023/A:1008973215925

Siegelman, N., Bogaerts, L., Christiansen, M. H., & Frost, R. (2017). Towards a theory of individual differences in statistical learning. *Philosophical Transactions of the Royal Society B: Biological Sciences*, *372*(1711), 20160059. https://doi.org/10.1098/rstb.2016.0059

Singh, L., Steven Reznick, J., & Xuehua, L. (2012). Infant word segmentation and childhood vocabulary development: A longitudinal analysis. *Developmental Science*, *15*(4), 482–495. https://doi.org/10.1111/j.1467-7687.2012.01141.x

Spaak, E., & Lange, F. P. de. (2020). Hippocampal and Prefrontal Theta-Band Mechanisms Underpin Implicit Spatial Context Learning. *Journal of Neuroscience*, *40*(1), 191–202. https://doi.org/10.1523/JNEUROSCI.1660-19.2019

Swets, J. A., Tanner Jr., W. P., & Birdsall, T. G. (1961). Decision processes in perception. *Psychological Review*, *68*(5), 301–340. https://doi.org/10.1037/h0040547

Tait, L., Özkan, A., Szul, M. J., & Zhang, J. (2021). A systematic evaluation of source reconstruction of resting MEG of the human brain with a new high-resolution atlas: Performance, precision, and parcellation. *Human Brain Mapping*, *42*(14), 4685–4707. https://doi.org/10.1002/hbm.25578

Teinonen, T., & Huotilainen, M. (2012). Implicit Segmentation of a Stream of Syllables Based on Transitional Probabilities: An MEG Study. *Journal of Psycholinguistic Research*, *41*(1), 71–82. https://doi.org/10.1007/s10936-011-9182-2

Tewarie, P., Hunt, B. A. E., O'Neill, G. C., Byrne, A., Aquino, K., Bauer, M., Mullinger, K. J., Coombes, S., & Brookes, M. J. (2019). Relationships Between Neuronal Oscillatory Amplitude and Dynamic Functional Connectivity. *Cerebral Cortex*, *29*(6), 2668–2681. https://doi.org/10.1093/cercor/bhy136

Tewarie, P., Liuzzi, L., O'Neill, G. C., Quinn, A. J., Griffa, A., Woolrich, M. W., Stam, C. J., Hillebrand, A., & Brookes, M. J. (2019). Tracking dynamic brain networks using high temporal resolution MEG measures of functional connectivity. *NeuroImage*, *200*, 38–50. https://doi.org/10.1016/j.neuroimage.2019.06.006

Tóth, B., Janacsek, K., Takács, Á., Kóbor, A., Zavecz, Z., & Nemeth, D. (2017). Dynamics of EEG functional connectivity during statistical learning. *Neurobiology of Learning and Memory*, *144*, 216–229. https://doi.org/10.1016/j.nlm.2017.07.015

van Diessen, E., Numan, T., van Dellen, E., van der Kooi, A. W., Boersma, M., Hofman, D., van Lutterveld, R., van Dijk, B. W., van Straaten, E. C. W., Hillebrand, A., & Stam, C. J. (2015). Opportunities and methodological challenges in EEG and MEG resting state functional brain network research. *Clinical Neurophysiology*, *126*(8), 1468–1481. https://doi.org/10.1016/j.clinph.2014.11.018

Vinck, M., Huurdeman, L., Bosman, C. A., Fries, P., Battaglia, F. P., Pennartz, C. M. A., & Tiesinga, P. H. (2015). How to detect the Granger-causal flow direction in the presence of additive noise? *NeuroImage*, *108*, 301–318. https://doi.org/10.1016/j.neuroimage.2014.12.017

Vinck, M., Oostenveld, R., van Wingerden, M., Battaglia, F., & Pennartz, C. M. A. (2011). An improved index of phase-synchronization for electrophysiological data in the presence of volume-conduction, noise and sample-size bias. *NeuroImage*, *55*(4), 1548–1565. https://doi.org/10.1016/j.neuroimage.2011.01.055

Wang, L., Hagoort, P., & Jensen, O. (2018). Gamma Oscillatory Activity Related to Language Prediction. *Journal of Cognitive Neuroscience*, *30*(8), 1075–1085. https://doi.org/10.1162/jocn_a_01275

Wang, L., Jensen, O., van den Brink, D., Weder, N., Schoffelen, J.-M., Magyari, L., Hagoort, P., & Bastiaansen, M. (2012). Beta oscillations relate to the N400m during language comprehension. *Human Brain Mapping*, *33*(12), 2898–2912. https://doi.org/10.1002/hbm.21410

Wang, P., He, Y., Maess, B., Yue, J., Chen, L., Brauer, J., Friederici, A. D., & Knösche, T. R. (2022). Alpha power during task performance predicts individual language comprehension. *NeuroImage*, *260*, 119449. https://doi.org/10.1016/j.neuroimage.2022.119449

Wang, X.-J. (2010). Neurophysiological and Computational Principles of Cortical Rhythms in Cognition. *Physiological Reviews*, *90*(3), 1195–1268. https://doi.org/10.1152/physrev.00035.2008

Wei, H. T., Francois-Nienaber, A., Deschamps, T., Bellana, B., Hebscher, M., Sivaratnam, G., Zadeh, M., & Meltzer, J. A. (2021). Sensitivity of amplitude and phase based MEG measures of interhemispheric connectivity during unilateral finger movements. *NeuroImage*, *242*, 118457. https://doi.org/10.1016/j.neuroimage.2021.118457

Weiss, S., & Mueller, H. M. (2012). "Too Many betas do not Spoil the Broth": The Role of Beta Brain Oscillations in Language Processing. *Frontiers in Psychology*, *3*. https://doi.org/10.3389/fpsyg.2012.00201

Youssofzadeh, V., & Babajani-Feremi, A. (2019). Mapping critical hubs of receptive and expressive language using MEG: A comparison against fMRI. *NeuroImage*, *201*, 116029. https://doi.org/10.1016/j.neuroimage.2019.116029

Youssofzadeh, V., Williamson, B. J., & Kadis, D. S. (2017). Mapping Critical Language Sites in Children Performing Verb Generation: Whole-Brain Connectivity and Graph Theoretical Analysis in MEG. *Frontiers in Human Neuroscience*, *11*. https://doi.org/10.3389/fnhum.2017.00173

Zhao, T. C., Boorom, O., Kuhl, P. K., & Gordon, R. (2021). Infants' neural speech discrimination predicts individual differences in grammar ability at 6 years of age and their risk of developing speech-language disorders. *Developmental Cognitive Neuroscience*, *48*, 100949. https://doi.org/10.1016/j.dcn.2021.100949

Zhou, Y. J., Pérez-Bellido, A., Haegens, S., & de Lange, F. P. (2020). Perceptual Expectations Modulate Low-Frequency Activity: A Statistical Learning Magnetoencephalography Study. *Journal of Cognitive Neuroscience*, *32*(4), 691–702. https://doi.org/10.1162/jocn_a_01511

Acknowledgements

First, I would like to thank my mentor, Pat Kuhl, for giving me the opportunity to join the Speech and Hearing Sciences program and pursue neuroimaging research. Pat's support allowed me to take the leap into research, and I am very grateful for the privilege of my training and participation in her lab. I would like to thank Alexis Bosseler and Samu Taulu from the MEG Center at the University of Washington, both of whom taught me so much about effective research with MEG. My mentors in neuroimaging software development, Eric Larson and Dan McCloy, have provided invaluable guidance and teaching throughout my entire time at the UW. I am so grateful for their generosity in sharing their time and expertise with me. I would like to thank my colleagues at ILABS, Julia Mizrahi, Ashley Drew, Maggie Clarke, Steve Bierer, and many others, for all the partnership, encouragement, and wisdom I have enjoyed from their company. I also am grateful to the members of my committees, Adrian K.C. Lee, Andrew Brown, and Sara Kover, for their patience and insightful feedback as I have worked on my program milestones over the years.

I would like to thank the family and friends whose love and support has kept me sane. I am grateful to my parents, Paul and Cathy Nordman, for their support during my program, along with the rest of my family. My friends Shannon DeJong, MC Westra, Christine Ley, Jon and Ke Hayase, and others in my church community have been instrumental in keeping me going through their encouragement and fellowship. Finally, I want to thank Jordan Sbarboro for uplifting my life with love.

Appendix A: Label Color Key

Frontal

- L CMF: caudalmiddlefrontal-lh
- R CMF: caudalmiddlefrontal-rh
- L FPOL: frontalpole-lh
- R FPOL: frontalpole-rh
- L LOF: lateralorbitofrontal-lh
- R LOF: lateralorbitofrontal-rh
- L MOF: medialorbitofrontal-lh
- R MOF: medialorbitofrontal-rh
- L POP: parsopercularis-lh
- R POP: parsopercularis-rh
- L PORB: parsorbitalis-lh
- R PORB: parsorbitalis-rh
- L PTRI: parstriangularis-lh
- R PTRI: parstriangularis-rh
- L PREC: precentral-lh
- R PREC: precentral-rh
- L RMF: rostralmiddlefrontal-lh
- R RMF: rostralmiddlefrontal-rh
- L SF: superiorfrontal-lh
- R SF: superiorfrontal-rh

Parietal

- L IP: inferiorparietal-lh
- R IP: inferiorparietal-rh
- L PSTC: postcentral-lh
- R PSTC: postcentral-rh
- L SP: superiorparietal-lh
- R SP: superiorparietal-rh
- L SPM: supramarginal-lh
- R SPM: supramarginal-rh

Temporal

- L BSTS: bankssts-lh
- R BSTS: bankssts-rh
- L IT: inferiortemporal-lh
- R IT: inferiortemporal-rh
- L INS: insula-lh
- R INS: insula-rh
- L MT: middletemporal-lh
- R MT: middletemporal-rh
- L ST: superiortemporal-lh
- R ST: superiortemporal-rh
- L TPOL: temporalpole-lh
- R TPOL: temporalpole-rh
- L TT: transversetemporal-lh
- R TT: transversetemporal-rh

Medial

- L CAC: caudalanteriorcingulate-lh
- R CAC: caudalanteriorcingulate-rh
- L ENT: entorhinal-lh
- R ENT: entorhinal-rh
- L ICING: isthmuscingulate-lh
- R ICING: isthmuscingulate-rh
- L PARC: paracentral-lh
- R PARC: paracentral-rh
- L PH: parahippocampal-lh
- R PH: parahippocampal-rh
- L PCING: posteriorcingulate-lh
- R PCING: posteriorcingulate-rh
- L PCUN: precuneus-lh
- R PCUN: precuneus-rh
- L RAC: rostralanteriorcingulate-lh
- R RAC: rostralanteriorcingulate-rh

Occipital

- L CUN: cuneus-lh
- R CUN: cuneus-rh
- L FFM: fusiform-lh
- R FFM: fusiform-rh
- L LOCC: lateraloccipital-lh
- R LOCC: lateraloccipital-rh
- L LING: lingual-lh
- R LING: lingual-rh
- L PCAL: pericalcarine-lh
- R PCAL: pericalcarine-rh

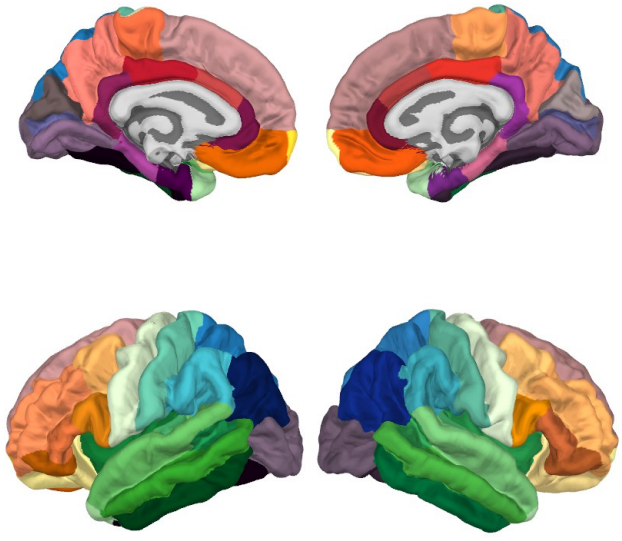

Appendix B: D-prime Values by Subject

Subject ID	D-prime
genz105_9a	0.503980691813442
genz106_9a	0.0568741690125577
genz108_9a	0.717580239007303
genz110_9a	0.258900208128528
genz111_9a	0.733931925100794
genz112_9a	-0.151843534281583
genz114_9a	0.00169408461951467
genz115_9a	-0.389750369467367
genz116_9a	0.17385039908194
genz118_9a	0.200003068771046
genz119_9a	0.723396500594928
genz120_9a	0.258900208128528
genz121_9a	-0.151843534281583
genz122_9a	-0.00169408461951481
genz123_9a	0.284715559622172
genz124_9a	0.847813226892774
genz125_9a	-0.330027331696692
genz126_9a	0.934295838993488
genz128_9a	0.129156076719324
genz130_9a	0.287469899815533
genz131_9a	0.238414611204317
genz133_9a	-0.129156076719325
genz205_11a	-0.761168377289932
genz206_11a	0.374114749418375
genz207_11a	0.021610546396112
genz208_11a	0.215638688820038
genz209_11a	0.855122309027922
genz210_11a	-0.330853230109886
genz212_11a	0.723396500594928
genz216_11a	1.35022323658851
genz218_11a	-0.419418877552533
genz219_11a	0.345871676705509
genz223_11a	0.635706500246436
genz224_11a	0.636751650992085
genz225_11a	0.0857727464249714
genz226_11a	0.723396500594928
genz227_11a	0.123722833518422
genz228_11a	0.68044085543666
genz229_11a	-0.493396407736305
genz231_11a	1.96454726556215
genz232_11a	0.200003068771046
genz233_11a	-0.108255395998955
genz235_11a	0.723396500594928
genz311_13a	0.460597361519089
genz313_13a	0.111009736192315
genz314_13a	-0.172417596027814
genz318_13a	-0.151843534281583
genz320_13a	0.804551707584284
genz322_13a	0.349975643955977
genz323_13a	-0.46329757031439
genz324_13a	0.636751650992085
genz325_13a	0.977679169287841
genz326_13a	0.330853230109886
genz327_13a	0.771752661367069
genz328_13a	1.04653616802534
genz329_13a	-0.338093888450173
genz330_13a	-0.192303560214127
genz331_13a	0.810863331639414
genz332_13a	-0.215638688820038
genz333_13a	1.54391352348497
genz334_13a	0.302283538422881
genz335_13a	0.417335842210599
genz337_13a	-0.215638688820038
genz401_15a	-0.155744091382539
genz403_15a	0.0656979641177952
genz406_15a	-1.03797864897782
genz409_15a	0.239113739043392
genz411_15a	1.04653616802534
genz412_15a	-0.591447522857928
genz413_15a	-0.302283538422881
genz414_15a	0.847813226892774
genz415_15a	1.21999024870304
genz417_15a	-0.0459530620080222
genz418_15a	0.0857727464249714
genz419_15a	0.550269038891372
genz420_15a	0.108255395998955
genz421_15a	0.258900208128528
genz422_15a	-0.770880566960818
genz423_15a	0.021610546396112
genz424_15a	0.804551707584284
genz425_15a	0.470593522094088
genz426_15a	0.0656979641177952
genz427_15a	0.847813226892774
genz428_15a	0.593530558199861
genz429_15a	0.427149484007427
genz430_15a	1.09012430630797
genz431_15a	0.374114749418375
genz432_15a	-0.172417596027814
genz507_17a	0.129156076719324
genz512_17a	0.419418877552532

Subject ID	D-prime
genz513_17a	0.434009346855875
genz514_17a	0.591447522857928
genz515_17a	0.172417596027814
genz516_17a	0.129156076719324
genz517_17a	0.547568830096071
genz518_17a	0.151843534281583
genz519_17a	0.847813226892774
genz520_17a	-0.761168377289932
genz521_17a	0.550269038891372

Subject ID	D-prime
genz522_17a	-0.503980691813442
genz523_17a	0.891034319684998
genz527_17a	0.00169408461951467
genz528_17a	0.0421846081423431
genz529_17a	0.021610546396112
genz530_17a	0.330027331696692
genz531_17a	0.0421846081423431
genz532_17a	0.200003068771046

Appendix C: Adolescent N400 Values by Subject

Subject ID	N400 Difference (1e-12)
genz105_9a	-20.9924664794048
genz106_9a	-23.5676385251644
genz108_9a	11.0938785018286
genz110_9a	-20.0017027246709
genz111_9a	-12.3363741531318
genz112_9a	18.6967093886624
genz114_9a	-19.2370495695572
genz115_9a	-8.80630744930772
genz116_9a	2.67513735998592
genz118_9a	-12.1195562430202
genz119_9a	-53.3637184643884
genz120_9a	6.31132686127594
genz121_9a	5.34879394204199
genz122_9a	13.6486304696046
genz123_9a	-1.32349566719358
genz124_9a	-25.3338926073358
genz125_9a	30.2129450691402
genz126_9a	18.0881597098176
genz128_9a	-22.0767120754606
genz130_9a	25.7973119857709
genz131_9a	2.24138292608777
genz133_9a	21.7616379469002
genz205_11a	8.29423697649378
genz206_11a	13.5633296759404
genz207_11a	-28.897338306949
genz208_11a	7.16110550465243
genz209_11a	0.922496501912632
genz210_11a	-13.7304228250996
genz212_11a	14.0537150281276
genz216_11a	-1.10359391580634
genz218_11a	-22.6263651603775
genz219_11a	19.579706073433
genz223_11a	-9.17071003530693
genz224_11a	-9.12064928991369
genz225_11a	13.3931189181076
genz226_11a	22.5909904779894
genz227_11a	-13.1540016929814
genz228_11a	-2.53809208618738
genz229_11a	-4.94192920942089
genz231_11a	21.7553584529203
genz232_11a	-39.4022591341638
genz233_11a	6.62450680737199
genz235_11a	-15.5259325230558
genz311_13a	17.8728908163727
genz313_13a	-8.71468759895409
genz314_13a	-10.3576732437005
genz318_13a	14.5617948379534
genz320_13a	-22.2885675224051
genz322_13a	-49.9527887642624
genz323_13a	17.0522784605816
genz324_13a	4.40118044650768
genz325_13a	4.80733320640807
genz326_13a	-10.9942126524966
genz327_13a	-7.08499053336805
genz328_13a	-4.99418429327407
genz329_13a	16.0395605096437
genz330_13a	-25.9253371783498
genz331_13a	11.7594753159766
genz332_13a	27.9805857940849
genz333_13a	12.4503714608941
genz334_13a	-2.92432935910295
genz335_13a	5.10668055614151
genz337_13a	5.14226321149647
genz401_15a	-14.6653848259873
genz403_15a	12.4510289242223
genz406_15a	8.85948122197761
genz409_15a	-17.9659332482246
genz411_15a	12.8173470695145
genz412_15a	12.2850434697757
genz413_15a	-1.02306313804441
genz414_15a	7.35522042653564
genz415_15a	20.1407432018986
genz417_15a	9.49529248890269
genz418_15a	-50.5284741346705
genz419_15a	31.5624863648069
genz420_15a	25.4241801829357
genz421_15a	-27.4190747050651
genz422_15a	-9.95137252642153
genz423_15a	-13.8557864139405
genz424_15a	4.28419115668286
genz425_15a	1.34919927292153
genz426_15a	-20.9816349402479
genz427_15a	-1.73114609752581
genz428_15a	-22.1547257508836
genz429_15a	-3.20854786949152
genz430_15a	-4.45823910705934
genz431_15a	-16.4827025739636
genz432_15a	-9.36798841857362
genz507_17a	7.4438620360874
genz512_17a	-27.784288210918

Subject ID	N400 Difference (1e-12)
genz513_17a	-7.5227087056082
genz514_17a	-5.04032661519635
genz515_17a	1.01570132380635
genz516_17a	-8.5859791632798
genz517_17a	-4.02187502005982
genz518_17a	8.88303234823129
genz519_17a	-1.49358007277808
genz520_17a	-9.6619635521697
genz521_17a	-8.09163073592829
genz522_17a	-14.750569931503
genz523_17a	10.7148780198004
genz527_17a	-8.69784028061028
genz528_17a	20.5685108936834
genz529_17a	10.8096490378752
genz530_17a	-19.9930345323038
genz531_17a	-24.6637881648301
genz532_17a	-10.1846008356606

Appendix D: Adult N400 Values by Subject

Subject ID	N400 Difference (1e-12)
genz_c101	4.25173652883491
genz_c102	15.8431119839093
genz_c103	3.7936057523589
genz_c104	8.08796338316935
genz_c105	3.42652263945995
genz_c106	-0.0718340955174502
genz_c107	4.9870250642932
genz_c108	-12.0702938976215
genz_c109	13.2104893669342
genz_c110	-30.5586556015542
genz_c111	-15.943439052593
genz_c112	-2.01758160342732
genz_c113	6.2876951209161
genz_c114	6.06696416885509
genz_c115	0.9388680749579
genz_c116	3.16941248705784
genz_c117	-14.5290338554513
genz_c118	-17.283573668026
genz_c119	-20.3079520356143
genz_c121	8.4334490288011
genz_c122	-3.5595110551189
genz_c123	-15.9295953517906
genz_c124	-14.1644753138485
genz_c125	0.783012619979281
genz_c127	-10.8158513984275
genz_c128	-6.07776496761266
genz_c129	-4.23466849643078
genz_c130	1.7181836959357
genz_c131	-26.9599796249239
genz_c132	16.3273177223211